CHALMERS

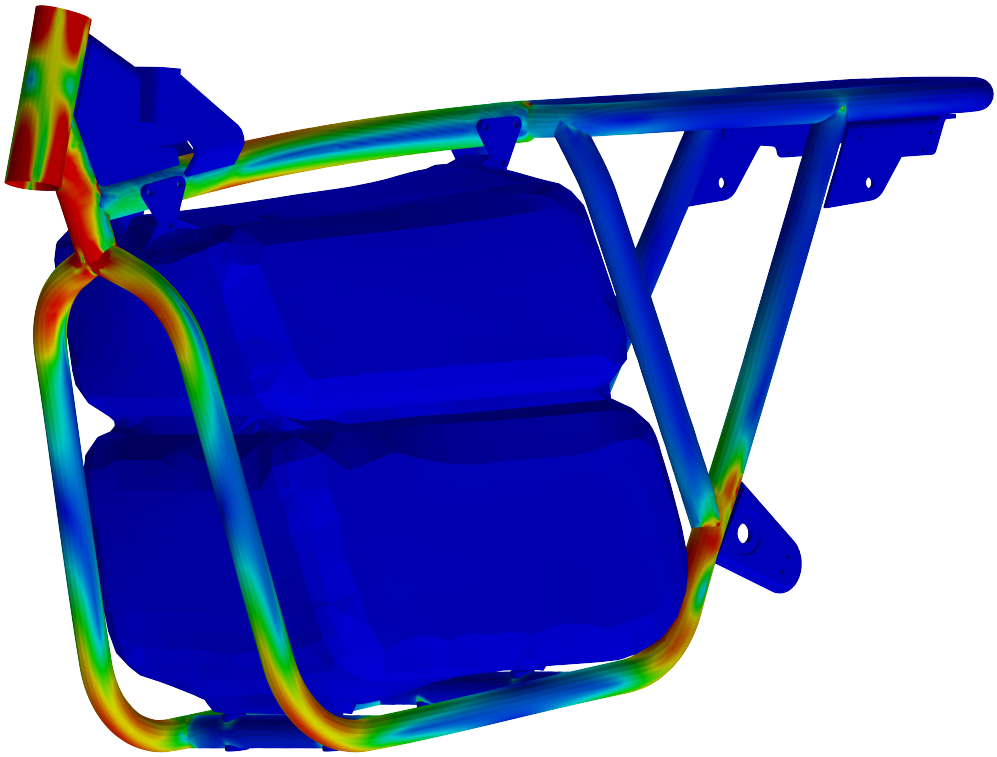

Method development for frame design of electric motorcycles

Master's thesis in Automotive Engineering

WILLIAM BLIXT
ADIL LOKAT

Department of Mechanics and Maritime Sciences
CHALMERS UNIVERSITY OF TECHNOLOGY
Göteborg, Sweden 2023

MASTER'S THESIS IN AUTOMOTIVE ENGINEERING

Method development for frame design of electric motorcycles

WILLIAM BLIXT
ADIL LOKAT

Department of Mechanics and Maritime Sciences
Division of Dynamics
CHALMERS UNIVERSITY OF TECHNOLOGY

Göteborg, Sweden 2023

Method development for frame design of electric motorcycles
WILLIAM BLIXT
ADIL LOKAT

Department of Mechanics and Maritime Sciences
Division of Dynamics
Chalmers University of Technology
SE-412 96 Göteborg
Sweden
Telephone: +46 (0)31-772 1000

Cover:
Colour plot of a FEM simulation

Chalmers Reproservice
Göteborg, Sweden 2023

Abstract

Compliance in a motorcycle frame is an important factor to consider when designing. Different load cases must be taken into consideration depending on the requirements of the bike and what the use case is. To think of the structural characteristics when designing can make the design process simpler and quicker. Extensive studies can take time and are not always necessary in early design if simple simulations has been done through the process. Early simulations can direct the design along the way to give good structural efficiency and smart solutions when integrating components as stressed members. To also have the simulations verified and calibrated to a physical test give confidence when doing simple iterative tests early in the design phase.

A method has been developed to enable iterative and fast design development of a motorcycle frame with consideration to structural characteristics, and to do this with limited access to tools. To allow for this the design must continuously consider the structural simulations to not end up with a overly complex model that requires big changes after simulating. Results show that the method used to design and simulate, can have an impact on what and how the results obtained from simulation can differ from each other and thus be less suitable for different scenarios.

Acknowledgements

We would like to direct our gratitude to the entire team at RGNT Motorcycles for having us and for all exiting new experiences. Special thanks to our supervisors Alexander Lewandowski and Ludvig Brodén. Without your guiding hands this project would never have succeeded. Many thanks to Petter Miltén for helping with the setting up the load cell used in the physical testing. Lastly a big thank to Thomas Abrahamsson, our examiner for giving valuable help and feedback throughout the project

Contents

1 Introduction

As the world is moving further and further away from combustion engines and fossil fuels towards electric energy in areas like the transportation and energy sector. This change puts a new set of requirements on the new type of products causing new challenges for the manufacturers to create products that are attractive for a consumer and meets all the laws and requirements posed considering safety and environment. This means that the workflow and design process might not be the same and thus need new methods that are more efficient or suitable for the application. This applies no matter if an old and established company are converting one existing product or if a new manufacturer wants to enter a new market. Some processes requires a complete overhaul while others can get away with minor changes. Regardless of what the outcome might be of the processes they still need to considered to harmonise with new components and architecture, even if the component itself will not face any changes. In the automotive sector it is the powertrain that is converting to electric drive where the internal combustion engine is exchanged for an electric motor, battery pack and electronics to power the system. These new components must integrate with the rest of the vehicle, thus new requirements must be met.

The motorcycle industry has two types of main target groups. In the developing world motorcycles are used as a day to day means of transport where small displacement, fuel efficient and cheap bikes counts for the majority of vehicles because of their nature of nimbleness and cheap operations [31]. In the western, more developed world the motorcycle is used mainly as a luxury item of leisure. Where the types of bikes being sold are vastly more performance oriented with engines that are more sophisticated and the materials used more exclusive, thus being more expensive [31]. It can be beneficial for manufacturers to develop electric motorcycles for both types of target groups. Initially the aim might be for a motorcycle targeted towards the consumer group with more expensive motorcycles who find the new and advanced technology attractive. As methods and manufacturing processes becomes cheaper and more suitable for mass production, manufacturers can start develop bikes that are used in urban traffic which is cheap to buy and operate. This is the method that Elon Musk, the founder of Tesla Inc, called the "Master Plan" which they have followed [23][22]. As Musk continues to write is that the manufacturing and assembly processes that had not been developed and refined for decades like other automotive manufacturers were expensive and inefficient which almost caused the company into bankruptcy which goes to show the importance of continuously revise the methods that exist.

1.1 Background

RGNT - Motorcycles is a young and evolving electric motorcycle manufacturer located in Kungsbacka, Sweden. They build a technological advanced bike with a classic, timeless look. RGNT - model, No.1 is the current model that they produce. It is built with a welded steel tube frame, rear mounted electric hub motor and cloud connected, used friendly interface through a touch display.

As one of the means of expansion, offering different types of motorcycles is an option to suit a wider range of costumer needs. It is therefore important to have an efficient method of evaluating different concepts, to be able to make informed decisions at an early stage. To streamline the design processes RGNT - Motorcycles asks of this project to come up with suggestions for a methodology to evaluate future frame designs structurally.

1.2 Purpose

The purpose of this study is to provide a verification for the methods embodied in the structural analysis when designing a frame for an electric motorcycle. The expected outcome of the study is to provide suggestions on how the method could be adapted in order to increase the accuracy of the simulations early in the design phase. This will complement the current setup and confirming the accuracy of it.

The study will consist of two major parts. The first part is to benchmark the current software used for structural analysis with other common software used in the industry. The goal for this study will be to see in what order of magnitude the results of the simulations correlates. Different methods of refining the simulations by the use of mesh adaptations and overall usability and adaptability of the software will be investigated.

Secondly a test rig will be constructed to evaluate the accuracy of the simulations compared to manufactured part. The test rig will aim to replicate a few load cases used in the simulations and the result will be collected by the use of load cells and strain gauges on suitable positions on the frame.

When constructing the testing rig, the aim is to have the rig as modular or adaptable as possible while not sacrificing precision. This will grant the possibility of longevity in the test rig, allowing for a wide range of future concepts and models to be tested. This will allow for an even further optimised method where different types of frames can be tested for a wider range of load cases.

The project will consider the structural analysis of the electrical motorcycle and focus on the frame and if stressed members could be used for optimisation. While conducting the study the handling aspects of having different levels of compliance in the frame will be investigated, in order to get a connection between desired levels of compliance and actual levels.

1.3 Boundaries

The project will take place during the spring semester 2022 and is 30 credits which corresponds to about 40h per week for each student. This sets the framework for the amount of time and length of the project which in turn means that the focus will have to be directed at certain key parts while some other parts may be simplified.

A detail construction will not be designed but rather the analysis of how certain key factors should be accounted for and incorporated in the design. The focus will mainly be on geometrical analysis rather than materialistic therefore a material study and analysis will not be considered unless obvious gains can be seen. On the other hand, there is room to point out, if necessary, possible improvement ideas for simple surrounding processes.

The purpose of the test rig is to verify the results of the simulations. It will therefore test a few load cases and not all, since the rig will be used to evaluate the simulations and not necessarily the frame.

2 Theory

In order to understand the main aspects of motorcycle frames and their requirements and FEA - concepts, this chapter aim to review the different terms and principles that are considered.

2.1 Frames and requirements

The first motorcycle as we know it was created by Gottelieb Daimler and Wilhelm Maybach in 1885, it was a bicycle with a small internal combustion engine attached as the source of propulsion [10]. It was known as the "Bone-Crusher" or "Bone-Shaker" since it was made of a wooden frame and iron wheels as seen in *Figure 2.1* [10]. This motorcycle set the base for what we come to know as a motorcycle with the controls for operation [11]. This motorcycle was too uncomfortable to ride which required a solution which showed itself in 1889 the air inflated tire was invented by John Boyd Dunlop [15]. The engines that were put in motorcycles had an even number of cylinders since it was found that it reduced vibrations compared to an uneven number of cylinders. The engines that were put in the motorcycles were small and did not have that much power, DeDion-Buton was the first manufacturer who mass produced motorcycles and did that with an engine that was used was a small lightweight one half horsepower 4 stroke engine [10]. The same concept was done by Indian Motorcycle whose motorcycle had 1,75 horsepower and came to be the best selling motorcycle until the first world war [21]. Up until this point the requirements on the frame of motorcycle was very similar to a bicycle, as seen in *Figures 2.1 & 2.2*

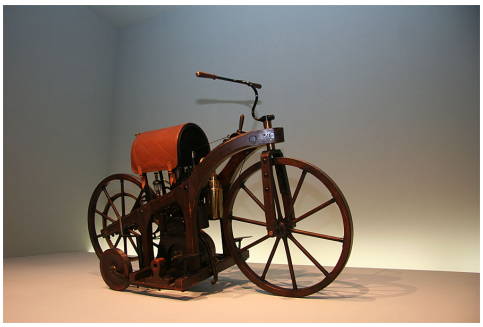

Figure 2.1: *The Daimler Reitwagen also known as the "Bone-Crusher"*

Figure 2.2: *An early Indian 1901, bicycle frame motorcycle*

The motorcycle had become a reliable and thus common mode of transport and proved to be a great resource for the war because of its simple and utilitarian nature. The motorcycle was used both as reconnaissance as well as message delivering [10]. When the war ended, the internal combustion engine was extensively used in many applications worldwide, not least in the motorcycle industry [29]. This meant that the size and power of the motorcycles were increased which meant that the frame had higher requirements and had to move away more and more from the bicycle like frame design [33].

As time goes, so does the development of the motorcycle and depending on where in the world they are the motorcycles fulfil a certain function. In developing parts of the world the motorcycle is a daily means of transport because of its lower price, great fuel economy and practical and nimble nature which is a useful characteristic in traffic jams in developing cities. In the more developed countries the motorcycle fulfil a function mostly for recreation and is more of a luxury than a necessity thus the requirements differ depending on how the user wishes to use the vehicle [30]. A sport bike is vastly different than a custom chopper both in terms of look and functionality.

2.2 Frame intro

As the motorcycle has been developed so has the frame since it is an integral part of the vehicle. Most of the components of a motorcycle is attached to the frame which means that it must be both practical as well as structurally sound since the forces from the ground are going through the frame [8].

In early days the frame of the motorcycle originated from the bicycle, and as the power, speed and expectations of the motorcycle has increased so has the requirements [8]. The combination of performance, practicality and design and its priority are different for different types of motorcycles. Regardless of how different manufacturers prioritise for their models it is sought after to have a frame that does not flex, is light and has high enough tolerances to allow for precise fitting of components such as the suspension and wheels [7]. These factors will affect the driver feel of the motorcycle as a frame that is not resistant enough to bending and twisting will change steering geometry as load is applied from road imperfection, cornering, braking and engine torque. This can make the driver exhausted and cause driver fatigue and make the bike uncomfortable since the driver effort will be higher [5].

This is a balancing act with the material cost, manufacturing cost and design of the motorcycle for the manufacturers. Therefore some types of bikes will have more or less focus on outright performance and structural efficiency and instead have design and manufacturing cost minimised on a bike that is not aimed for performance driving[8]. With more and more vehicles becoming electrified, they stand before different requirements which must be met.

There are different ways to maximise stiffness and minimise weight as different frame types will do in different ways, geometry, material and using other components as stressed members are some ways to achieve this [8]. The stiffness to weight ratio is known as the structural efficiency and although this is very dependent on model to model even within bikes with the same frame type there is a general trend of what types of frames that has higher structural efficiency [8].

Some of the most common types of frames are described below and their advantages and disadvantages. Any motorcycle embodies several essential compromises, there is no perfect design that suit all. The use case of the bike dictates what characteristics that are sought after, a motorcycle with handling in focus might have a stiffer frame and compromise on comfort [8][5]. The two main basic goals of the frame is to withstand the static and dynamic forces. The static forces is the weight of the bike, rider and to hold the components of the bike. The dynamic forces are the forces that interacts with the bike while driving, and when these forces act on the bike it should maintain precise steering, good road holding, handling and comfort [8][7]. Precise steering is achieved by a frame that is resistant to twisting and bending which prevents the relation of the wheels to change. The road holding of the bike is the stiffness between the wheels, in other words if the bike is not resistance to twisting and compliance and can not maintain the stiffness between the wheels the road holding of the bike is not sufficient [8]. All of these factors affect the handling of the bike, although for the handling, there are other factors that must be well thought about before the frame stiffness will cause any apparent effect, for example the weight and weight distribution, suspension geometry and tuning and overall vehicle architecture will have a bigger impact on handling if not well designed [5].

2.2.1 Tubular frame

The first motorcycles that came into production were using tubular frames since they originate from the bicycle frame. This design is simple and cheap to manufacture, this is the reason why the tubular frame is the foundation for many other frame types that uses some traits from this frame type. As the engines got bigger and more powerful the tubular frame adapted in to many different variants. Examples of these are the single cradle frame which hugs the engine on either side of it with a single tube. There is also the double cradle frame which is the evolution of the single cradle frame. The double cradle frame is not that common though since the introduction of the twin spar frame which has taken its place. This design has evolved to more suitable types of frames that can withstand the higher loads and meet the higher requirements therefore there are not that many outright tubular frames in production today as they were in the early days. Many of the frame types that are covered below which are commonly used today originally comes from the tubular frame.

2.2.2 Trellis frame

The trellis frame is also a type of tubular frame but is uses small, triangulated tubes from the steering head to the swing arm as directly as possible. Because of the smaller tubes and the more direct path the structural efficiency is good [24],[6]. This light and string type of frame also allows for good accessibility for maintenance. The cost of manufacturing compared to tubular frames however is increased since a more complex shape require a more complex jig to for welding. The cost of manufacturing compared to the gained performance is quite high, thus the trellis frame not being used to a great extent by manufacturers [33],[8]. When using long thin tubes, the likelihood for vibrations from the engine is high which can be counteracted by having shorter tubes and increase the diameter of the tubes until a satisfactory result. This is the case for the any type of frame design but the design trellis frame increases the likelihood for it [8]. Figure 2.3 shows a trellis frame. The trellis frame is used in the Ducati Monster 1000, KTM 1290 Super Duke R, and Honda VTR 250 for example.

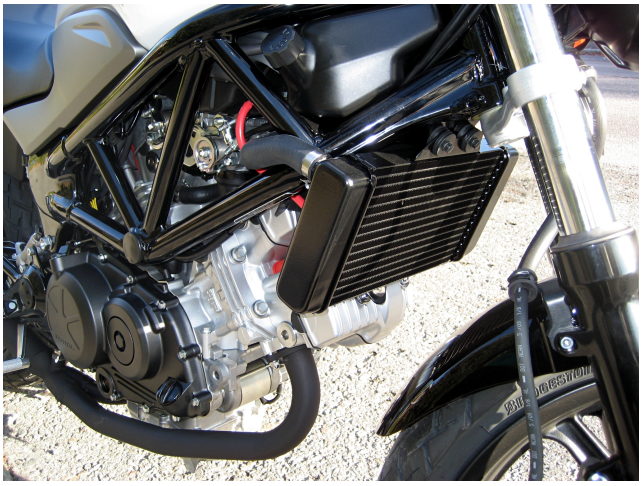

Figure 2.3: *Trellis frame*

2.2.3 Monocoque

In aeroplanes and high performance cars you can find a monocoque, a frame where the stresses are taken up by the skin which is structural instead of having fairings and a smooth outer surface on top of a inner structural frame [8]. In a motorcycle this is not as beneficial as the previous mentioned applications since its shape and size make it difficult with packaging and accessibility which requires holes and cutouts, thus counteracting the advantages with the monocoque design philosophy. Monocoque motorcycles are almost always custom specialised competition bikes and rarely street bikes [8], as seen in *Figure 2.4* which makes them expensive, thus not ideal for road bikes. The Kawasaki Ninja ZX-14 2006, and the Ducati 1199 2012 used a monocoque as their frame.

Figure 2.4: *Monocoque frame*

2.2.4 Twin spar frame

The twin spar frame is the most common type of frame in modern sport bikes and racing bikes. It is a variant of the Perimeter or Beam frame consists of two beams running on each side of the engine in the middle [8],[33]. The beams connect the swing arm mounting with the steering head thus providing great stiffness which is suitable for sport bikes and high-performance applications. The structural efficiency of this type of frame is not great and if not made by a lighter metal it would be very heavy. But the gained lateral and torsional stiffness this type of frame provides is the sought after trait that prompts manufacturers to keep using this type of frame in the high performance category. The shape of the Twin spar frame also allows for good packaging possibilities and accessibility for engine work. These advantages, mainly the stiffness take higher priority than weight since the gains in performance compared to a slightly lighter frame.

2.2.5 Stressed members

To reduce the weight of the frame and increase the structural efficiency a stressed member can be used. This means that the motorcycles other components can be used as a part of the load bearing structure. Most common is to use the engine and gearbox assembly as a stressed member and thus removing that part of the frame which leads to higher structural efficiency. This is a very common technique used by manufacturers since the engine already has built in stiffness that can be utilised making the while motorcycle more efficient in terms of structural efficiency [8]. Investigations show that the bolted connection will not have as good of a structural consideration as if it were welded [28], but the structural efficiency can be increased.

2.3 Effect of frame stiffness

It is inevitable that a motorcycle frame will flex when exposed to the forces acting upon it when driving [7]. The magnitude of flex and what compromise and combination of characteristics however is up to each manufacturer and what they are willing to do. Since different motorcycles are driven in different ways and are aimed for different costumer groups there is no correct way of designing or no ideal way of having the characteristics. It is different for every manufacturer and every bike model and its purpose [8]. Thus, the different purposes face different requirements and the effect of frame compliance can be more or less significant [5],[28]. A racing bike can not flex as much as a regular road bike since the changes that happen when the bike flexes can cause unpredictable behaviour and be potentially dangerous while a road bike can have a cheaper and more comfortable design since the requirements are not as high [8]. The three main ways a motorcycle frame will flex is lateral, longitudinal and torsional, which according to the coordinate system in figure 2.5 is along the y-axis for lateral deflection, along the x-axis for longitudinal deflection and around the x-axis for torsional deflection. The stiffness for the lateral and longitudinal load case is defined as N/mm, and the

stiffness for the torsional load case is defines as $N/\deg$ [7]. The load cases which are being considered are defined in section 2.4 Load Cases.
The most significant deformation of the complete bike occurs along the z-axis which is designed in to the suspension and taken up by the forks, springs and dampers, the stroke of the suspension is significant compared to the deformation of the frame, thus the effect of it is negligible [7].

2.3.1 Significance depending on type of bike

As mentioned different bikes have different requirements of stiffness depending on the use case [8]. A motorcycle that is aimed for track driving have a suspension geometry that is carefully thought out and designed for the purpose. As a racing motorcycle is driven om the limit, any slight variation to the geometry while driving can cause the bike to induce nervous behaviour or worst case lose control and crash. In this application, the stiffness of the frame and stiffness of the full bike be the reason for unpredictable suspension geometry changes while driving if not good enough [7][5]. On the other hand, if the motorcycle is designed as a day to day city cruiser where performance driving is not the objective, the main goal is to hold everything together and be sufficiently stiff to not break when exposed to the loads [8]. In such application, comfort and convenience is more important, thus having a lighter bike that is easy to manoeuvre through city traffic. For a city bike the nimbleness is more important maximum stiffness [33].

2.3.2 Perceived robustness from stiffness

The main reason for considering stiffness when constructing a bike is for the bike to be predictable when driving. Often a lesser bike on paper can outperform a better one if is more predictable and thus confidence inspiring for the rider. It is the experienced stiffness that is the key rather than the absolute stiffness [5]. One example pointed out by *Tony Foale in MOTORCYCLE HANDLING AND CHASSIS DESIGN, the art and science* [8] is that a poor seat mounting is more often a problem than lack of frame stiffness because it makes the rider unpredictably move around on the bike causing a lack of confidence. Similarly, other factors can disguise the lack of stiffness like good suspension geometry, tire size, which dampens and takes up forces making the bike feel predictable [28].

2.3.3 Stability considerations

The stability of the bike is a factor that frame stiffness affects [28]. The effect frame stiffness have on stability was investigated [28]. Motorcycle stability can be defined in many ways, depending on what motion the motorcycle is executing, and different factors like speed, suspension geometry and frame stiffness enhances of defeats the instability that might exists [7]. Weave and wobble are the two modes of instability that are of main interest. Weave is an oscillation that affects the whole motorcycle where its mainly induced by the rear end. Wobble is front end oscillation around the steering axis where the rear end does not have any significant contribution [7]. In the study "The Influence of Frame Structure on the Dynamics of Motorcycle Stability" by G. E. Roe and T. E. Thorpe [28], two tubular frames were part of the analysis, one frame was of duplex cradle type and the second was a duplex frame with a suspended engine which also acts as a stressed member [28]. The different factors that might affect a motorcycles dynamic stability was investigated and how significant the effect of the frames stiffness. For weave stability the torsional stiffness of the frame converges to a optimum value while the lateral stiffness should be as high as possible since the stability increase with the stiffness. Moreover it is the opposite for wobble stability where the torsional stiffness gives a more significant improvement [28].

2.4 Load Cases

The dynamic loads and forces that the motorcycle gets exposed to are generated in the contact patch of the tire and the resultants of these forces can be derived and applied at parts of the frame for analysis [7],[8]. The forces that appear when driving is rarely singled out to one specific axis or direction [7]. Instead of trying to capture all of these together in simulation the load cases are separated to defined directions which can be captures both in simulation and in physical testing. These load cases are defined to evaluate the torsional stiffness, lateral stiffness, and longitudinal stiffness of the frame [7]. All of theses cases are considered between the swing arm pivot axis and the steering head. The boundary conditions can set up in a way where the steering head is locked in space and the load is being applied at the swing arm pivot, or the opposite where the swing arm pivot is locked and the load is being applied at the steering head [7]. The case where the swing arm pivot is locked and the force is being applied at the steering head is the easier to replicate during the physical testing. When evaluating the full motorcycle it is also of interest to consider the swing arm and fork in since these will have their own properties and stiffness when loaded. The magnitude of the load can be arbitrary since it is the stiffness that is of interest [7], [8].

2.4.1 Load case - Lateral stiffness

To evaluate the lateral stiffness a load is applied on the steering head tube laterally, along the global y-axis. The swing arm pivot point is fixed in space a figure 2.5.

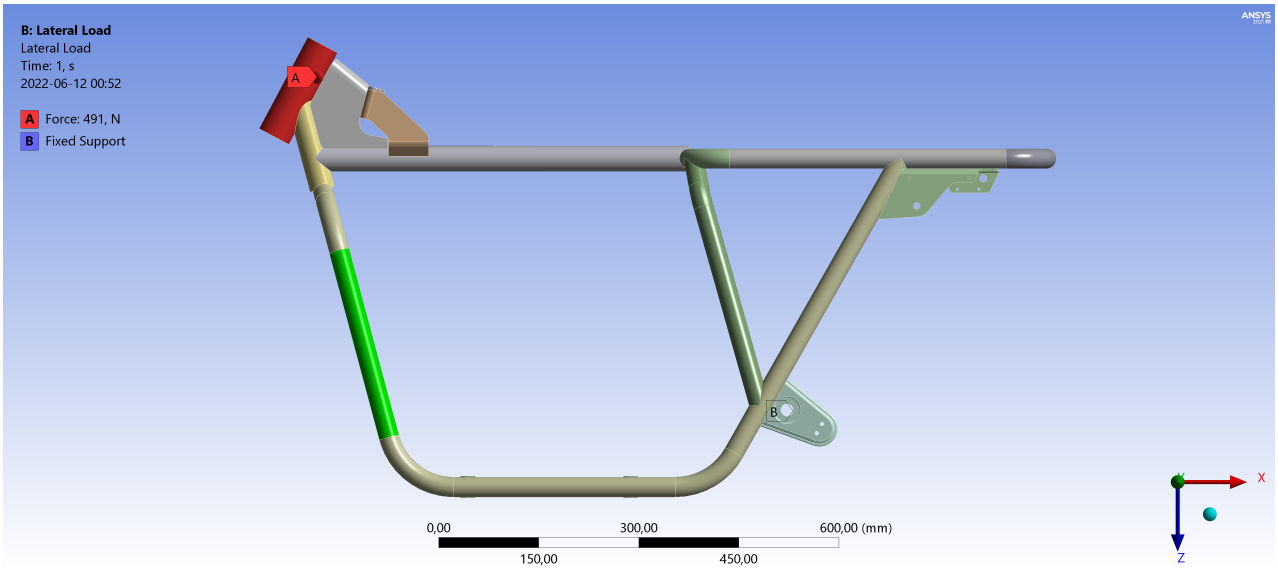

Figure 2.5: *Boundary conditions for the Lateral load case*

2.4.2 Load case - Torsional stiffness

To evaluate the torsional stiffness a torque is applied along the axis perpendicular to the steering axis pointing towards the swing brackets. The swing arm pivot point are fixed in space. As seen in figure 2.6

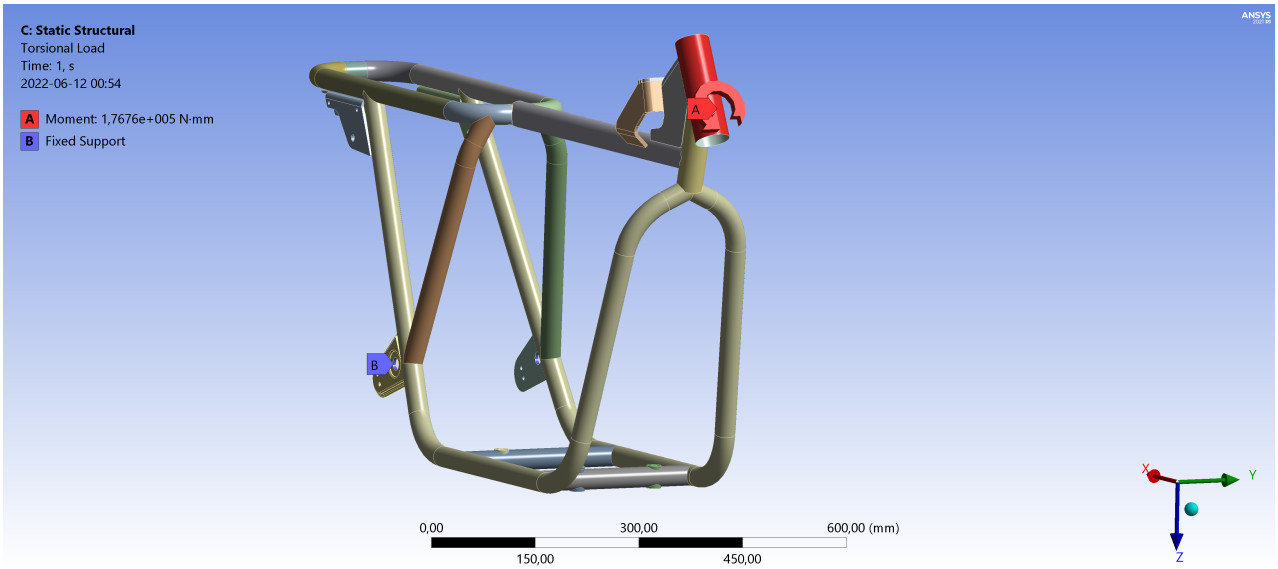

Figure 2.6: *Boundary conditions for the torsional load case*

2.4.3 Load case - Longitudinal stiffness

For the longitudinal simulation a remote force is applied where the center of the front wheel would be positioned acting with components both in x-direction, longitudinally and in z-direction, vertically. The force is applied on the steering head tube resulting in a torque around the y-axis replicating the characteristics of heavy braking as figure 2.7.

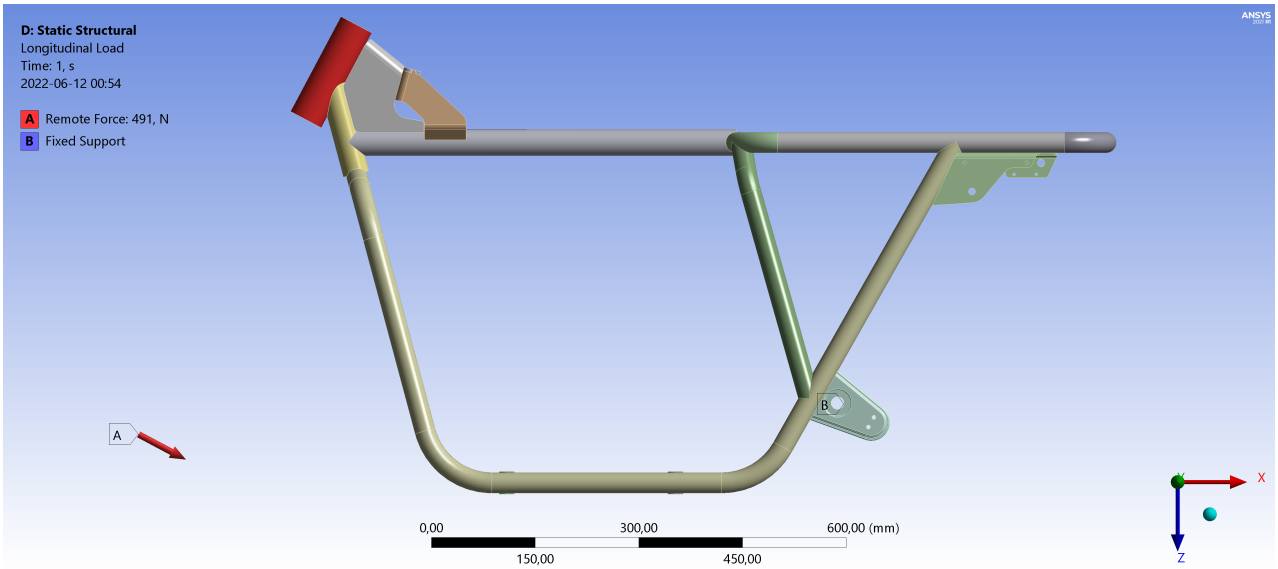

Figure 2.7: *Boundary conditions for the longitudinal load case*

2.5 Finite element method

The Finite Element Method (FEM) or Finite Element Analysis (FEA) is one of the most used tools in Computer Aided Engineering (CAE). It is a computational method that can be used for solving stress distributions through complex bodies, heat transfer in and between different bodies, flow simulations of different fluids and much more. It finds one its first traces in the 1940s with the publications 'Solution of problems of elasticity by the framework method' by Hrennikoff and 'Variational methods for the solutions of problems of equilibrium and vibrations' by Courant [4]. The name Finite Element Method was coined in 1960 in the publication 'The finite element method, in plane stress analysis' by R.W. Clough and have been kept since[4]. The first computer software using FEM was developed in 1965. That software later got to be the commercial software NASA Structural Analysis (Nastran).[4] In the 1970s more FEM software started to emerge and throughout the decades together with advancements in computer technology the software have gotten more and more advanced.[4]

2.5.1 Mesh

Before conducting a FEA firstly the geometry that is to be analysed needs to be translated into a mesh of points that captures the defining features. This mesh is made out of nodes connected into elements, which will be covered later. The mesh is automatically generated by the computer and software however the defining settings for the mesh needs to be addressed manually [4]. Generating a mesh is a trade-off between accuracy and computational time. An infinitesimally small mesh converges towards an exact solution while a gradually larger mesh reaches a less accurate solution at a faster pace. One way to address this trade off is to run several simulations with different mesh sizes and see if the solution converges within a set limit. Depending on the use case three different types of meshes can be used. A structured mesh has a constant size and shape over its entirety. A structured mesh is the least computational heave type since the connectivity of the mesh can be calculated instead of stored explicitly [4]. The disadvantage however is that the mesh is very bad at coping with complex geometries. Another option is to have an unstructured mesh. This mesh adapts to complexities in the model by reducing the mesh size around features in the geometry. This gives a much better model but at a much greater computational cost. The third sort is a hybrid between both structured and unstructured mesh. This is a compromise where areas of constant shape is given a structured mesh and details are more unstructured, in order to capture the details [4].

When looking at the quality of the mesh an ideal mesh consists of a compromise between accuracy and complexity. A highly detailed mesh will cost very much computational power and time compared to a rough. A far to rough mesh will however give far too inaccurate results that in an industrial application can have severe implications. The ideal mesh should therefore capture the details of the model, have as few elements as possible, gradually change in size over a sufficient distance and be as close to equiangular and equilateral as possible [4].

One way of testing if the mesh is of sufficient quality is to do a convergence study. It is done by running the same simulations with different levels of mesh. There are two main types of convergence testing; h-convergence and p-convergence[16]. In an h-convergence test the mesh size is repeatedly shrunk, leading to more nodes and a more computational heavy model. For every iteration the fluctuation in stress or deformation or the parameter of interest are traced to see if the model converges towards a value. When conducting a p-convergence test, instead of shrinking the mesh size the polynomial order of the mesh is increasing for every iteration. P-convergence testing is beneficial to use since it requires no verification steps for the user so it can usually run automatically by the FEM software[16]. When performing a mesh convergence test it is often not necessary to globally refine the mesh. It is most often only necessary to refine areas with high stress gradient. It is therefore common to perform non-uniform mesh refinements in order to achieve the highest precision for the lowest computational cost[16].

There is a risk when simulating with sharp corners. When simulating the first iteration i can show as particularly high levels of stress around sharp edges. If doing a convergence test it usually gets larger and larger, the finer the mesh. This is caused by a mathematical error in the model and it is causing a stress singularity. A stress

singularity is a mathematical error caused by having sharp edges in areas of significant stress. This leads to infinitely high amounts of stress, which will cause the convergence test to diverge.[16] Stress singularities does not make the entire model inaccurate but the maximum stress value will be wrong. To mitigate the risk of stress singularities it is wise to adjust the edge in the CAD model by adding a chamfer or a fillet. This is not unreasonable to add in a CAD model since in reality there is nothing like a perfect sharp corner. There will always be a rounded edge, albeit small[16].

2.5.2 Element types

There are different types of elements that can represent the geometry that should be analysed. They can be represented in 1 dimension, 2 dimensions or 3 dimensions, or 1D, 2D, 3D [20]. When a simple beam or truss is analysed a 1D element is suitable to use. 2D elements are normally used when there is a surface geometry that should be evaluated, and when the geometry is more complex and had more volume a 3D element is used.

A beam element, 1D, is useful when the geometry allows for it, for example a line or a curve[20]. The advantages of using beam elements is that the modelling and computational time is very fast. It is also easy to change the geometry very quick. For a beam you can specify a cross section and if that is not optimal you can change the assigned cross section and run the simulation again without having to redesign [26].

2D elements are often used for surface geometries, where the elements has triangle och quadrilateral as the shape. It is very useful to solve elasticity problems with a surface element [20]. The 2d elements are also versatile and useful when 1D elements are not sufficient. Compared to a 3D element the simulation time saved when not having to mesh a small thickness is significant [26].

For more complex geometries where the 1D and 2D elements can not capture the geometry in a representable way solid elements are used, 3D [20]. The 3D elements should only be used when the other types in not good enough. There is more detail captured in a 3D mesh but the computational power and time is increased. No matter which element types that are being considered the question is always, is there a significant enough gain to move to a more complex element type [26].

Once the dimension of the element has been determined there are different element types with different shapes and number of nodes like seen in figure **??**. For 1D, there are usually linear beam elements that are being used. For 2D and 3D there are a different types of elements, where the main shapes are triangular and quadratic elements [26]. Triangular elements tend to output a stiffer result compared to quadratic elements [20]. Both types of shapes can have different number of nodes that build up the element. The more nodes that the element have the more computationally heavy the simulation will be but can potentially capture more accuracy in the results [26].

3 Method

The aim of the thesis is to investigate and determine a method for the design process of a frame for a electric motorcycle and comparing a three different software in with increasing price and complexity levels, to get a smooth and reliable result. The different steps taken and factors evaluated will be covered in this chapter.

3.1 CAD Models

When conducting a finite element analysis, what is first needed is a mathematical model that interprets the actual part and describes it in a manor that is applicable to the analysis model. For simple geometries a mathematical model can be made using very few mathematical nodes connected in a simple point matrix, however the more complex the physical model gets the more complex the mathematical model needs to be in order to maintain accuracy when simulating. For this scope, describing the motorcycle frame as a point matrix is not feasible to do without the use of a Computer Aided Design (CAD) software. It is therefore a necessity for this purpose to begin with an as detailed as possible CAD model of the primary structure of the motorcycle frame to build the FE-Analysis upon.

As a part of the development of a methodology two different CAD software are compared in order to give a statement on suitability for RGNT. The used software are Autodesk Inventor Professional 2022 [1] and Autodesk Fusion 360 [2]. Those programs were chosen with both budget and current ecosystem used taken to account. The distinctive features of Autodesk Fusion 360 is that it is a web based program, leading to a convenient file storage system that enables multiple users to work on the same files simultaneously, aided by cloud computing which reduces the need och high performance computers. The advantage of using the Inventor program is a more competent CAD software with more advanced features for creating and working with more complex CAD models in a more accurate and efficient way.

For this application the most important parts to be featured in the CAD model are selected to be the main frame, swing arm connection brackets, top spring & damper brackets, reinforcement brackets surrounding the steering neck, battery box and the supporting brackets for the battery box, since these makes the primary structure of the motorcycle seen in *Figure 3.1.* The battery box with connecting brackets are included as an investigation if they can be regarded as stressed members of the frame and therefore serve a dual purpose both as a container for the batteries as well as a reinforcement for the structure.

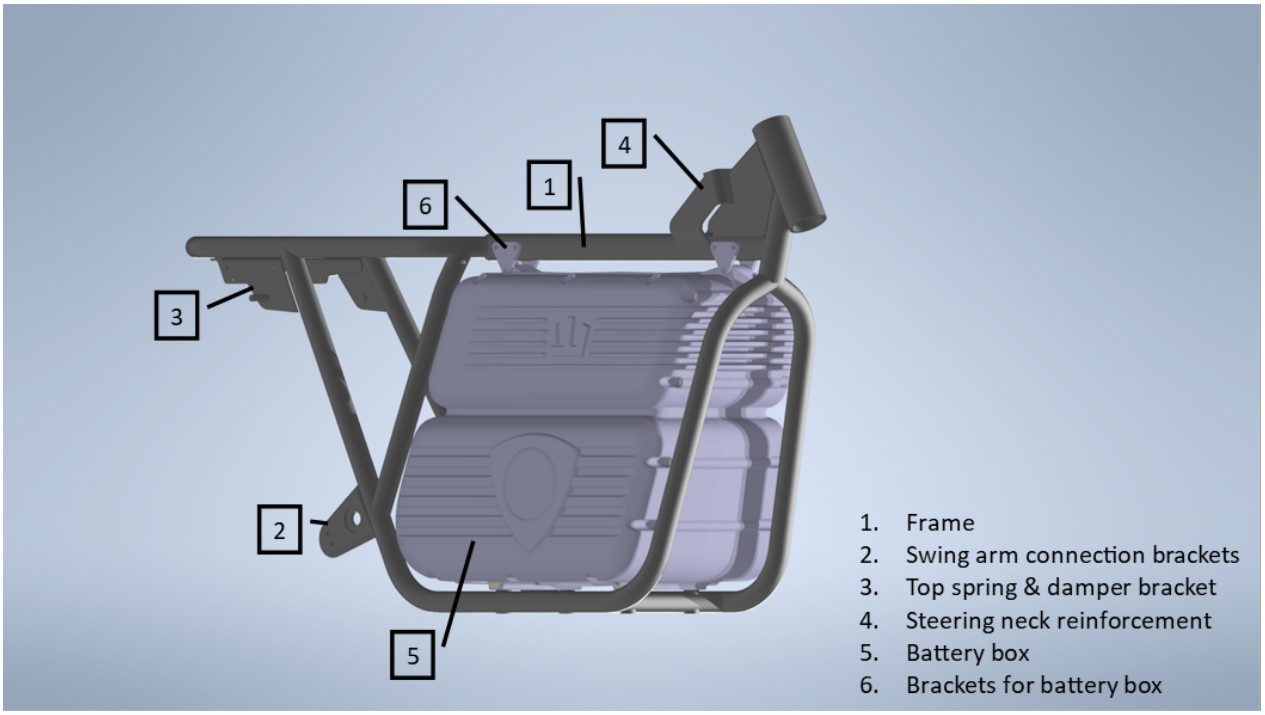

Figure 3.1: *CAD model of the motorcycle frame and battery box*

3.1.1 Frame

The existing CAD model of the motorcycle frame was made using mainly Autodesk Fusion 360. Some parts of the design was made using other CAD software and imported in a general file format. The main focus within previous development have not been to make the model suitable for FEA simulations, resulting in substantial issues when trying to simulate with the existing CAD model. As a consequence it was impossible to reach a continuous mesh for the FEM solver to calculate on. Therefore a new CAD model of the frame needed to be made to conduct the simulations on. The new model was made using the feature 'Frame generator' within the Autodesk Inventor Professional software. The dimensions and features of the CAD model was collected from the existing model together with drawings to exactly replicate it. The new model began as a 3D sketch in Inventor. All frame members were drawn as splines and constrained by both dimension and angles to important members and planes, as shown in *Figure 3.2*.

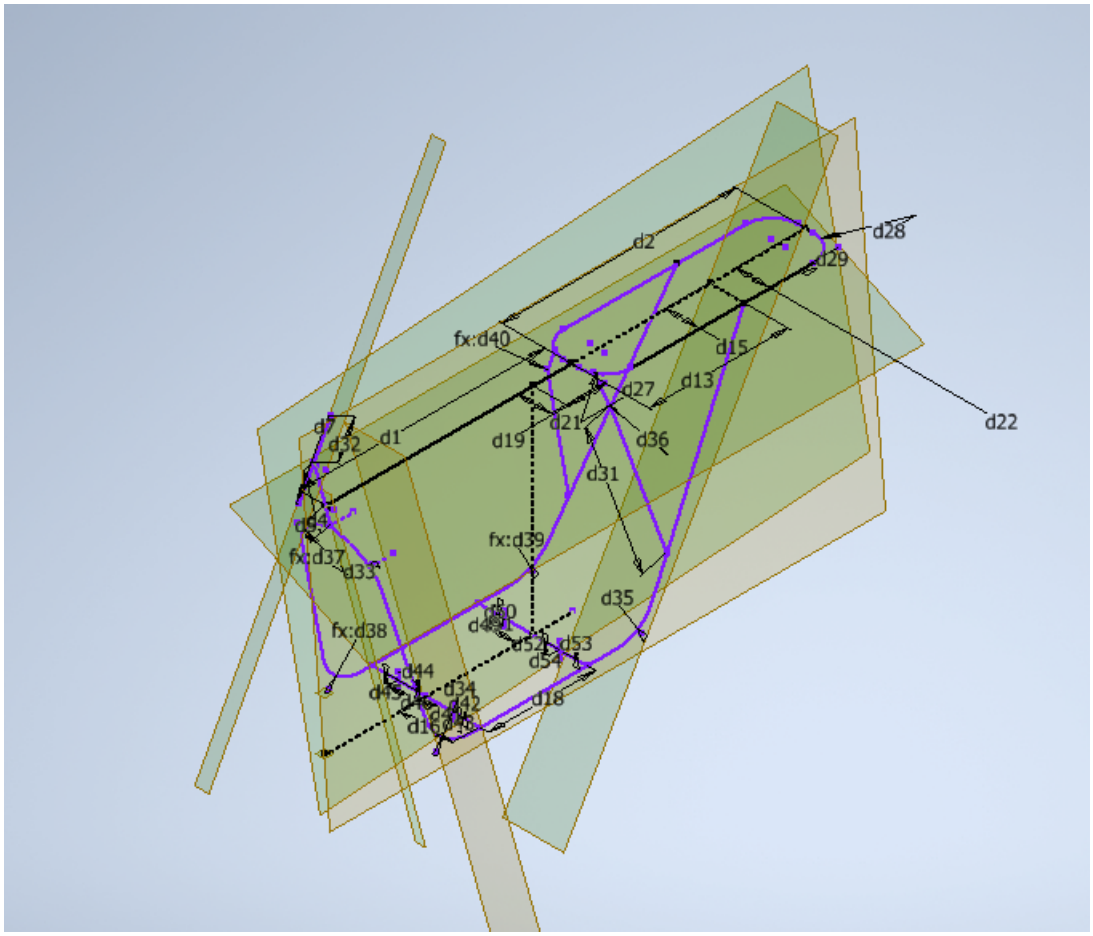

Figure 3.2: *3D sketch of the frame together with defining planes*

With the finished 3D sketch the frame generator tool was used to build a frame along the sketch elements. First all sketch nodes with the same cross sectional dimensions were marked. Cross sectional shape, material family and dimensions was selected according to existing model. The connection between the 3D sketch and the frame is illustrated in *Figure 3.3*

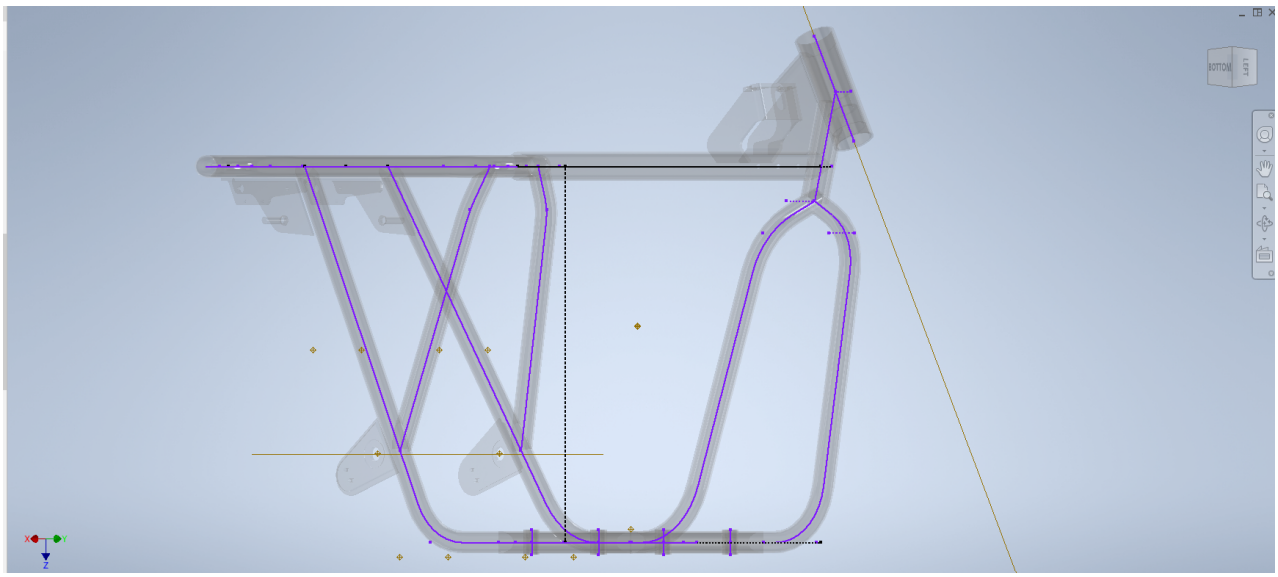

Figure 3.3: *Generated frame with defining sketch in blue*

The cross sectional properties of the members are matched with the existing model and added as an input to the frame generator shown in *Figure 3.4*

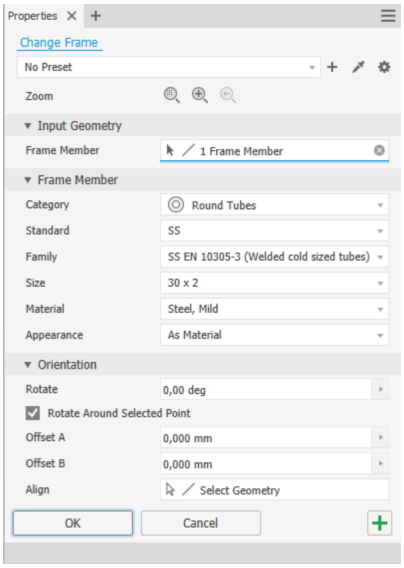

Figure 3.4: *Defining parameters for the frame generator*

When creating the frame as a sketch all intersections between frame members occurs on exact coordinates. This eliminates the risk of gaps in the model and minimises the manual work of connecting the individual members. The frame generator also allows for post processing on the frame to overlapping members. At the intersections between frame members, miter cuts and notches were added to the suitable members. This accurately represent the real frame while keeping the model suitable for analysis in FEM. Carry over parts were imported from the preexisting model and are constrained to the new frame, since these elements needs not to be remade. Mounting holes for the battery box attachment brackets were also added to the fame.

3.1.2 Battery box

Over its design phase the original battery box CAD file has been transported between numerous CAD software. This has resulted in a CAD file with no trace of the defining operations, making a simplification process more challenging. Due to it being one of more substantial part of the motorcycle both size wise and due to it replacing what normally would be the place of the engine in a conventional petrol powered motorcycle acting as a stressed member, the shape of the battery box have been heavily exposed to design. This makes the battery box inapt for FE analysis due to the complexity of the shape with following requirements of mesh resolution and computational power. To include it in the analysis it was first necessary to adapt the current battery box CAD to a simpler shape, while maintaining its mechanical properties. This was done by stretching defining surfaces of the box and patching them together to a geometrically similar shape without design details. This was done using Ansys Spaceclaim, the included CAD software within Ansys.

In Spaceclaim, the CAD model of the battery box was imported in the general CAD format STEP [13]. All exterior surfaces were marked and copied. The surfaces were then pasted and the original body hidden from the model. The surface representation of the box was then used as the foundation for creating shell elements, being surfaces without thickness. The original CAD model was kept as a reference to make sure that the simplified version still resembled the body and to be able to recover errors. With a combination of the embedded function blend, solidify missing faces and merge faces the patchy model of the box was connected to a complete surface model of a simplified battery box as shown in *Figure 3.5*. By striving towards minimising the amount of faces while maintaining the general shape of the actual part, an accurate representation of the defining shape of the battery box was reached.

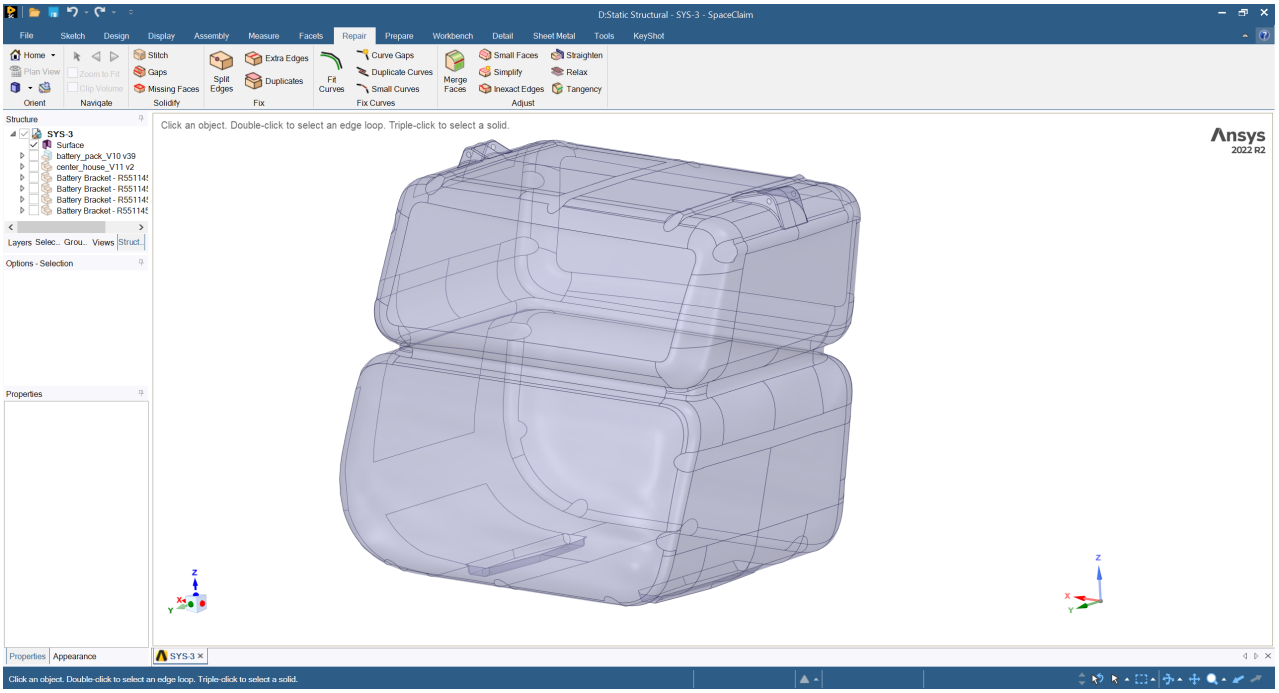

Figure 3.5: *Spaceclaim workbench for creating the battery box simplification*

3.1.3 Battery substitute

Due to the simplifications made to the CAD of the battery box when adapting it to the mesh another unknown is added to the correlations study. Since the battery box is not identical to the actual box on the motorcycle, differences between simulation and physical testing can be dependent on both the accuracy of the model and the simplification of the battery box. Therefore a substitute for the battery box was designed of which the aim was for the substitute to be easy to manufacture and easy to replicate in CAD to both simulate and test accurately. The battery substitute uses the same mounting points that exists for the original battery box, thus the forces that would be transferred in a representable way compared to the original application and act similarly and predictable. The battery substitute was triangulated between the mounting nodes on the frame to increase the stiffness of the whole assembly when mounted. With the battery substitute, tests could be performed to investigate how a stressed member affects the dynamics of the frame and if there is any noticeable benefits and something that should be continued to be used.

The main emphases was put on having the construction easy to replicate when manufacturing since differences between the CAD model and the physical part could lead to the distribution of forces being being different thus the result not correlating. The battery substitute was made from steel and welded together as one part, it was then mounted with fasteners in the frame similarly as the RGNT battery box would be mounted. With the battery substitute manufactured and mounted it could be tested physically and be compared to simulation results.

3.2 FEM Models

Figure 3.6: *Principal image of FEM simulation output*

As a part of developing a suitable methodology for analysing future frames for RGNT motorcycles, three different FEM software was used with different levels of complexity and capability. Testing these three software will give an understanding of the cost of choosing a cheap software compared to overpaying for a software far more advanced than the use case requires. The software will be evaluated on both user experience and accuracy compared to the physical tests.Correct material properties for the frame needed to be defined, all of the tubular frame are made of EN 10305-3 E355 grade steel, SS 2172 Ovako 520M grade steel on all sheet metal parts and SS355J2 steel on the steering head. The data for corresponding material was sourced through metal suppliers Tibnor [32] and Ovako[25]

Table 3.1: Material properties for the metals used in the frame

Name	Density $[Ton/mm^3]$	Youngs modulus $[MPa]$	Tensile limit $[MPa]$	Yield Limit $[MPa]$	Poisson's ratio ν
EN 10305-3 E355, SJ2172	$7.85 * 10^{-9}$	$2.1 * 10^5$	590	435	0.3
SS355J2, Ovako 520M	$7.8 * 10^{-9}$	$2.10 * 10^5$	470	345	0.3

3.2.1 Autodesk Inventor Nastran

Autodesk Inventor Nastran works as an add on to the Autodesk Inventor CAD software. This makes updating the CAD convenient, not needing to convert or export the model between software. while also enabling for modelling while designing to identify potential upgrades early on. The user interface is similar to the user experience of the CAD software in Inventor making the transition into the add on understandable and easy to work with in finding the different functions, shown in *Figure 3.7*.

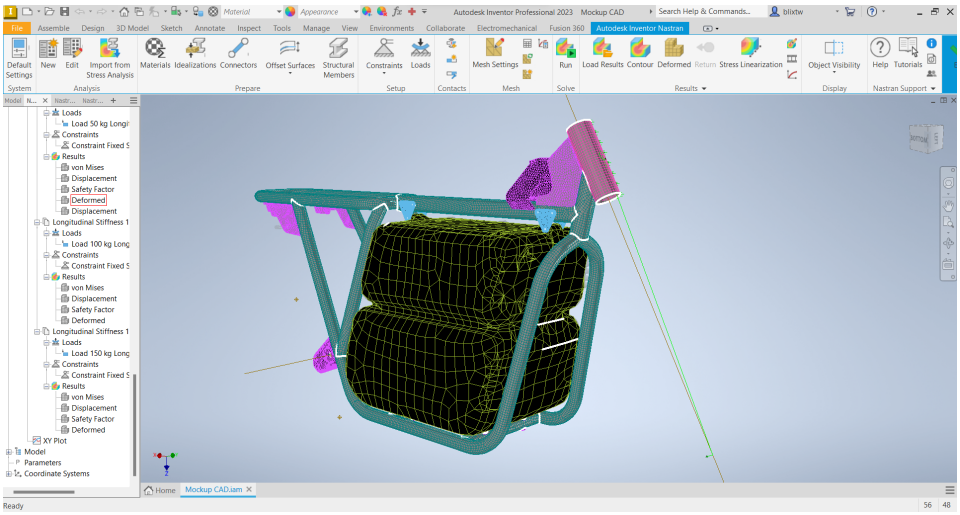

Figure 3.7: *Overview of the Inventor Nastran workspace*

When opening the Nastran workspace the first part was to set up the boundary conditions for the simulation. There is no need for a strict path to follow however it is wise to begin with creation of an idealisation of the model. This step will decide if the part will be simulated as beam-, shell- or solid elements, depending of the geometry. All tubular components of the frame are constant thickness and cross section. This enables the option of using beam or shell elements which reduces the amount of elements necessary to accurately describe the geometry and thus reduces compute time. If selecting beam elements, the cross section needs to be defined with shape and dimensions. If selecting shell elements only the thickness of the geometry is needed to be added since the outer surface of the geometry is used to define the shape.

The other parts of the frame, not consisting of tubular elements were defined as solids since they do not have a continuous thickness and does not have the same cross section.

All intersecting parts of the assembly needs to be connected. The contacts between all parts of the frame needs to be defined. Most modern FEM software includes automatic contact identifiers, Autodesk Inventor Nastran included. This however did not produce contacts that allowed for the model to solve, possibly due to the amount of different connecting parts. Therefore all contacts needed to be checked or redefined manually. All contacts connecting the parts of the frame were defined with an edge to surface condition. That created one set of contact points on the edge one of the selected tubes and connects it with the closest elements on the surface of the selected connecting tube.

The connections to the solid parts were connected using a surface to surface connection. This allowed for more connected elements on the edge since the mesh of the solid elements also spans through the thickness of the geometry.

The mesh settings were applied part wise in order to have the best trade off between computational accuracy and time according to *Table 3.2*

Table 3.2: Mesh properties for the different parts

Part	Mesh size [mm]	Mesh type	Mesh shape
Battery tube insert	3	Solid	Tetrahedral
Head Tube Gusset	8	Solid	Tetrahedral
Shock Absorber Bracket	8	Solid	Tetrahedral
Steering Lock Lower Bracket	5	Solid	Tetrahedral
Steering Lock Upper Bracket	5	Solid	Tetrahedral
Swing Bracket	5	Solid	Tetrahedral
Tubular frame	5	Shell	Quadrilateral

Improperly sized mesh will result in an either too stiff or too weak model and it is therefore important to gradually test smaller sizes of mesh to be certain that the mesh converges towards a certain amount of stress. The total amount of nodes from the meshing was 173 599. This is not a measure on the accuracy of the model but will give an indication on the computational load of the simulation.

Nastran does not embody any intuitive solution of displaying which contact conditions are to be considered as satisfactory so achieving a simulation that successfully runs without singularities in the stiffness matrix was an iterative process, composed of changing the pinball region of the contact condition together with altering the size of the mesh.

The process of adding both the battery box and battery substitute is similar. First the parts needs to be correctly constrained in the CAD part of Inventor, so that they are represented where intended in Nastran. Both bodies were represented as shell elements since the battery substitute consists of square tubes with a constant thickness and the battery box in reality can be described as close to constant thickness. It was tried to connect the boxes to the frame using bolted connections, which corresponds to a one dimensional beam with pretension to connect the bodies. This repeatedly resulted in a singularity in the stiffness matrix and a failed simulation. This could potentially be fixed by adding a separation contact between the connecting brackets and the frame to prevent the parts from penetrating each other. This is however not tested and verified. Instead the brackets were bonded together likely resulting in a stiffer connection than in reality.

3.2.2 Ansys Mechanical

The CAD models needs to be transferred to Ansys from the used CAD software. Although Ansys can utilise some add-on that allows it to convert most common CAD formats it is wise to use the generic CAD format STEP [13] to make sure that all geometry is included. First a static structural analysis was initialised within Ansys workbench. The CAD model was imported to geometry and the file was opened in spaceclaim, the included CAD software within Ansys. In spaceclaim the solid CAD model was converted into surfaces since shell elements are desired. This can be achieved either by selecting and copying the surfaces of the frame and replacing the solid parts when pasting or by defining the surfaces as midsurfaces. When generating midsurfaces the program defines an average thickness and applies it to the whole part selected and creates a corresponding surface at either the innermost surface, middle or outer surface of the part. It is also in Space Claim that CAD bodies not to be included in the analysis were suppressed in order to reduce the size of the model and thus save computing time. When finished in Space claim the model was opened in the modelling program within Ansys named model. The model program is similar in purpose as the Inventor Nastran environment, namely the pre-processor of the program. The material of the different parts were assigned using the same material data as in Nastran (*Table 3.1*The standard mesh size was set to 5 mm. Comparing with Inventor Nastran, Ansys manages to auto mesh to a satisfactory result using only that setting together with quadratic order of elements, generating mid side nodes between all elements. However in the same manor that Inventor Nastran did not succeed in generating automatic contacts Ansys also needed for the contacts to be defined manually for the model to solve. The same approach was applied here. All parts in immediate contact were covered by the bonded constrain where all mesh nodes at the end of the connecting tube were bonded to the surface of the other connected tube. All parts that are connected with a gap between were connected using an offset bonded contact. One key advantage of the Ansys post processor is that all contacts can be visualised to give a picture on how well the contacts are defined, as shown in *Figure 3.8* below.

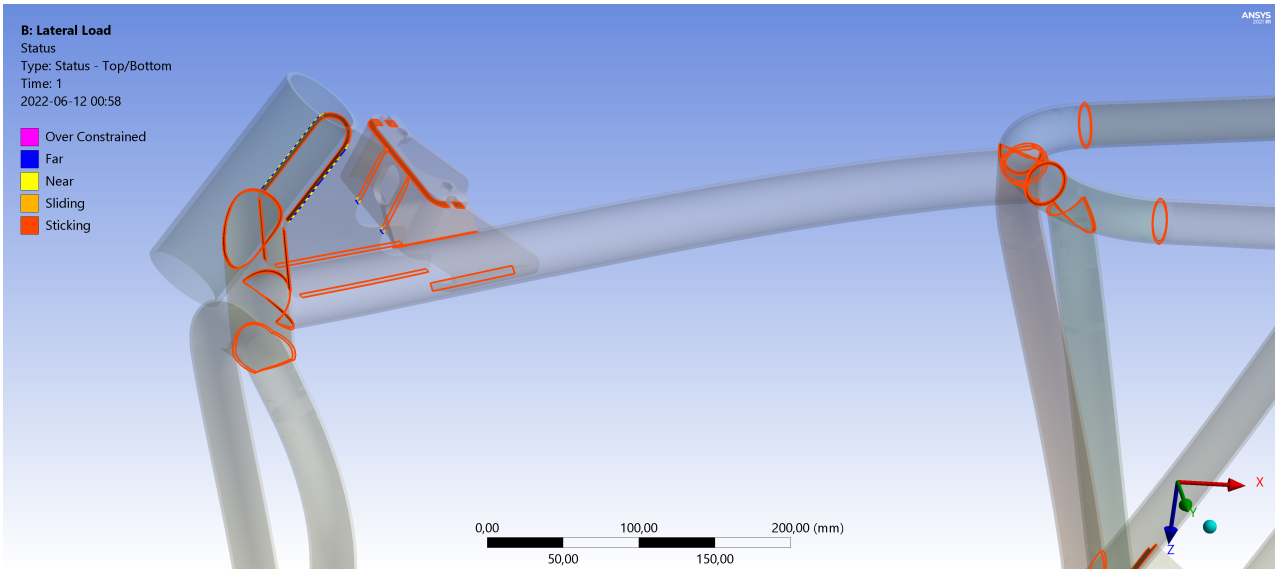

Figure 3.8: *Contacts visualised between the different parts around the head of the frame. Red areas are defined as bonded. Yellow and gradually blue means that the contact is gradually weaker.*

In order to track the results of the simulation remote points were added to particular areas of interest that can easily be found and compared when making the physical tests. These points were governed by displacement probes, meaning that the values of the displacement of that particular node of interest was saved. One beneficial feature within the Ansys software is the possibility conducting a parametric study. This allows for different values of input and corresponding effects on the output to be tracked and tabulated for more efficient use of time. The input loads were divided in steps of 491 N between 491 N to 1964 N with the corresponding torques and load components for the different load cases. This makes the process of confirming linear behaviour of the model and is used while comparing to the physical testing.

An important step when conducting FEM simulations is to make sure that the size of the mesh does not affect the result of the simulations. One way of doing this analyses is by making repeated simulations with differing mesh sizes and comparing the results of the analysis. This was appropriately done in Ansys by using the parameterised input tool allowing for repeated simulations with controlled parameters to be altered, while keeping all other aspects constant. A similar tool for measuring convergence was not found in neither Inventor Nastran or Fusion 360, so the derived suitable mesh size found in Ansys were used for those software as well. The chosen mesh sizes for the simulation are 15, 10, 7, 5, 4, 3 $[mm]$

3.2.3 Autodesk Fusion 360

In Autodesk Fusion 360 the simulation workbench is similarly to Inventor an extra add on to the main CAD software. That means that adaptations to the CAD model are equally simple to implement as in Inventor, as long as the original CAD model is made in Fusion 360. The user interface is logical and simple to use shown in *Figure 3.9.*

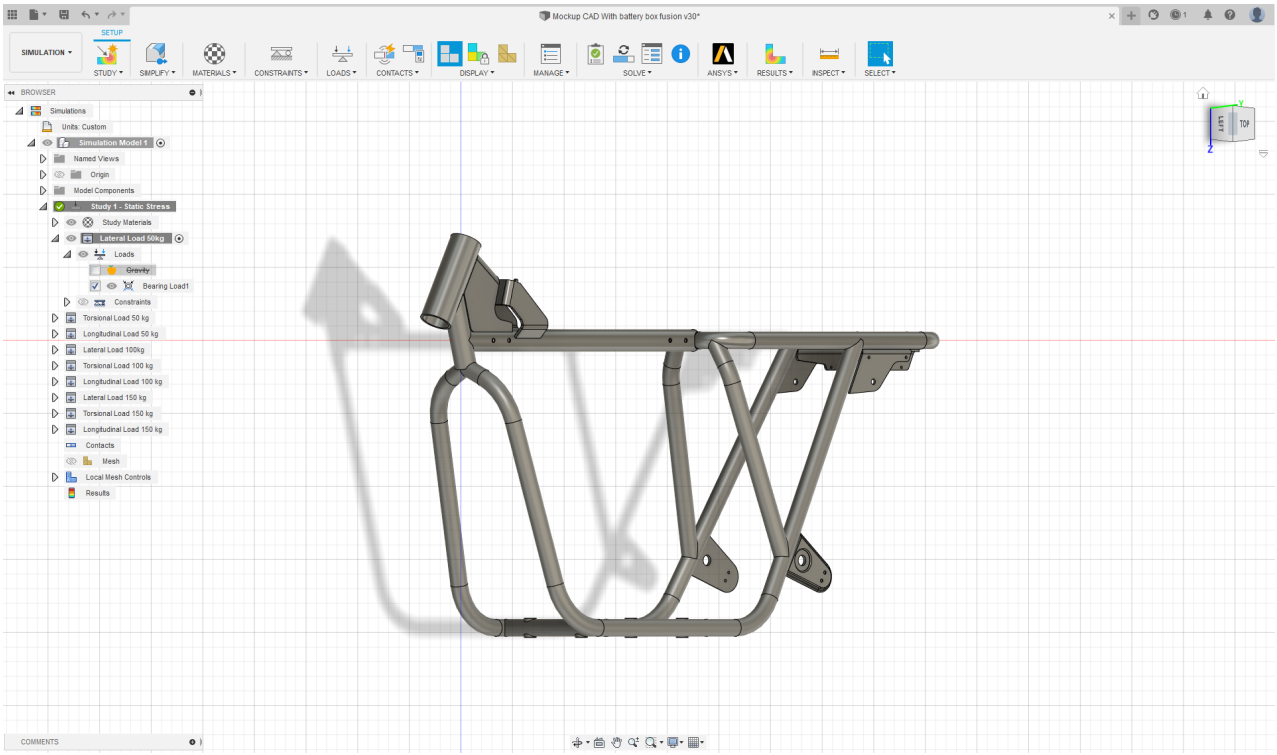

Figure 3.9: *User interface within the simulations workspace of Fusion 360*

The user interface contains the most fundamental elements of a FEM pre-processor GUI. The main features are divided in sub-categories with specifics hidden within. The first step was to apply the material properties according to *Table 3.1.* This was done within the 'Materials' menu, where the exact properties were added as a manual entry and applied to the corresponding parts. Next step was to apply the correct boundary conditions by setting constraints. The swing brackets were fixed in all degrees of freedom from the constraints menu. The following step was to apply a load corresponding to the load cases defined. Multiple load cases were added for a staggered simulation outputting multiple answers instead of manually running every load case one at the time. Next step was to define the contacts between the nodes of the frame and the accessory parts that in reality are welded to the frame. There is an option of automatic contact definition done by the program. For this simulation all contacts were manually assigned since the automatic tool produced an unsuitable result. All parts in direct contact are defined with a bonded connection. Parts with some gap that in the real frame are connected are applied with an offset bonded connection.

The last step was to generate a mesh. This is the part where Fusion 360 lacks the most amount of control compared with the other programs. Since Fusion is only capable of producing 3 dimensional mesh elements the mesh size needs to be substantially smaller in order to not produce an overly stiff model.

When simulating there is an option of defining a fixed mesh size however this also applies to all parts of the frame, meaning that there is no option of having different sizing of the different parts The mesh size was selected to be at roughly 3 % of the model base, as a trade off between compute time and feasibility shown in *Figure 3.10.*

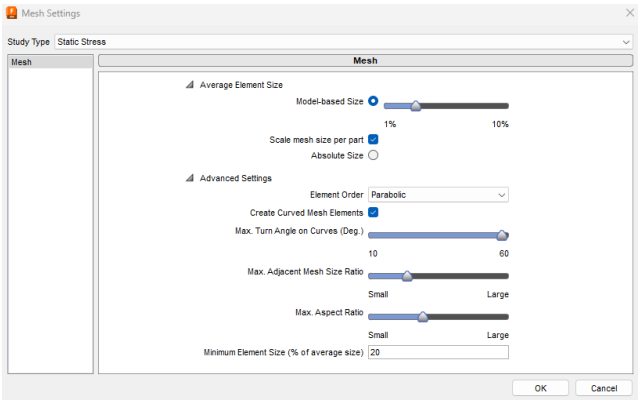

Figure 3.10: *User interface for setting up mesh parameters*

2nd order elements were selected, named parabolic in this suite, to improve accuracy over curved parts. Fusion 360 gives the option of convergence testing the mesh and it is set for a target of 5 % mesh convergence. This generated 1 135 109 nodes, which is roughly 6 times as many as generated with shell elements in Inventor Nastran and is presented in *Figure 3.11*.

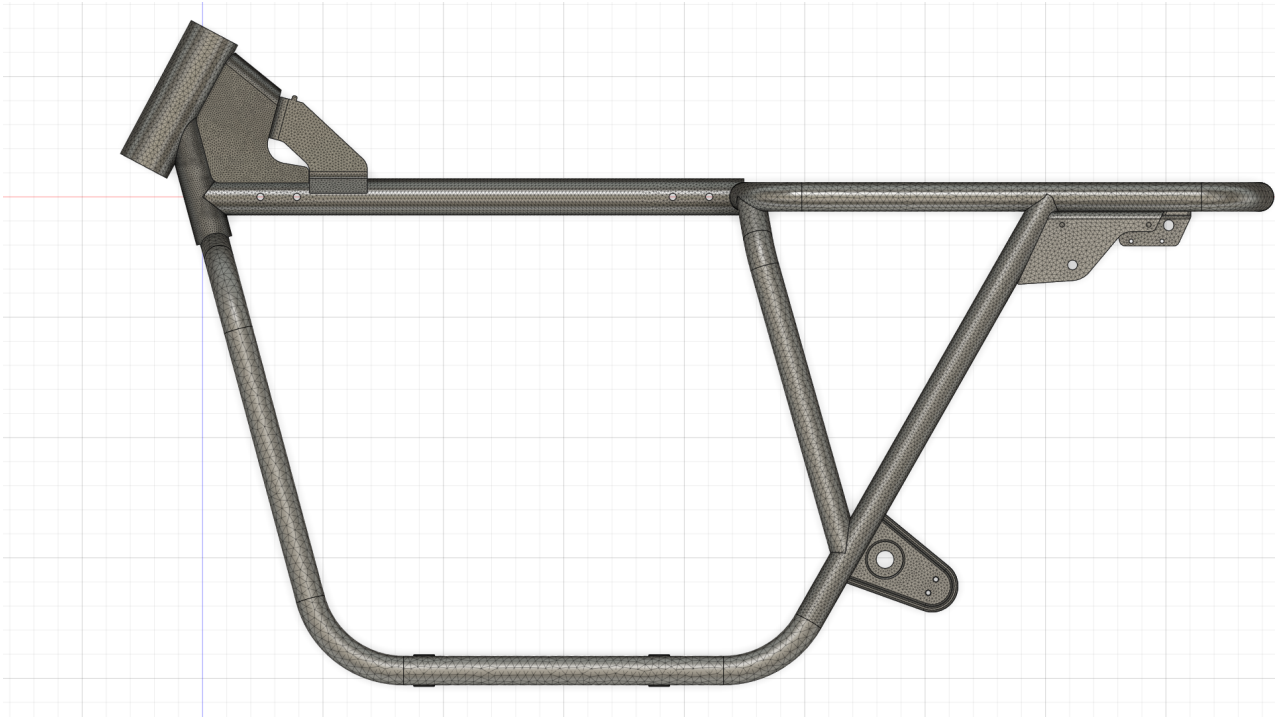

Figure 3.11: *Mesh produced in Fusion 360*

3.3 Physical Testing

To correlate the simulations of the frame with the manufactured frame, physical testing was done for a few selected load cases. The load cases that where of interest to test where lateral loading and torsional loading. The selected load cases where well defined in Motorcycle Dynamics Vittore Cossalter [7] with reference values of stiffness for 1000 cc sport bikes. As mentioned previously, sport bikes usually have a Twin-Spar frame which is designed with the main objective to withstand lateral and torsional deformation to a greater extent than most other types of frame including the tubular frame of which the analysis concerns, thus the reference values in [7] is merely an indication of relative stiffness rather than an absolute value to be met. The aim of the tests is to correlate the stiffness of the frame by measuring the deflection with a known load applied according to [7].

3.3.1 Construction of test rig

A test rig was constructed to allow for testing the lateral and torsional load cases on the motorcycle frame. Requirements that were stated for the test rig was that is should be small so that it does not take up to much space, be modular to allow for test on different motorcycle frames for comparison, and be cheap and easy to manufacture.

This was done by having the frame tilted on its side according to *Figure 3.12*. The centre beams of the test rig are the mounting point for the frame and is what holds the test rig together with a bolted connection. When different frames with different dimension are being tested the spacing between the centre beams can be adjusted to fit more frames than the one considered in this study. The test rig can also be stored away taken apart and thus not take up much space when not in use. The side pieces of are made of 50x50 mm square steel profile with a wall thickness of 2 mm and welded together. The centre beams are 50x50 mm solid steel beams which also hold the solid steel shaft which the frame is attached to. The base of the test rig is fixed and load is applied to the steering head with a car jack. The load is measured with a load cell and the deflection of the frame is measured with a dial indicator.

Figure 3.12: *Overview of test rig*

3.3.2 Measuring equipment

The test were aimed to be simple, repeatable and reproducible to allow for tests on different and future frames. These test will not be a part of the day to day operation for RGNT but rather something that can be done when required to ensure quality and test other frames. Therefore the equipment and testing procedure were formed so that the test can be done with already existing equipment. The lead time and automation requirements where not of high priority. The main strength of the rig is comparative studies. Either with another completely different frame or to evaluate improvements and updates.

The equipment used for measuring the deformation of the frame and flex of the test rig was two different types of dial indicators which measures the deflection in mm with a resolution of 0,01 mm. The specifications of the dial indicators can be found in the data sheet in [19] & [18]. To apply load to the frame car jacks were used, both a hydraulic and a scissor jack was used as in *Figure 3.13 & 3.14*. The scissor jack was used for the lateral loading test and the hydraulic jack was used for the torsional loading test. The hydraulic jack could put more force on the frame during the test but it could not hold the force steadily which meant that the step size of the force was required to be larger. The scissor jack however could be more precise on the applied load which meant that the interval could be smaller. The method of loading however, can be arbitrary since the load which is being applied is measured by a load cell which output the load in kilograms with a resolution of 0,01 kg. The load cell is controlled by an Arduino controller board.

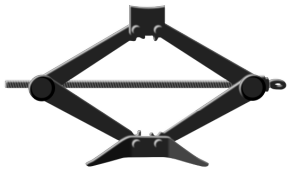

Figure 3.13: *Scissorjack*

Figure 3.14: *Hydraulic jack*

3.3.3 Flex of test rig

In the Finite element analysis software, the support of how the frame is constrained is ideal which is not the case in reality. Both the test rig and the fixation of how the frame is attached to the test rig will flex and deform when load is applied which will produce non representative data of the actual frame deflection. To obtain the correct values of the deflection of a applied load, the flex of the test rig and the attachment of the frame was measured. The frame and test rig was measured on multiple locations with dial indicator to be able to identify the unwanted flex and thus subtract it from the deflection of the frame. The locations of where the dial indicator were placed are shown in *Figure 3.15*.

Figure 3.15: *Placement of dial indicator for test rig flex measurement*

To determine how the flex of the test rig affects the measurements of deflection of the frame the test rig was measured at several positions to obtain better understanding of its behaviour when loaded. This showed that the vertical beam of the test rig was rotating around its most bottom point from which the relation between test rig flex and its effect on frame deformation measurement could be determined according to *Equation 3.1* from *Figure 3.16*

$$d_1 = \frac{d_2 \cdot H_1}{H_2} \tag{3.1}$$

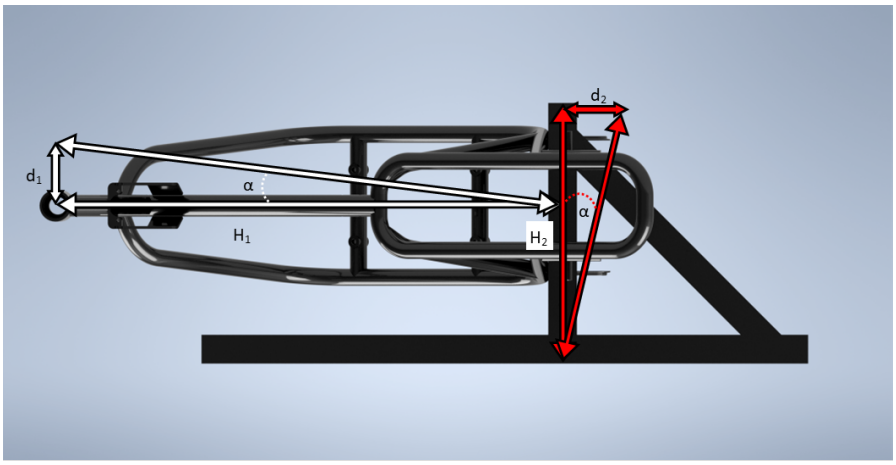

Figure 3.16: *Figure explaining the variables for the equation*

3.3.4 Testing procedure

Before the testing can begin there are some preparation that must be conducted. The preparation and the testing procedure is similar to test both lateral and torsional test, the placement of the load cell, jack and the dial indicator however will be different.

Preparation

First the test rig must be mounted to the solid steel table using the bolted claps according to *Figure 3.17*. Once the test rig is securely mounted, the frame can be attached to the test rig with the corresponding shaft. If the tests are conducted on a frame with a different diameter on the swing mounting, the shaft can be changed

to secure the frame of interest. When the frame and test rig is mounted and fastened, the load cell and jack can be put in place depending on which test that is being conducted.

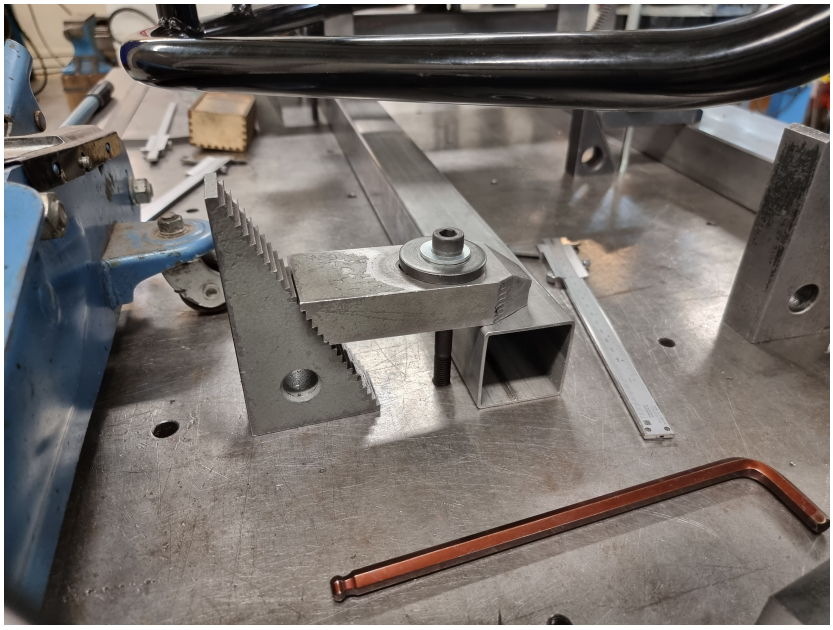

Figure 3.17: *Mounting of test rig*

Lateral test

When the lateral test is being conducted the jack load cell and dial indicator should be placed according to *Figure 3.18*. To know the placement of the dial indicator is important so that this position can be probed in the FEM software when correlating. The placement of the dial indicator was derived from the FEM analysis, it should be a point that is easy to locate and measure. For the lateral test the dial indicator was placed as shown in *Figure 3.18*.

Figure 3.18: *Placement of dial indicator for lateral test*

Torsional test

The torsional test require additional pieces of the test rig to capture torsion and not lateral deformation of the frame. The first part is the pivot which is placed according to *Figure 3.19*. This pivot acts as the rotational point according to the reference case in chapter 2.4 Load Case. This point should be perpendicular to the attachment point of the swing to satisfy the reference case and thus be the same as the FEM software is simulating. The second part which is needed is a shaft that goes through the steering head where the jack and load cell is acting upon. This shaft allows the vertical force from the jack to transform to a torque acting on the frame according to *Figure 3.19*. The jack should be placed on a known distance to calculate the acting torque. The placement of the dial indicator varies on the torsional test compared to the lateral since the frame will deflect in a different manner, thus the dial indicators were placed as shown in *Figure 3.19*

Preload

Before the test and data collection can begin, the frame must be preloaded to eliminate any play that might exist from manufacturing tolerances. The force required to eliminate any play will be different for different frames and its corresponding shaft for attachment. To determine the preload force the dial indicator were placed and zeroed. Then the frame was loaded with an interval of 50 N and the deformation displayed by the dial indicator noted for each interval. When the data was compiled and plotted the preload force could be determined when the graph showed linearity. With the known preload force applied the setup is complete.

Testing procedure

Once the test rig and frame is mounted, and the frame preloaded, the dial indicator can be zeroed and the test begin. The load on the frame was increased with a step size of 100 N until the frame had deflected 20 mm which was the the maximum stroke of the dial indicator. When the deflection had reached about 20 mm the load was decreased with step size of 100 N until the load was back to the preload force. For each step the load and and deflection was noted. The test were conducted multiple times with completely unloading the frame and reapplying the preload and repositioning the dial indicators.

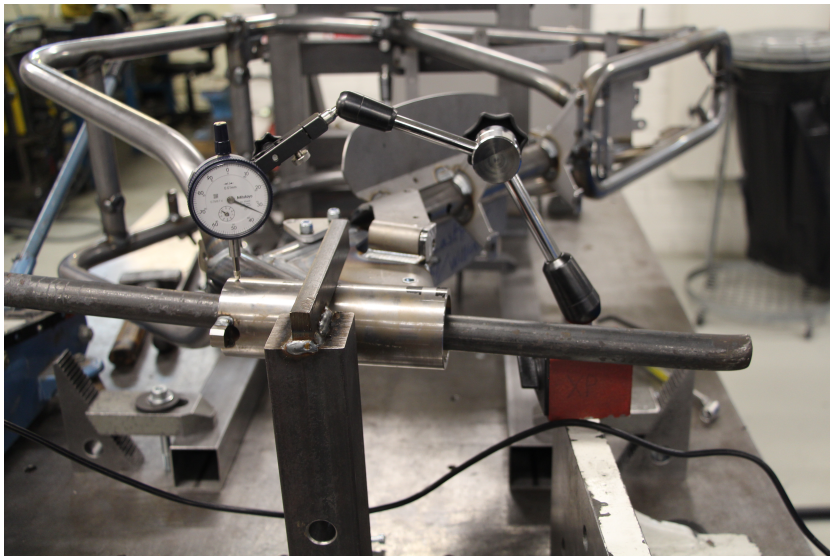

Figure 3.19: *Placement of the pivot*

Data Processing

The collected data must be processed from applied load and deformation before it can be translated into frame stiffness. Both the deformation of the frame and the applied load are not representative as they are as raw data. The measured deformation at the steering head has been distorted by the flex of the test rig, thus this must be adjusted for proper data. Since we apply a preload this must also be taken in to consideration for a representative result. If these factors are not considered the correlation between the physical testing and the finite element analysis will be greatly affected.

As previously mentioned the stiffness are defined in different ways for the different load cases. Since the test does not measure the rotation of the frame and the corresponding stiffness is in N/deg, *Equation 3.2* is used to convert the deflection data to rotation.

$$rot = \arctan(\frac{deflection[mm]}{L[mm]}) \tag{3.2}$$

Where the deflection is the measured value from the test and the L is the leverage arm from the pivot point to the dial indicator as seen in *figure* 3.19. Once the data for each of the tests where compiled and transformed the data points could be plotted and a linear curve was fitted to the points. The inclination of the graph gives the stiffness. Extracting the stiffness this way means that the preload force can be disregarded since the curve fitting is done with the delta between the points. This way any outliers in the data will not skew the result, moreover the behaviour is expected to be linear which also will be enlightened in the result.

4 Results

In this chapter the results will be presented. This includes the result for the CAD design, simulation and how the different software compare, testing, and the correlation between the two. Different cases and element types are compared as well as the capabilities of the different software.

4.1 CAD Model

The CAD model is existing in its entirety within an assembly to be used in Inventor. All different parts are included in the file in order to include the different models without the need of opening and maintaining different assemblies illustrated in *Figure 4.1*. The result of each entity of the assembly follows.

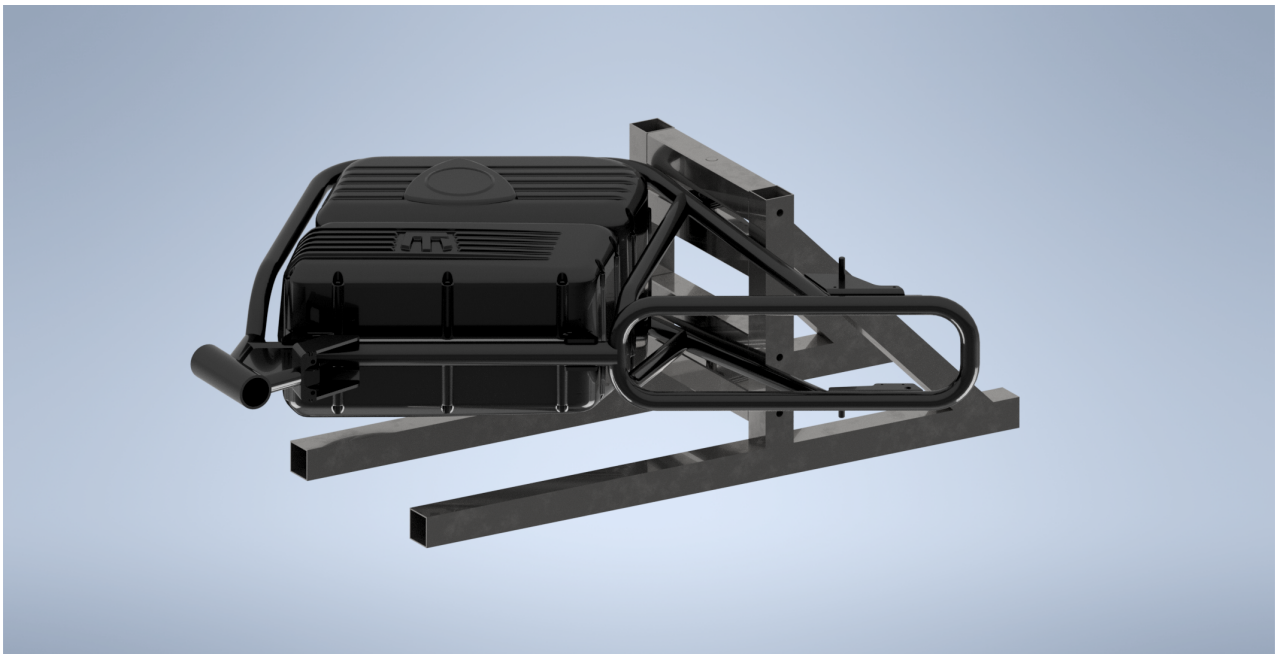

Figure 4.1: *Overview of the frame mounted in the test rig*

4.1.1 Frame

The replacement model of the frame shown in *Figure 4.2* are made using the built in functionality frame generator within Autodesk Inventor Professional 2022. It is made up from a 3D sketch of all the frame nodes and then assigned a cross section in the tool. Defining features from the pre-existing CAD model are imported and placed accordingly to replicate the finished motorcycle frame.

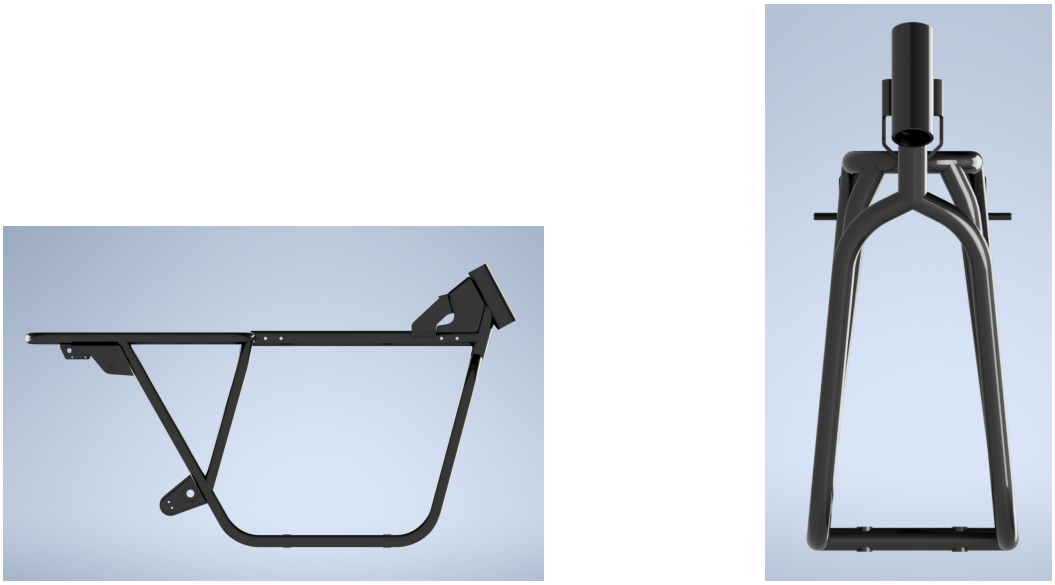

(a) *Side view*

(b) *Front view*

Figure 4.2: *The new CAD model of the frame*

4.1.2 Battery box

The surface model of the battery box are made using Spaceclaim. It is a more simple outline of the actual model that is adapted to better be used in a simulation, while keeping the defining geometrical features of the actual part. In *Figure 4.3* The two top pictures shows a rendering of the surface model and the bottom two pictures shows the pre-existing CAD model.

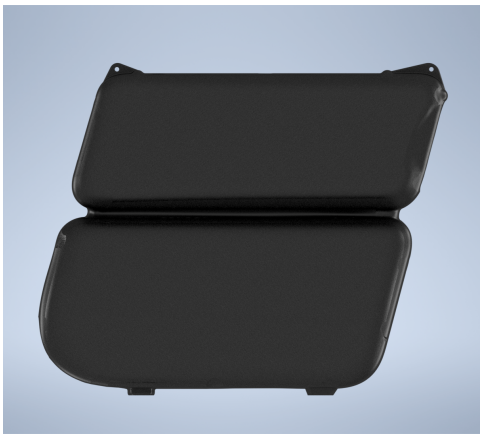

(a) *Side view of the replacement model*

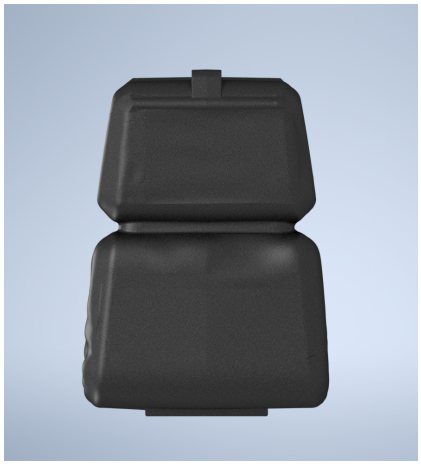

(b) *Front view of the replacement model*

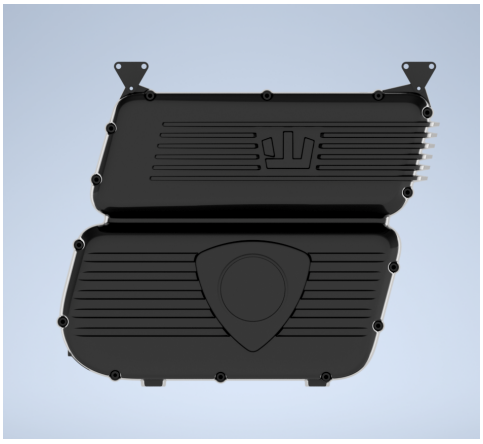

(c) *Side view of the original model*

(d) *Front view of the original model*

Figure 4.3: *Surface model of the battery box in comparison with the original*

4.1.3 Battery substitute

The battery substitute was manufactured and mounted in the frame and the test result could be compared to the simulation results. Because of how the mounting points were designed on the frame it is hard to create stiffness from it in other ways than the xz-plane of the motorcycle. The mounting points in the frame was sub optimal and not complete as in production which meant that there is a uncertainty connected with the test with the battery substitute. In *Figure 4.4* the top two pictures shows the replacement frame of the battery box and the two bottom pictures shows the frame together with the motorcycle frame.

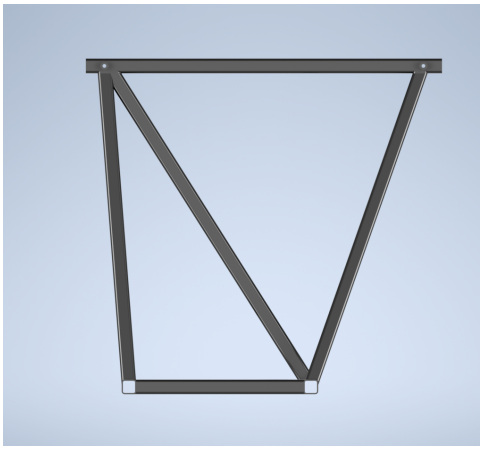

(a) *Side view of the battery substitute*

(b) *Front view of the battery substitute*

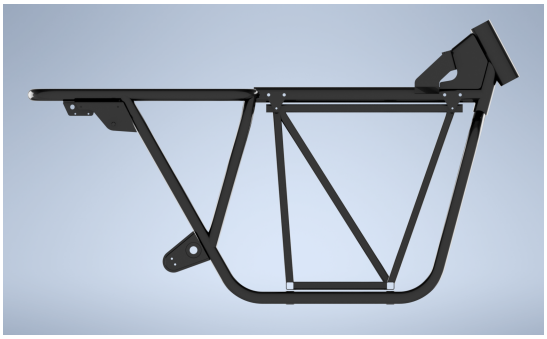

(c) *Side view of the frame with battery substitute*

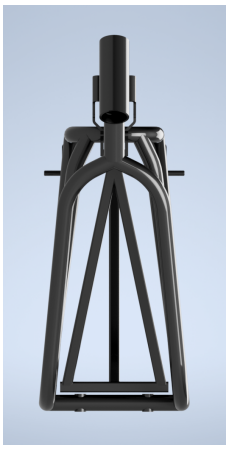

(d) *Front view of the frame with battery substitute*

Figure 4.4: *Battery substitute*

4.2 FEM Models

The results of the FEM analysis will be presented in this section. Validation of the mesh, results from each load case and the effect of a stressed member will be covered in the analysis of the FEM results.

4.2.1 Mesh Convergence

For each load case, the mesh was validated by running a mesh convergence analysis to capture a detailed enough result while not being to inefficient and taking to much processing time. The mesh size was started with 15 mm and going down in step size until the error was within a reasonable error. As can be seen in *Table 4.1* the error is small, thus convergence has been met. Finally the mesh size chosen was 5 mm since the convergence was deemed okay. The mesh convergence study in *Table 4.1* was done in Ansys Mechanical since that was the only software of the ones tested that had the functionality to do a parameterised study of mesh convergence. From a user experience and time efficiency point of view Autodesk Inventor Nastran and Fusion 360 was lacking in this regard since you would have to do the study manually and thereby having to spend more time and effort. A quick validation of the mesh was done in both Nastran and Fusion 360 based on the results in Ansys Mechanical to determine a reliable result.

Table 4.1: Mesh convergence analysis in Ansys Mechanical

Mesh Size	Deformation Lateral		Deformation Torsional		Deformation Longitudinal	
mm	mm	Delta	mm	Delta	mm	Delta
15	4,397	0	0,718	0	2,742	0
10	4,314	1,88%	0,670	6,56%	2,625	4,25%
7	4,303	0,26%	0,667	0,54%	2,602	0,88%
5	4,205	2,28%	0,681	-2,06%	2,642	-1,53%
4	4,225	-0,48%	0,727	-6,77%	2,697	-2,08%
3	4,195	0,69%	0,694	4,54%	2,618	2,93%

4.2.2 Lateral Load-case

The Lateral load case was simulated using an applied load of 491 N at the bearing surfaces on the steering neck. The Load was simulated using shell elements in Ansys and Nastran, beam elements in Nastran and solid elements in Fusion 360. The stiffness is calculated by dividing the force with the maximum displacement of the frame according to *Equation 4.1.* The result from the simulation in Ansys are shown in *Figure 4.5.*

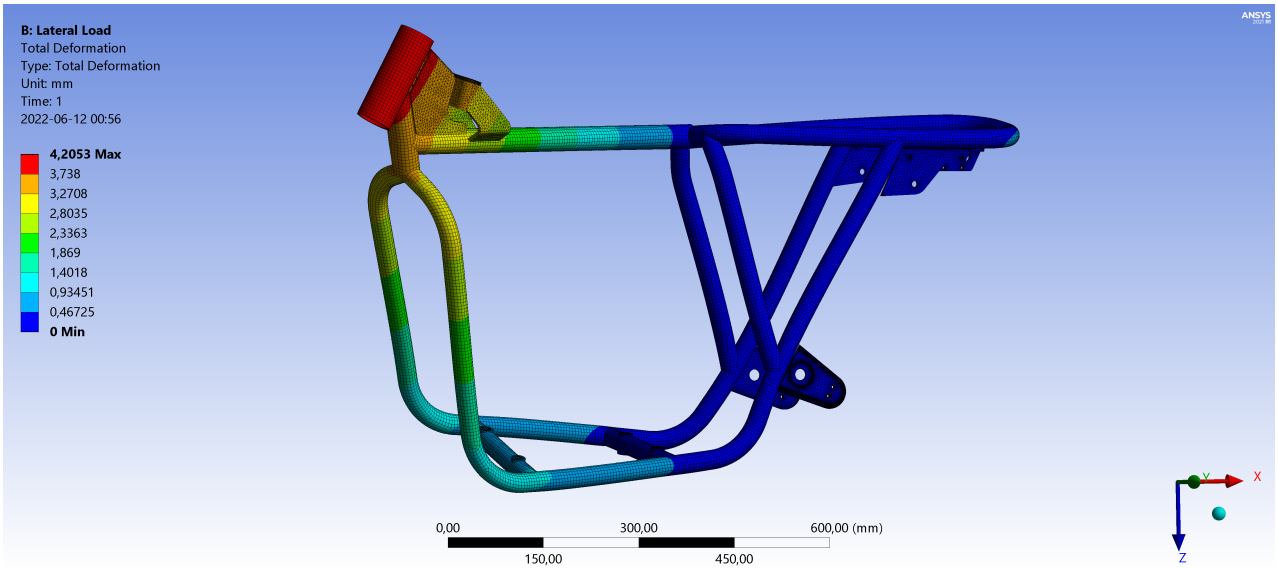

Figure 4.5: *Deformation from a load of 491 N simulated using shell elements in Ansys*

$$k = \frac{F}{\delta} \tag{4.1}$$

The different simulated stiffness values are presented in *Table 4.2* below with a description on the included components, element types and software

Table 4.2: Lateral

Stiffness [N/mm]	**Software**	**Element type**	**Component**
127,76	Nastran	Shell (2D)	Frame
126,91	Nastan	Beam (1D)	Frame
122,17	Ansys	Shell (2D)	Frame
275,84	Fusion 360	Solid (3D)	Frame

The resulting values of stiffness indicates that Nastran and Ansys produce results within a 5% margin. The simulations in Fusion 360 differs from the other software with 125%, which is significant.Presented in *Appendix A.1* are the simulation plots for the lateral load case where the colour map shows the magnitude of displacement

for the frame. The different software uses different methods regarding the distribution of the colour map and the order of magnitude for the visualisation of the displacement hence the slight variance in how the plots looks in the different programs. In general it is clear that all software manages to show similar trends in where the displacement occurs, which points towards a convergence in results when comparing the simulations.

4.2.3 Torsional Load-case

In the torsional load case a torque $[M]$ of $176Nm$ was applied on the steering head at the point on the steering axis perpendicular to an axis connecting the swing arm pivot point. The results are presented as a stiffness $[k]$ by dividing the force with the rotation about the axis of applied rotation. The output from the simulations are described in displacement of the nodes. The simulation plots from Ansys are presented in *Figure 4.6* To connect this to degrees of rotation it needs to be converted according to equation 4.3 where δ_{dist} corresponds to the distance between the point of applied torque and the point of measurement in the physical testing. δ_{ymax} is the distance that the measured node displaces along the y-axis.

$$\delta_{dist} = 37.5[mm] \tag{4.2}$$

$$k = \frac{M}{atan(\frac{\delta_{ymax}}{\delta_{dist}})} \tag{4.3}$$

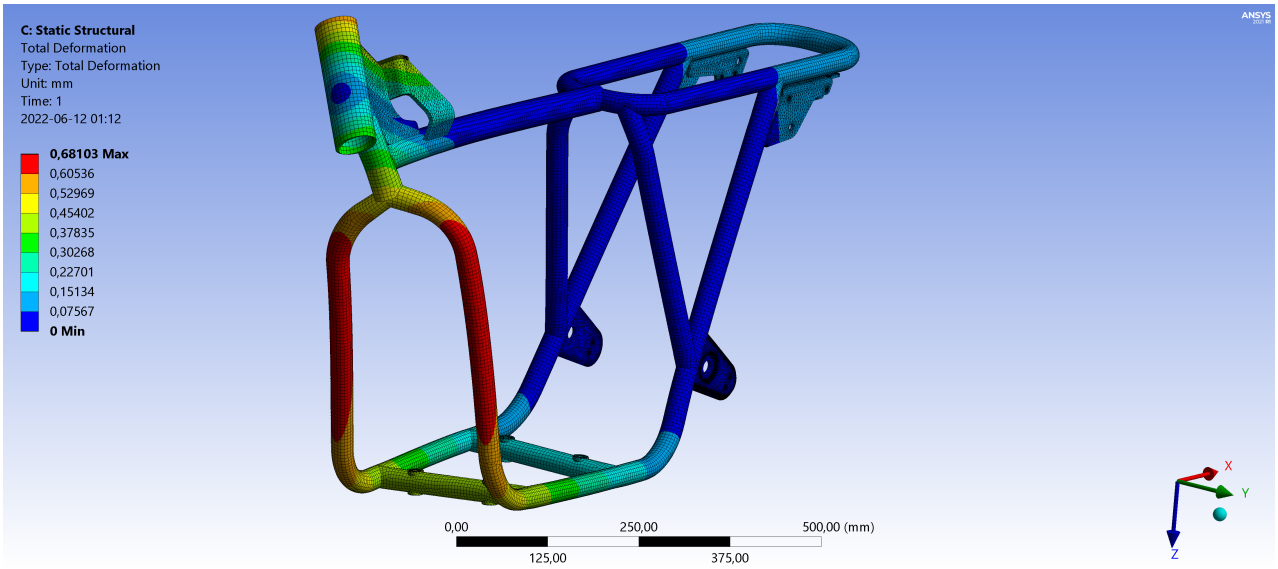

Figure 4.6: *Deformation from an applied torque of 176 Nm simulated using shell elements in Ansys*

The calculated stiffness from the different software are presented in *Table* **??**

Table 4.3: Torsional

Stiffness [N/deg]	**Software**	**Element type**	**Component**
336,42	Nastran	Shell	Frame
380,00	Nastan	Beam	Frame
336,80	Ansys	Shell	Frame
166,89	Fusion 360	Solid	Frame

Presented in the *Appendix A.2* are the plots from the torsional load case simulations in the different software. Looking at the directions of deformation, it is clear that the general behaviour of deformation is similar for all software used. The exception is Fusion 360 which reached greater amounts of displacement and thus a lower value of stiffness in the frame.

4.2.4 Longitudinal load-case

For the Longitudinal load case, a remote force acting perpendicular to the steering axis along the global x-axis and z-axis was applied at the imagined position of the wheel hub of the front wheel acting on the bearing surfaces on the steering head. The application of a remote force did not work when using beam elements as this causes rotation on the node connecting the steering neck with the rest of the frame. Therefore simulations using beam elements were disregarded for this load case. The corresponding values of stiffness were calculated by dividing the applied force with the translation of the steering neck and presented in *Table 4.4*

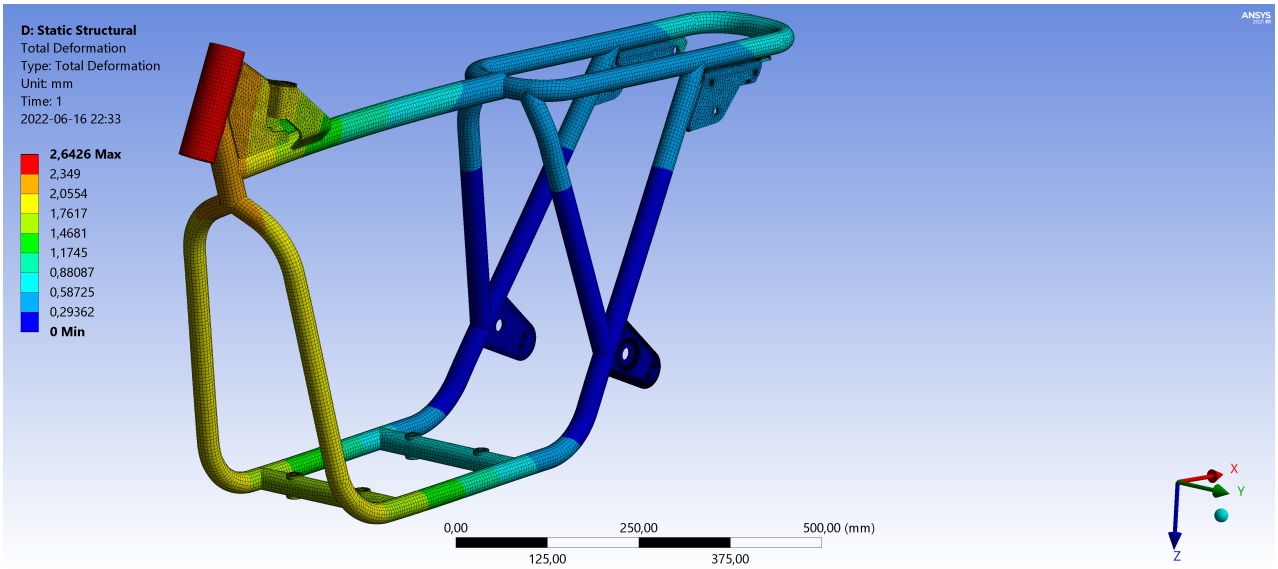

Figure 4.7: *Deformation from a Longitudinal load of 491 N simulated using shell elements in Ansys*

Table 4.4: Longitudinal

Stiffness [N/mm]	**Software**	**Element type**	**Component**
334,44	Nastran	Shell	Frame
526,49	Fusion 360	Solid	Frame
354,76	Ansys	Shell	Frame

The Deformation and stress plots from the different software are presented in *Appendix A.3*

4.2.5 Stressed member simulations

The surface model of the battery box and the battery substitute was simulated and the effect of stressed member has was be evaluated. The battery box added stiffness to the whole assembly as expected and stabilised the bottom plate of the frame where the battery box is fastened with 4 screws to the frame. The simulations also shows that the batter replacement frame improved the stiffness even further. This is not an unexpected behaviour due to it having a more rugged design and being made out of steel. The more interesting comparison is between the battery substitute in simulation versus physical testing. The principal behaviour for the lateral load case is shown in *Figure 4.8*. Detailed plots from all software and load cases are presented in *Appendix A.4*.

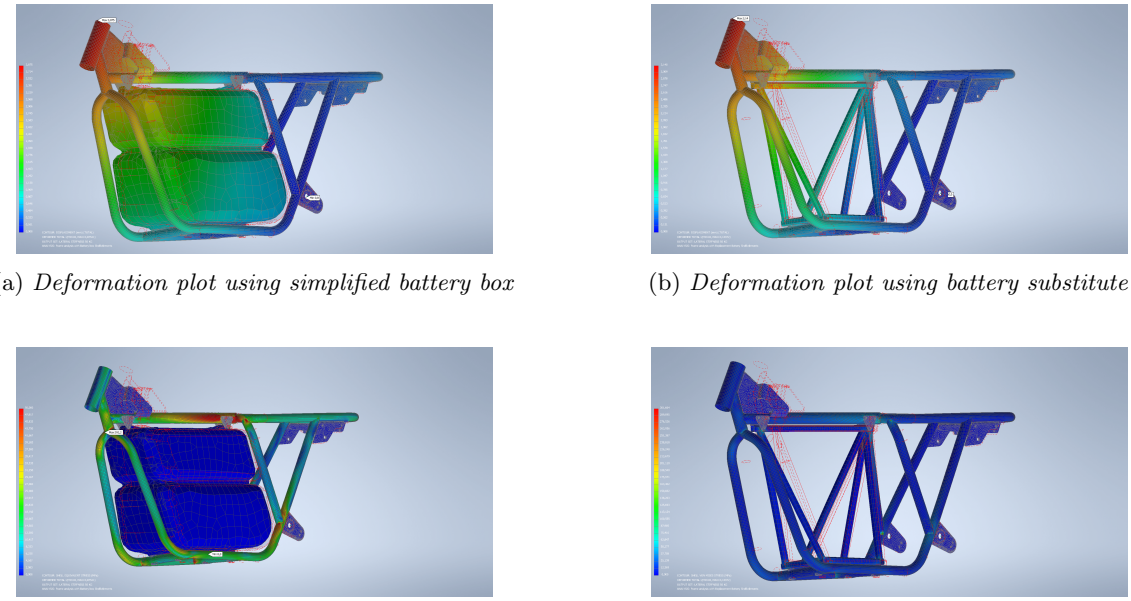

(a) *Deformation plot using simplified battery box*

(b) *Deformation plot using battery substitute*

(c) *Stress plot using simplified battery box*

(d) *Stress plot using battery substitute*

Figure 4.8: *Deformation and stress plots from the lateral load case using both the simplified battery box and the battery substitute*

stiffness of the models are calculated according to the previous method described in *Sections 4.2.2, 4.2.3 and 4.2.4* and presented below in *Table 4.5*.

Table 4.5: Simulated stiffness for the frame together with the simplified battery box and the battery substitute frame

Stiffness	**Components**	**Load case**
163.59 [N/mm]	Battery substitute	Lateral
132.54 [N/mm]	Battery box	Lateral
526.65 [N/deg]	Battery substitute	Torsional
335.45 [N/deg]	Battery box	Torsional
396.65 [N/mm]	Battery substitute	Longitudinal
343.29 [N/mm]	Battery box	Longitudinal

4.3 Physical Testing

The physical tests performed on the frame in the rig and its corresponding data will be analysed and presented. This data will later be used for comparison with the simulated results in the FEA.

4.3.1 Construction of test rig

The test rig was built and assembled to allow for the test to be performed. The requirements stated that it should be cheap, modular, and have flexibility to test different frames with different dimensions. This was achieved with the test rig as seen in *Figure 4.9*. It is made up of two sides which were welded together, the sides are being held together with 4 removable beams that also hold the motorcycle frame as seen in *Figure 4.1*. The beams that hold the frame can be adjusted to fit frames with different dimensions to allow for a versatile test rig. The dimensions of the rig can be seen in *Figure 4.10*. The dimensions were set with regards to the available material to keep the cost down, while still being big able to conduct test with good enough results.

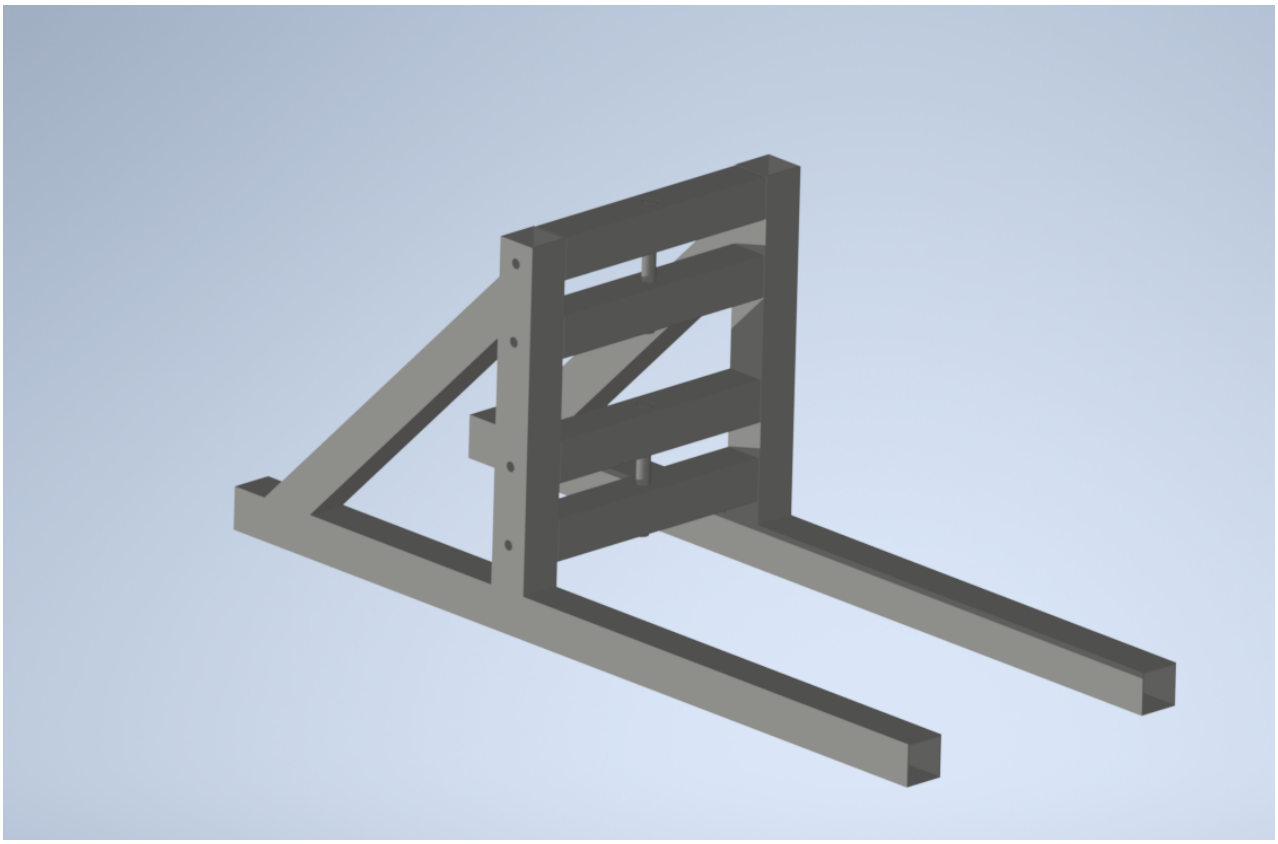

Figure 4.9: *CAD model of the test rig*

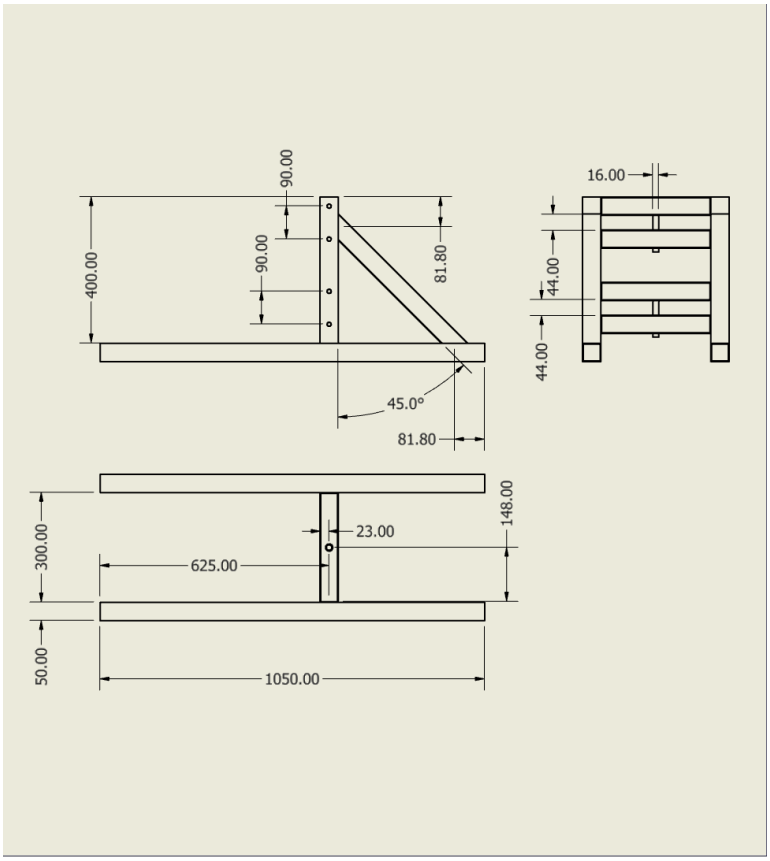

Figure 4.10: *Drawing of test rig*

4.3.2 Flex of test rig

The flex of the test rig was measured to be able to subtract the effect of the equipment on the test result to not skew the data. Although the rig was designed to minimise potential flex it was also modular to be able to be stored away and the parts were fasted with screw connections which meant that the potential flex that could occur was of a higher concern than if the rig would have been welded as one part. The flex that the rig induced on the test result is presented in *Figure 4.11* below. The impact on the test result that the flex imposes on the measurements would lead to unreliable results unless addressed. The more uncertainties that exist the less the test result can be trusted. The lateral test case was the case that was of concern, thus was addressed with this method. The torsional test case did not have any flex that could be measured on the dial indicator, thereby the data did not have to be adjusted for rig flex.

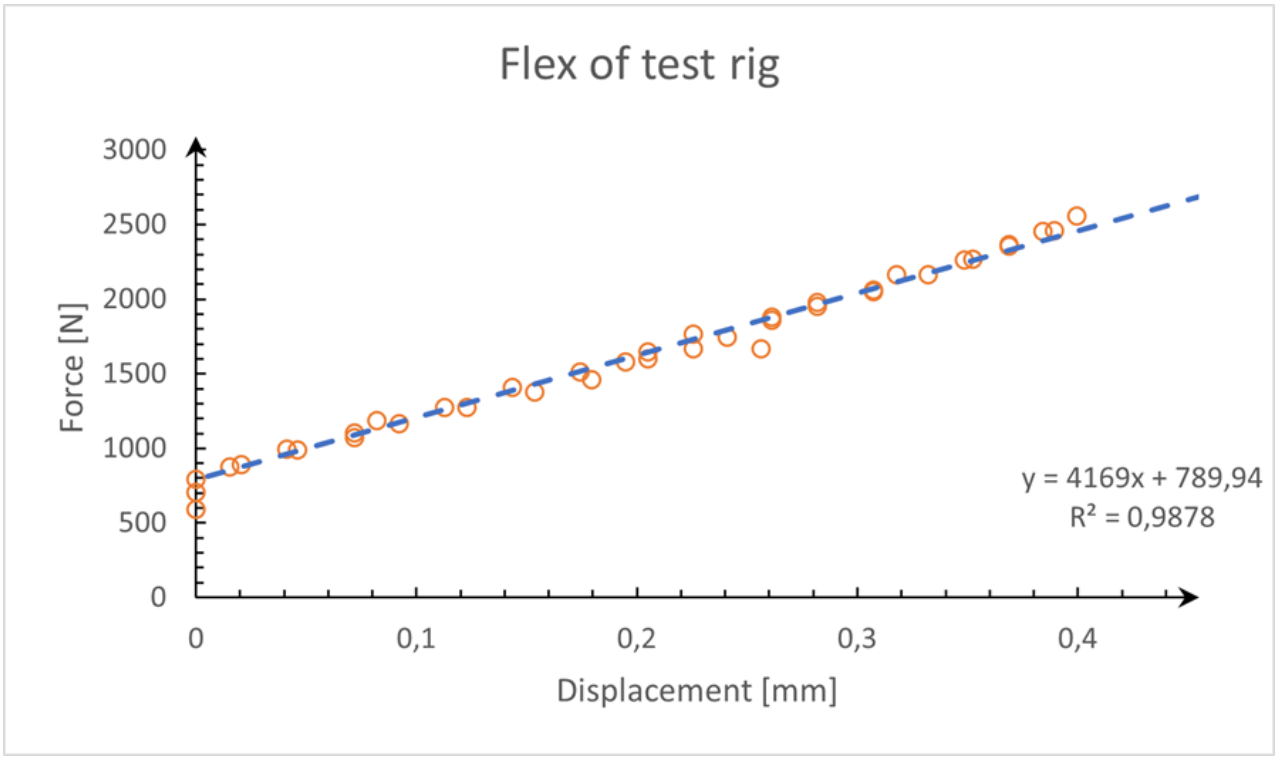

Figure 4.11: *The deflection of the test rig with force applied*

As can be seen the displacement is linear to the force applied and correlates good with a linear equation, thus the the effect on the displacement of the frame can be easily adjusted for to the correct value with the linear equation. The value of the slope in the equation is the stiffness of the rig, $4169 N/mm$. The graph does not intersect with the origin since the rig, frame and jack had to be pre loaded before the measurement started. This way the measurement equipment and the applied force did not need to be calibrated and start at zero at the same time. If that would be required the test procedure would not have been as robust and sensitive to error.

4.3.3 Lateral load case

Similarly to the measurements for the flex of the test rig different placements of the dial indicators gave the results for the lateral load case test, *Figure* **??**. The load and displacement was measured and since the frame was pre-loaded prior to the first data point the extrapolated line does not intersect the origin. However, it is the slope of the line which gives the stiffness of the frame during lateral loading.
The R^2 value is close to 1 which indicates that the data points are close to the interpolated line thus the data is not scattered with many outliers which in turn indicated good data. The values in the graph however is the raw data captured during the test and must be adjusted for the flex of the test rig to achieve the correct stiffness as seen in

5 Concluding remarks

5.1 Conclusion

From the study the conclusion drawn is that both Autodesk Inventor Nastran and Ansys Mechanical produces feasible results. The results correlate well with each other when comparing the results and they provide a less sensitive model. In comparison the simulations made using Autodesk Fusion360 are less reliable for this application. Minor changes in the parameters for the simulation gave very different results after simulating. The largest drawback is the lack of compatibility for beam and shell models. This leads to over stiff models with far more computational nodes than necessary when working with thin-walled bodies. In a prototyping stage with solid parts it shows useful however not when analysing more complex systems. In this application our recommendation is that Autodesk Inventor Nastran gives the most value since it both includes a competent CAD software with a sufficient FEA software. It is more expensive than Autodesk Fusion360 but is better suited as a CAD software when building the frame and produces much more reliable results. Ansys would also suit the needs but is much more expensive than Inventor and does not include any suitable CAD software.

At the beginning of the project the CAD model that existed was not suited for structural simulations. This led to an unexpected amount of time needed to remake the model into something more suitable. With that time more work could have been invested in further refining the simulations model possibly reaching even better results. More load cases could have been tested and with greater precision. This is something that should be taken into account in when planning for future projects and design iterations. The outcome of continuously doing structural simulations early in design projects can be possibility of reducing unnecessary mass, more efficient construction which can lead to both reduction in price and an increase of range. In this project computational power was a limiting factor. If better computers would have been an option the simulation times could have been reduced leading to more simulations made and a better final outcome of the project.

The outcome from the stressed member simulations are that the mounting solution is equally important as the member itself. Due to not being able to properly mount the battery box replacement to the frame in the physical testing we saw a substantially worse correlation to the simulations in the torsional tests. This can be interpreted as a less perfect mounting compared to the simulated model. The test frame used lacked threaded inserts in the upper mounting for the battery. With those inserts mounted on the frame a better result is expected. It would have been of great interest to be able to further test with another frame to get a better understanding of the implications of having the battery box as a stressed member to investigate possible reduction in weight och an increase in stiffness since the box makes for much of the frames bulk.

The test rig is regarded as a suitable method for testing lateral and torsional stiffness. Much of the flex of the rig was possible to measure and subtract from the test resulting in a less tolerance sensitive and more light weight rig. Areas of possible improvement would be in the mounting interface between the test rig and the pressure point of the hydraulic jack. Ideally the jack would press against the rig instead of the table in order to minimise the need of a mounting the rig at all. Since the frame was powder coated and missing any tightly toleranced bearing surfaces around the mounting points there are some play after mounting. This can be disregarded from testing if the measurements starts at a force where there is no slack in the interface. It could also have been done if the mounting solution could have been pretensioned. By mounting the frame in the steering head bearing surfaces some amounts of slack could have been reduced as well but this would present other problems and would have required a different test rig. It would have been interesting to be able to properly test the longitudinal load case as well, however it would have required more time than available for the project.Even though the test rig can be improved it proved of correlation to a satisfactory extent.

All simulations gave a more stiff model than the actual case. This is likely caused by inaccuracies in the welded joints of the frame, since a welded joint rarely completely fuses the materials together. The frame used for the testing was originally made to evaluate the welds, which could have led to a not fully representing model. As a final remark we believe that a combination of beam, shell and solid element in the FE model would give the ideal set up between speed and accuracy.

5.2 Recommendations for future work

Our opinion is that it was possible to with a quite simple testing rig to reach results close to the simulations. As a future work it would be interesting to see if the same rig and approach can be used in more cases. For this study only one physical frame was used. It would be great to test with more frames of the same model to reduce the impact of the individual frame. It would also be of great interest to try more makes of motorcycle frames to benchmark RGNT with competitive brands to learn for future models.

This study surrounded greatly in finding the best suited software for RGNT. Having made that recommendation it would be beneficial to continue to refine the model within Autodesk Inventor Nastran to see how close to reality is possible to reach. It could possible be necessary to add more components and load cases to the model and it would be great to have a method for confident inclusion as well. It would also be interesting to work with local refinements on the mesh to see if the amount of mesh nodes can reliably be reduced even further.

As for improvement to the physical testing it would be valuable to include strain gauges as well to the testing. This would give one more dimension to the confidence, not only looking at the displacement of the frame but also looking into strain in the different parts. It was seen during these physical tests that the mounting method used required to preload the frame before starting the tests, due to a loose fit in the swing brackets. Future investigation should be targeted towards a method to pretension the frame to the test rig to reduce the risk of miscalculations.

A final recommendation to RGNT is to invest in Autodesk Inventor Nastran to conveniently incorporate structural simulations early in the design phase to minimise the needs of future physical testing.

References

[1] Autodesk. *Autodesk Inventor: Programvara för mekanisk konstruktion med ambitiösa idéer.* URL: https://www.autodesk.se/products/inventor/overview?term=1-YEAR&tab=subscription (visited on 05/13/2023).

[2] Autodesk. *Fusion 360: Mer än CAD, det är det framtiden inom design och tillverkning.* URL: https://www.autodesk.se/products/fusion-360/overview?term=1-YEAR&tab=subscription (visited on 05/13/2023).

[3] S. Bhavikatti. *Finite Element Analysis.* New Age International Ltd, 2004. ISBN: 9788122425246.

[4] Z. Bi. *Finite element analysis applications : a systematic and practical approach.* London [England] : Academic Press, 2018. ISBN: 9780128103999.

[5] J. Bradley. *The Racing Motorcycle, A technichal guide for constructors.* Broadland Leisure Publications, 1996. ISBN: 9780951292921.

[6] K. Cameron. *Why Ducati's Trellis Frame Was So Good: Ducati's success was built on a beautiful but flexible steel frame that worked like magic.* URL: https://www.cycleworld.com/why-ducatis-trellis-frame-was-so-good/ (visited on 06/14/2022).

[7] V. Cossalter. *Motorcycle Dynamics.* Annalia, Fabrizio, Flavio, 2006. ISBN: 9781447532767.

[8] T. Foale. *MOTORCYCLE HANDLING AND CHASSIS DESIGN, the art and science.* Tony Foale Designs, 2006. ISBN: 84-933286-2-6.

[9] K. Hanjalic et al. A robust near-wall elliptic-relaxation eddy-viscosity turbulence model for CFD. *Int. J. Heat Fluid Flow* **25** (2004), 1047–1051.

[10] W. Harris. *How Motorcycles Work.* URL: https://auto.howstuffworks.com/motorcycle6.htm (visited on 05/20/2022).

[11] S. Hensiek. *History of the Riding Car: The First Mercedes Motorcycle Ever Produced.* URL: https://worthly.com/most-expensive/motorcycles/history-riding-car-first-mercedes-motorcycle-ever-produced/ (visited on 06/14/2022).

[12] A. Iserles. *A First Course in the Numerical Analysis of Differential Equations.* Cambridge University Press, 2004. ISBN: 0-521-55655-4.

[13] ISO Central Secretary. *Industrial automation systems and integration — Product data representation and exchange — Part 21: Implementation methods: Clear text encoding of the exchange structure.* en. Standard ISO 10303-21:2016. Geneva, CH: International Organization for Standardization, 2016. URL: https://www.iso.org/standard/63141.html.

[15] *John Boyd Dunlop Biography - The First Commercial Pneumatic Rubber Tire.* URL: http://www.bicyclehistory.net/bicycle-inventor/john-boyd-dunlop/ (visited on 06/14/2022).

[16] P. M. Kurowski. *Finite Element Analysis for Design Engineers.* SAE International, 2004. ISBN: 978-0-7680-5310-4.

[17] *MATLAB manual. Ordinary Differential Equations.* Version 7.8. Mathworks, 2008. URL: http://www.mathworks.com/access/helpdesk/help/techdoc/ref/ode45.html.

[18] Mitotoyo. *Dial Gauge, Flat Back, ISO Type.* URL: https://shop.mitutoyo.se/web/mitutoyo/en_SE/all/$catalogue/mitutoyoData/PR/2971AB/datasheet.xhtml (visited on 05/13/2023).

[19] Mitotoyo. *Dial Test Indicator, Horizontal Type Item number: 513-404-10E.* URL: https://shop.mitutoyo.se/web/mitutoyo/sv_SE/all/$catalogue/mitutoyoData/PR/513-404-10E/datasheet.xhtml (visited on 05/13/2023).

[20] Modelling optimization involving different types of elements in finite element analysis (2013). DOI: https://doi.org/10.1088/1757-899X/50/1/012036.

[21] I. Motorcycles. *BECOMING LEGENDARY: AMERICA'S FIRST MOTORCYCLE COMPANY.* URL: hhttps://www.indianmotorcycle.com/en-us/history/becoming-legendary/ (visited on 06/14/2022).

[22] E. Musk. *Master Plan, Part Deux.* URL: https://www.tesla.com/sv_SE/blog/master-plan-part-deux (visited on 06/14/2022).

[23] E. Musk. *The Secret Tesla Motors Master Plan (just between you and me).* URL: https://www.tesla.com/blog/secret-tesla-motors-master-plan-just-between-you-and-me (visited on 06/14/2022).

[24] D. J. Noce. The Engineering Process for the Design of a Motorcycle Chassis and Suspension (2012).

[25] Ovako. *Material data sheet Steel grade S355J2.* URL: https://steelnavigator.ovako.com/steel-grades/s355j2/ (visited on 05/13/2023).

[26] Ł. S. Ph.D. *What are the Types of Elements Used in FEA?* URL: https://enterfea.com/what-are-the-types-of-elements-used-in-fea/ (visited on 05/12/2023).

[28] G. E. Roe and T. E. Thorpe. The Influence of Frame Structure on the Dynamics of Motorcycle Stability (1989). DOI: https://doi.org/10.4271/891772.

[29] M. G. M. Ryan. *RADIO, AIRPLANES, AND WORLD WARS: NEXT STEPS FOR THE PROFESSION OF ARMS.* URL: https://mwi.usma.edu/radio-airplanes-and-world-wars-next-steps-for-the-profession-of-arms/ (visited on 06/14/2022).

[30] P. J. B. Shuhei Nishitateno. The motorcycle Kuznets curve. *Journal of Transport Geography* (2014). DOI: https://doi.org/10.1016/j.jtrangeo.2014.03.008.

[31] P. J. B. Shuhei Nishitateno. The motorcycle Kuznets curve. *Journal of Transport Geography* **36** (2014), 116–123. DOI: https://doi.org/10.1016/j.jtrangeo.2014.03.008.

[32] Tibnor. *Stålprodukter för hydraulik 2021.* URL: https://www.tibnor.se/medias/stalprodukter-for-hydraulik-2021.pdf?context=bWFzdGVyfHJvb3R8M%5C%5CTk4Njc1fGFwcGxpY2F0aW9uL3BkZnxoYz%5C%5CUvaDg1Lzg5MTM3MTEyNjc4NzAvc3RhbHByb2R1a3Rlci1mb3I%5C%5CtaHlkcmF1bGlrLTIwMjEucGRmfGJjNDFkMDVmM5C%5CUwZTA0NjcwZjBjODgwNTg1ZmMyMDc4ZWRjOWI2OTM3ZGU&attachment=true (visited on 05/13/2023).

[33] T. Watson. *History of Motorcycle Frames.* URL: https://www.rideapart.com/features/254262/history-of-motorcycle-frames/ (visited on 06/14/2022).

A FEM Simulations

A.1 Lateral Load case

A.1.1 Deformation

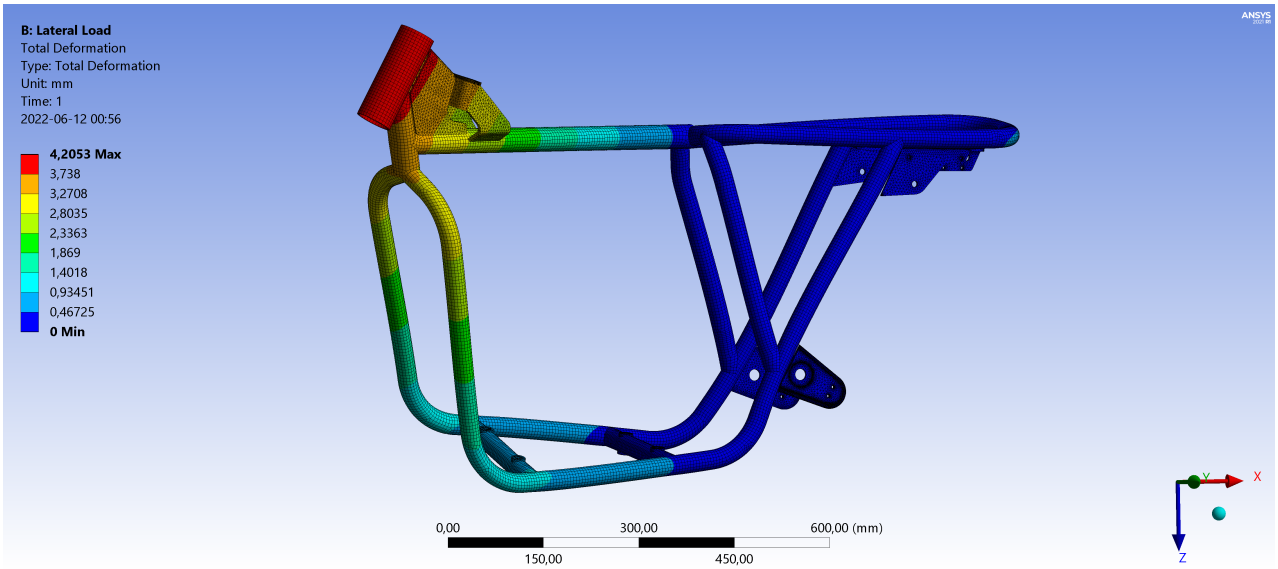

Figure A.1: *Deformation from a load of 491 N simulated using shell elements in Ansys*

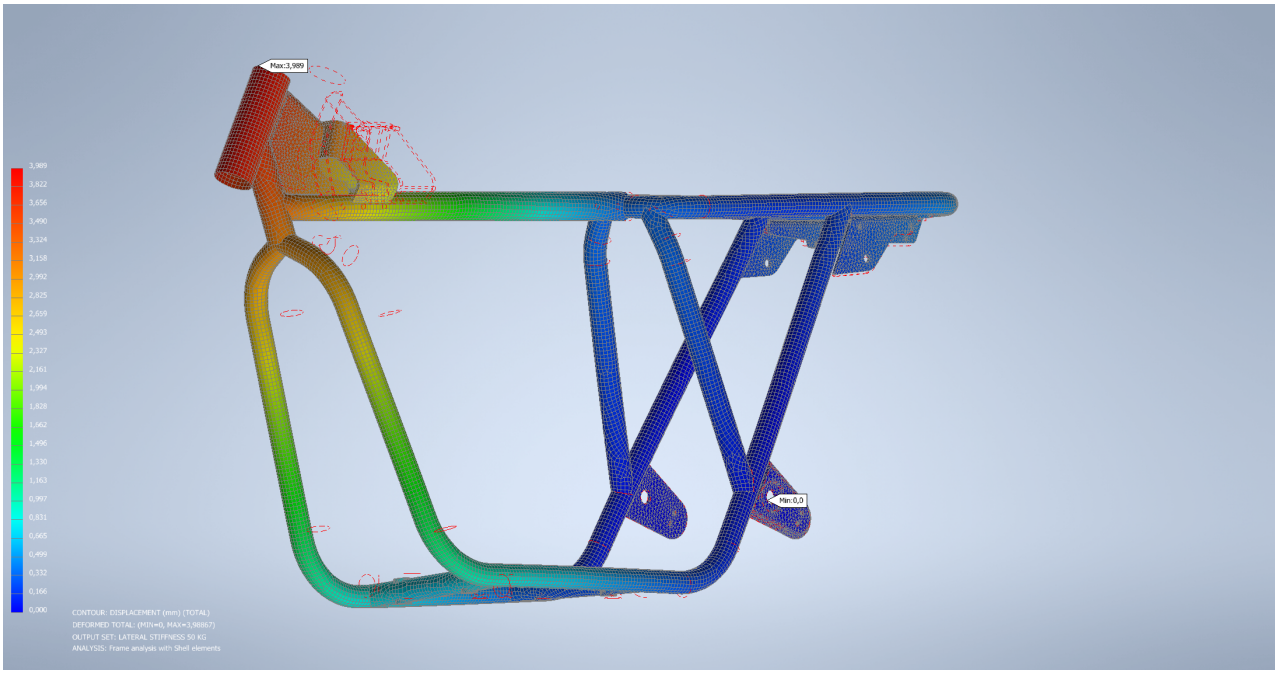

Figure A.2: *Deformation from a load of 491 N simulated using shell elements in Autodesk Inventor Nastran*

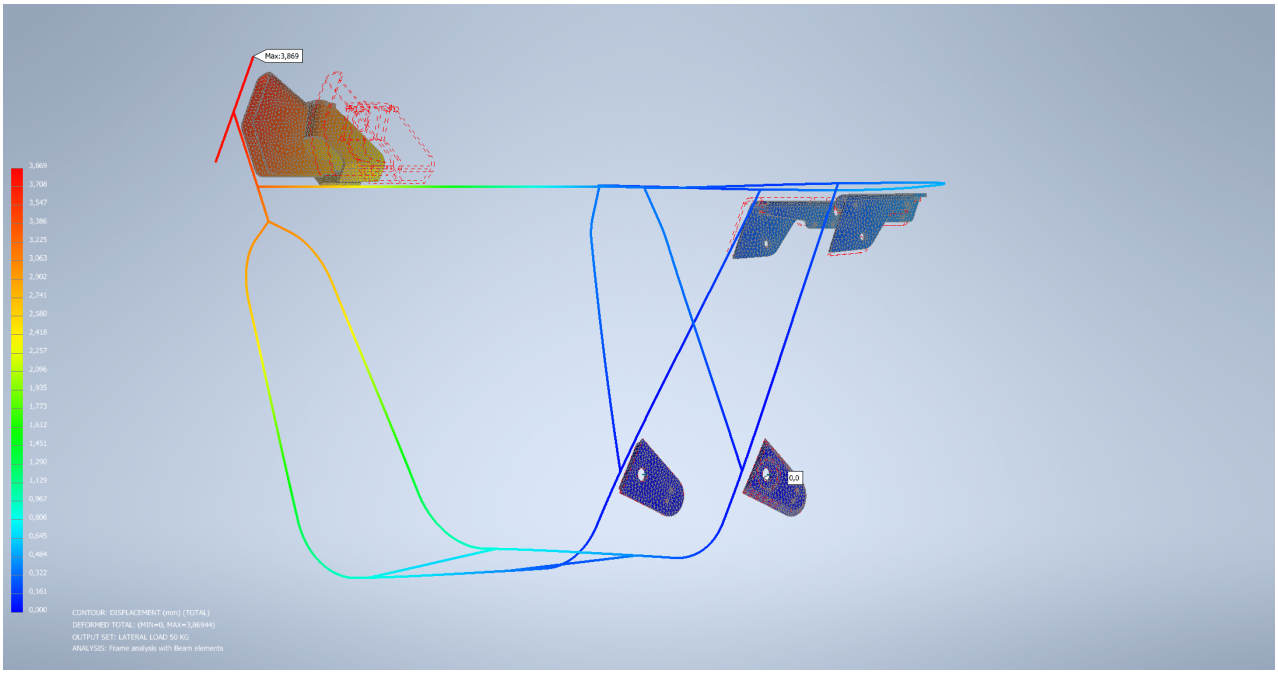

Figure A.3: *Deformation from a load of 491 N simulated using beam elements in Autodesk Inventor Nastran*

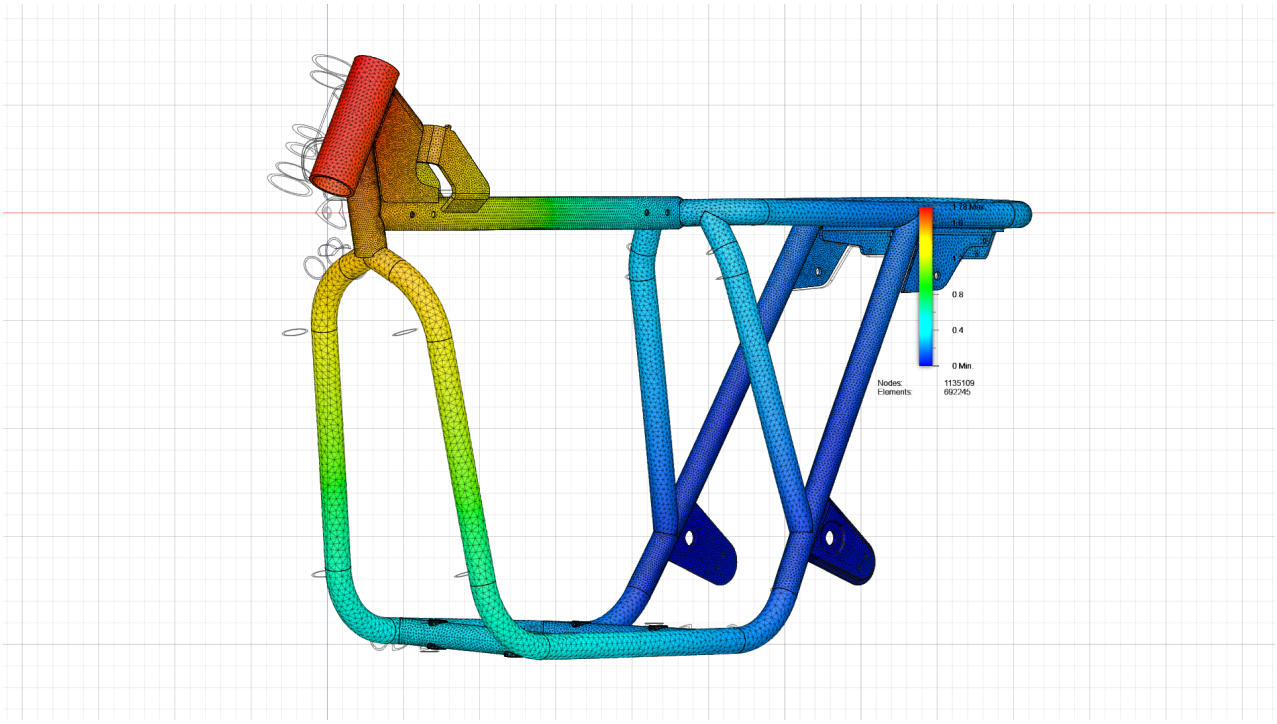

Figure A.4: *Deformation from a load of 491 N simulated using solid elements in Autodesk Fusion 360*

A.1.2 Stress

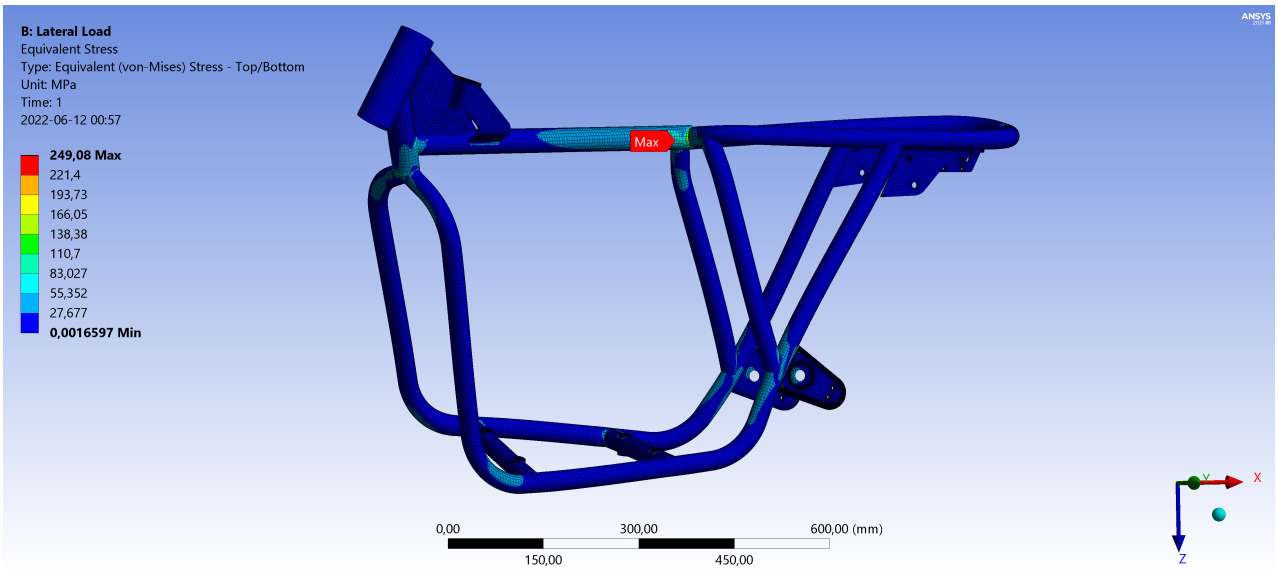

Figure A.5: *Stress plot from a lateral load of 491 N simulated using shell elements in Ansys*

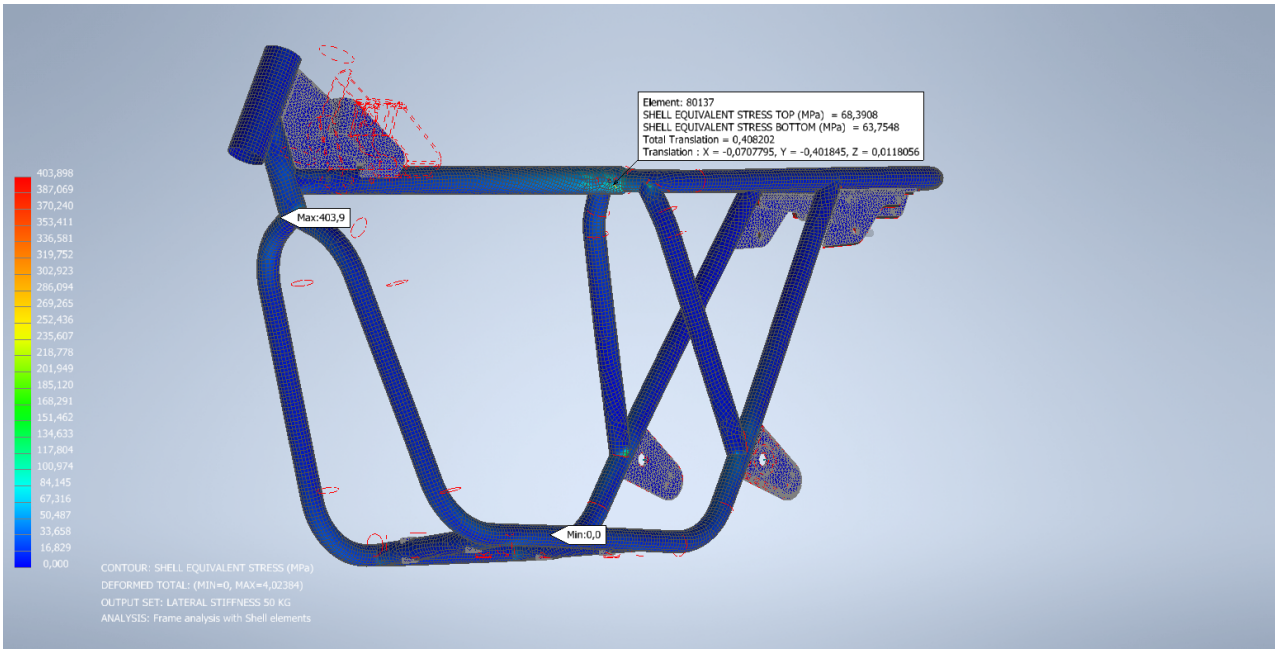

Figure A.6: *Stress plot from a lateral load of 491 N simulated using shell elements in Autodesk Inventor Nastran*

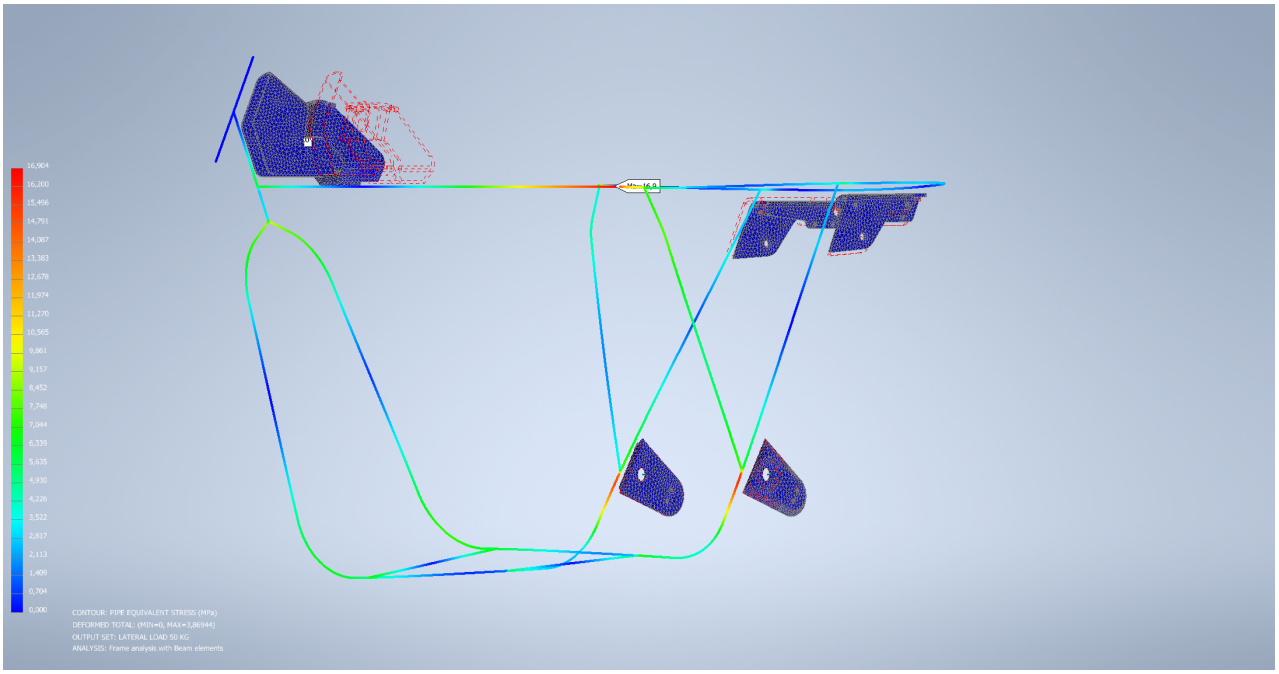

Figure A.7: *Stress plot from a lateral load of 491 N simulated using beam elements in Autodesk Inventor Nastran*

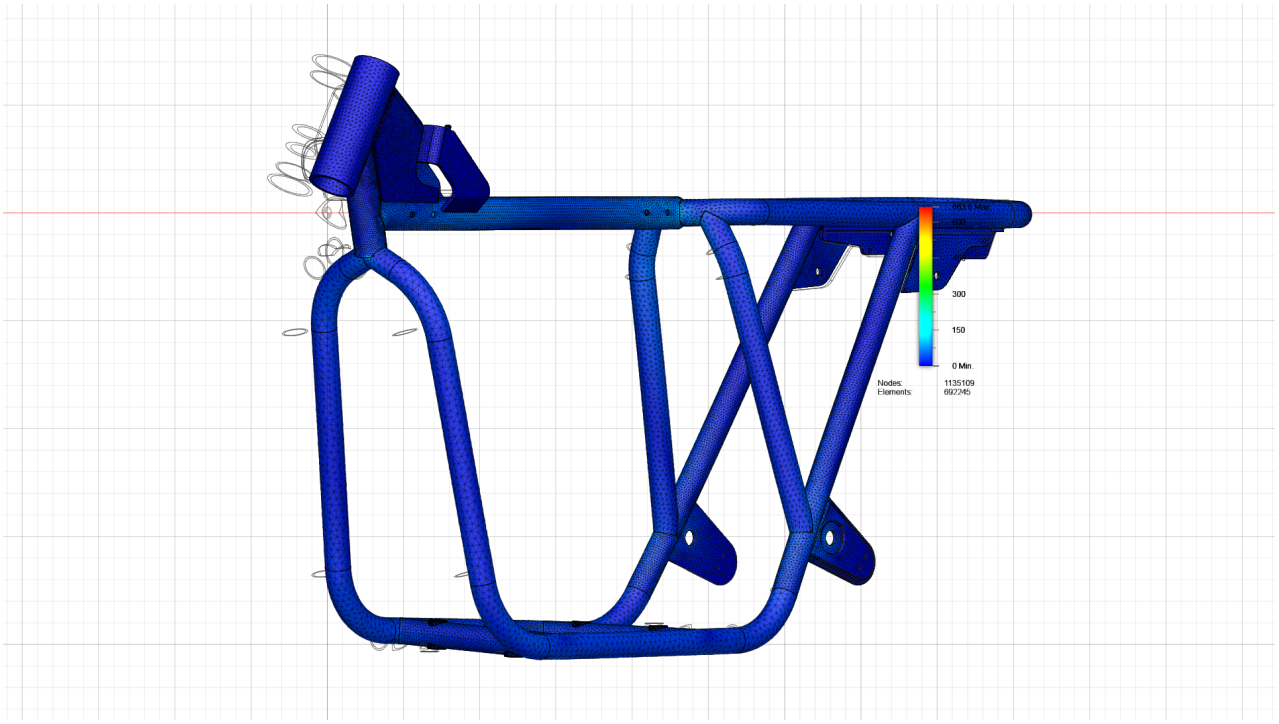

Figure A.8: *Stress plot from a lateral load of 491 N simulated using Solid elements in Autodesk Fusion 360*

A.2 Torsional Load Case

A.2.1 Deformation

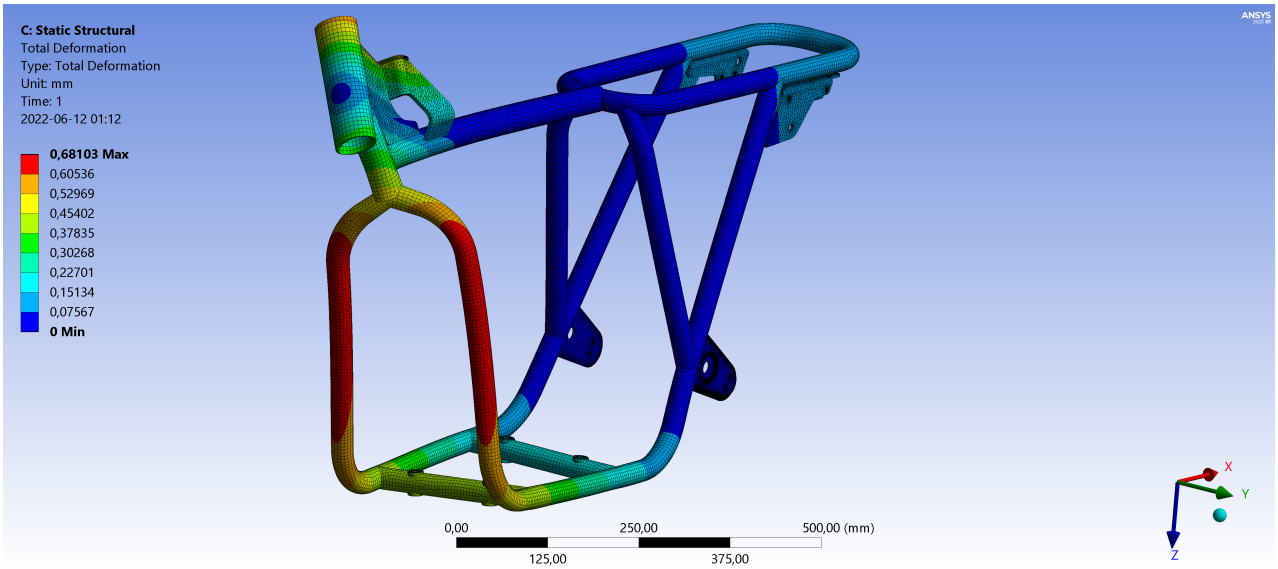

Figure A.9: *Deformation from an applied torque of 176 Nm simulated using shell elements in Ansys*

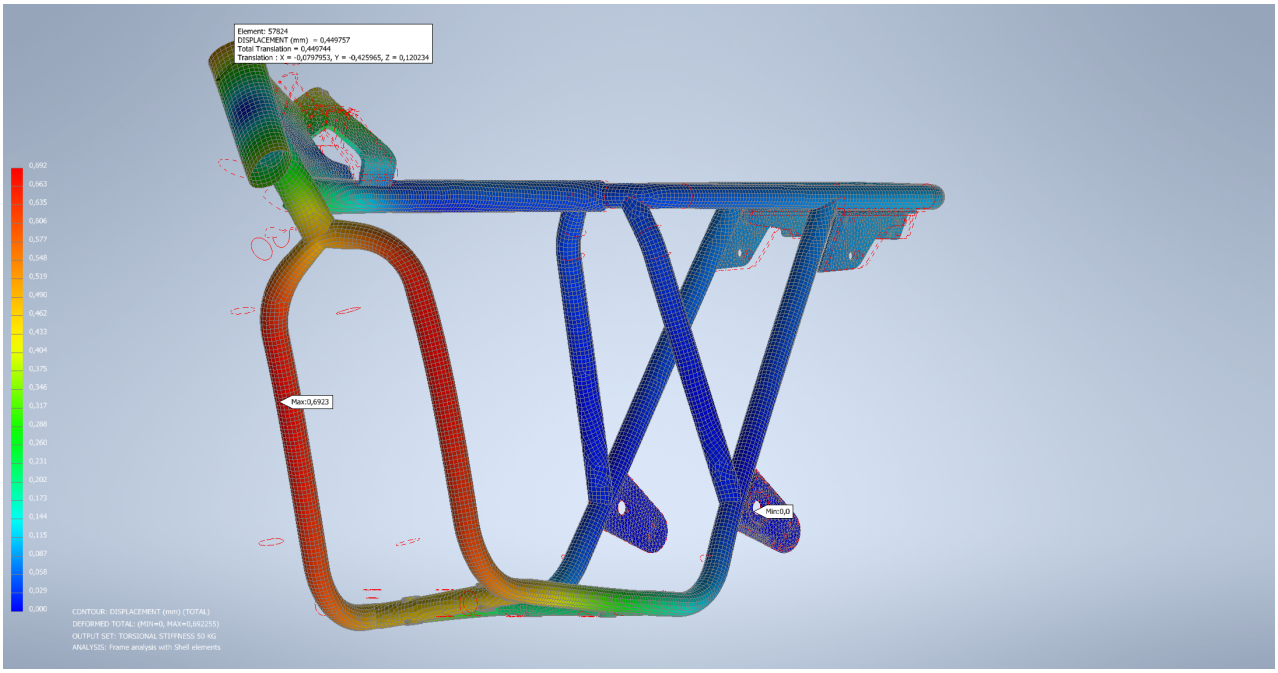

Figure A.10: *Deformation from an applied torque of 176 Nm simulated using shell elements in Autodesk Inventor Nastran*

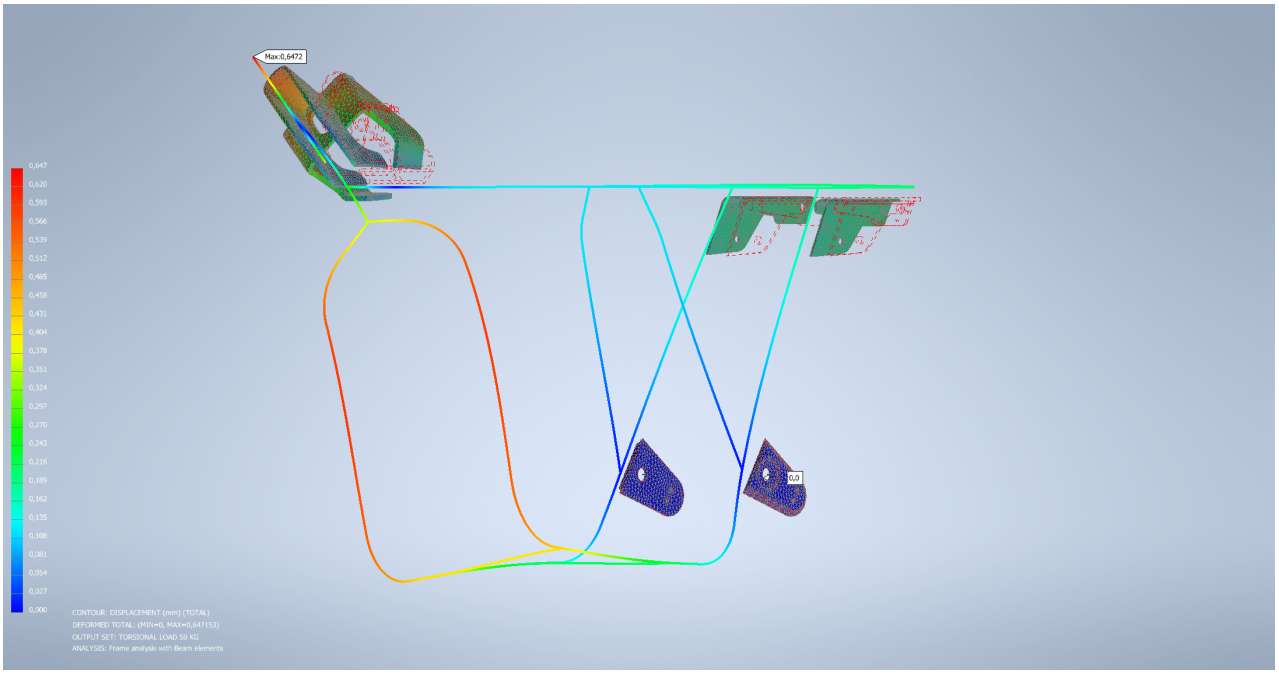

Figure A.11: *Deformation from an applied torque of 176 Nm simulated using beam elements in Autodesk Inventor Nastran*

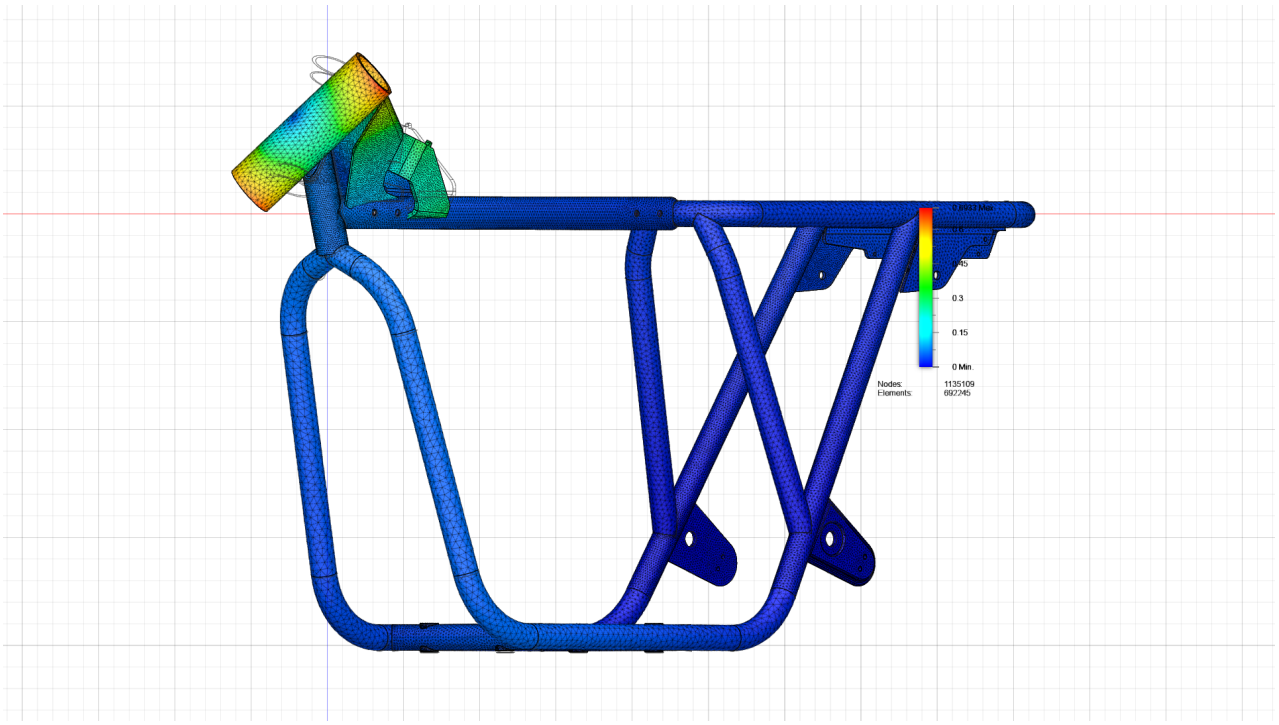

Figure A.12: *Deformation from an applied torque of 176 Nm simulated using solid elements in Autodesk Fusion 360*

A.2.2 Stress

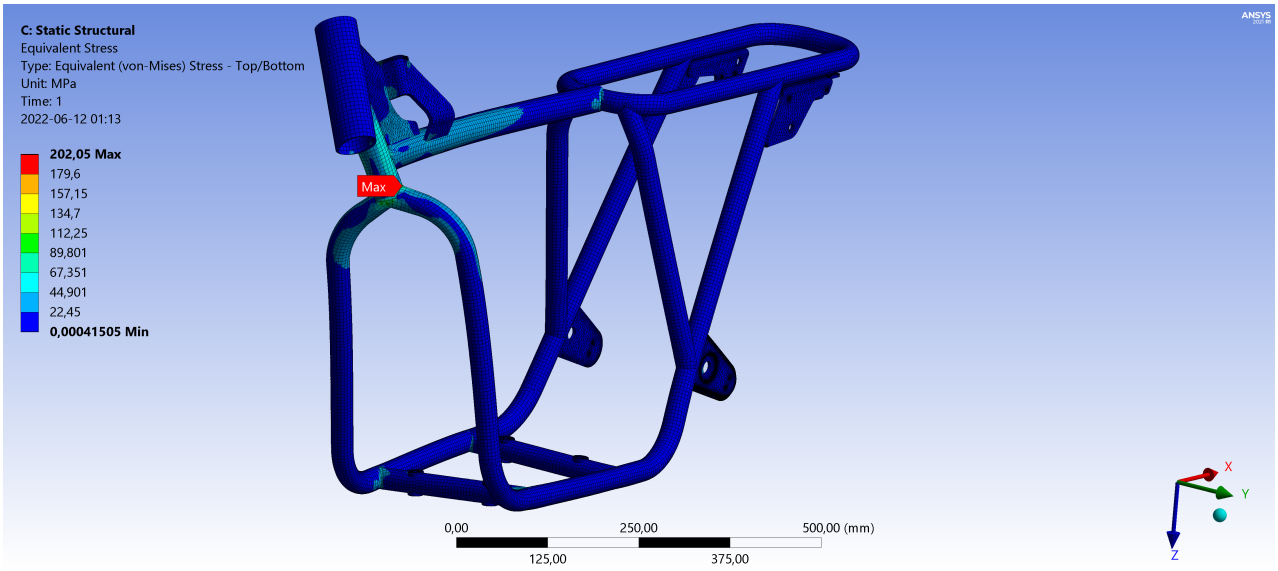

Figure A.13: *Stress plot from an applied torque of 176 Nm simulated using shell elements in Ansys*

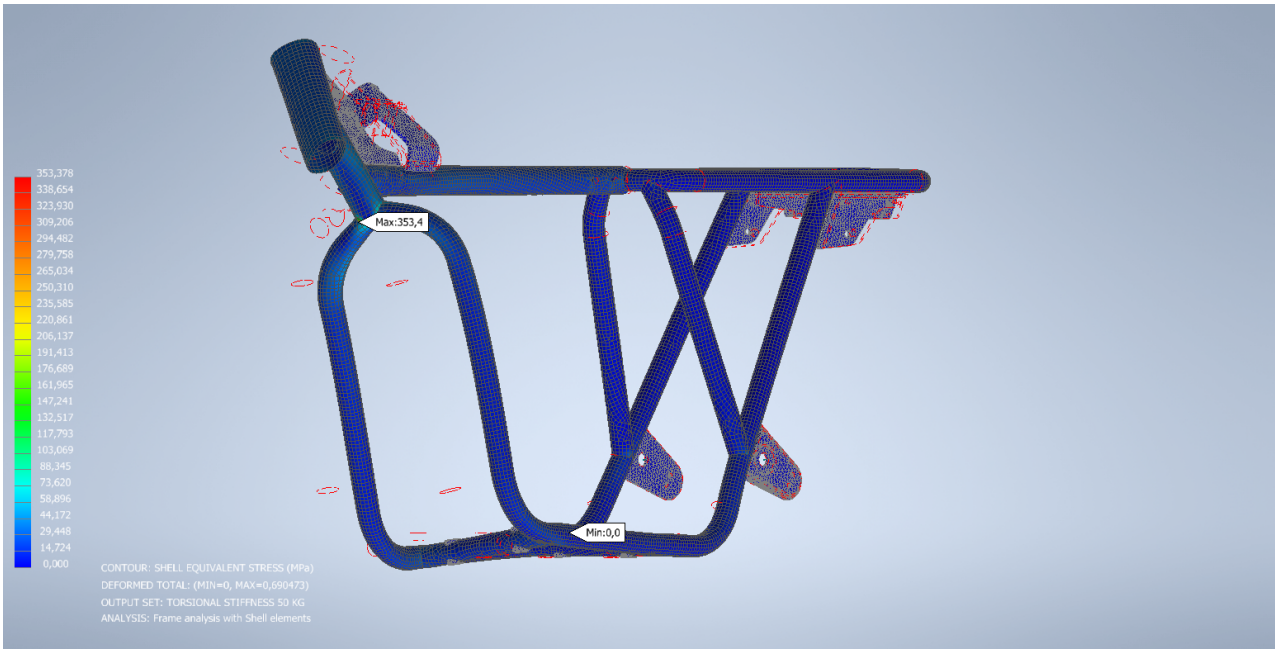

Figure A.14: *Stress plot from an applied torque of 176 Nm simulated using shell elements in Autodesk Inventor Nastran*

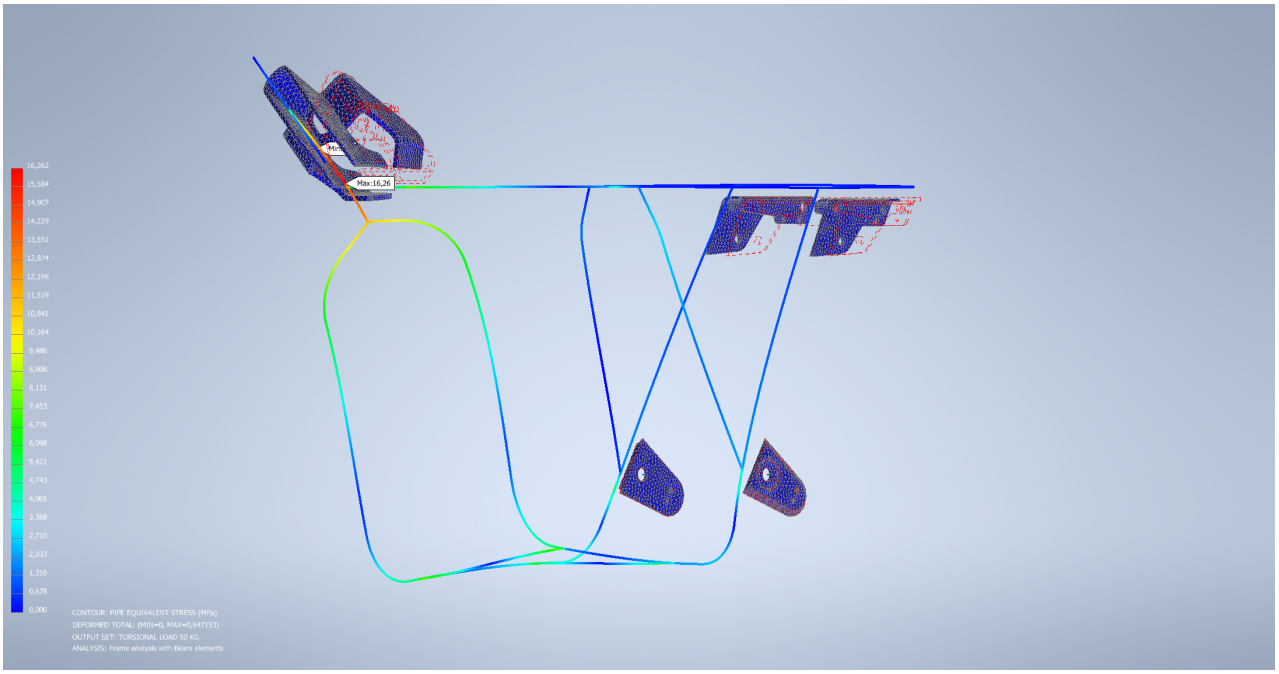

Figure A.15: *Stress plot from an applied torque of 176 Nm simulated using beam elements in Autodesk Inventor Nastran*

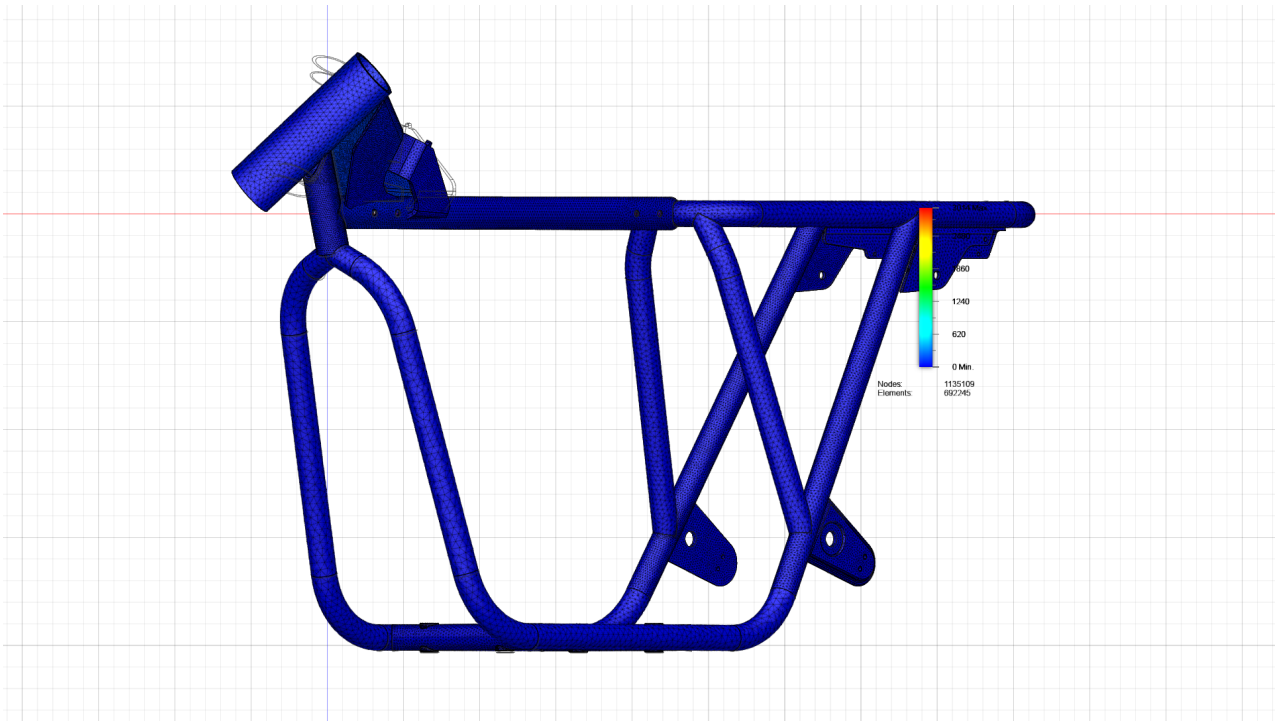

Figure A.16: *Stress plot from an applied torque of 176 Nm simulated usning Solid elements in Autodesk Fusion 360*

A.3 Lontitudinal Load Case

A.3.1 Deformation

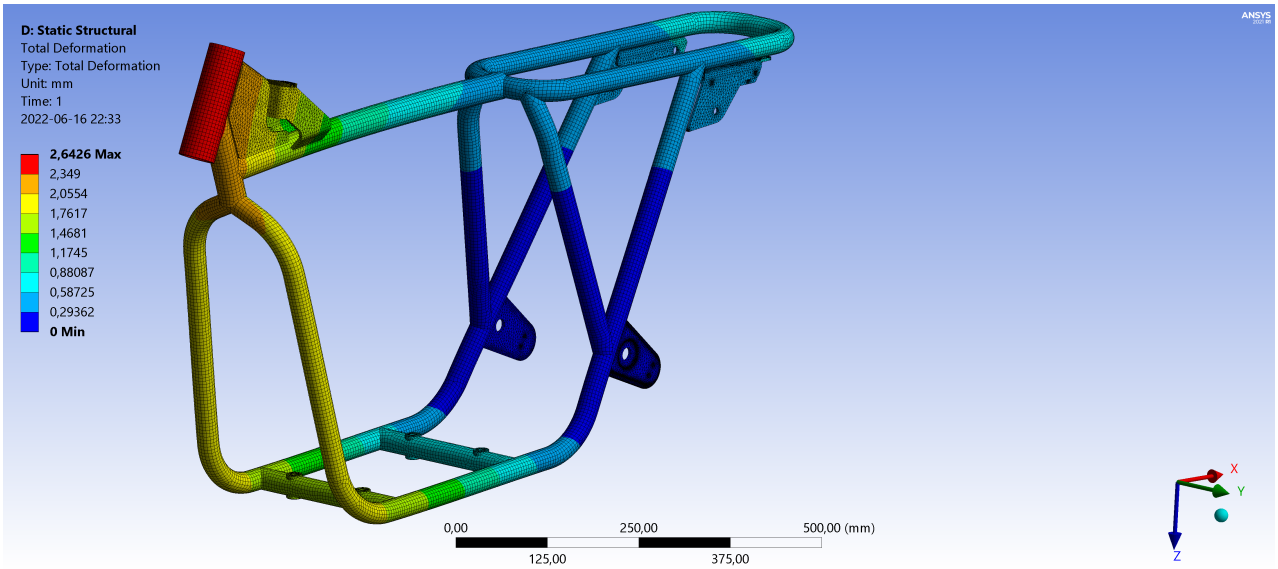

Figure A.17: *Deformation from a Longitudinal load of 491 N simulated using shell elements in Ansys*

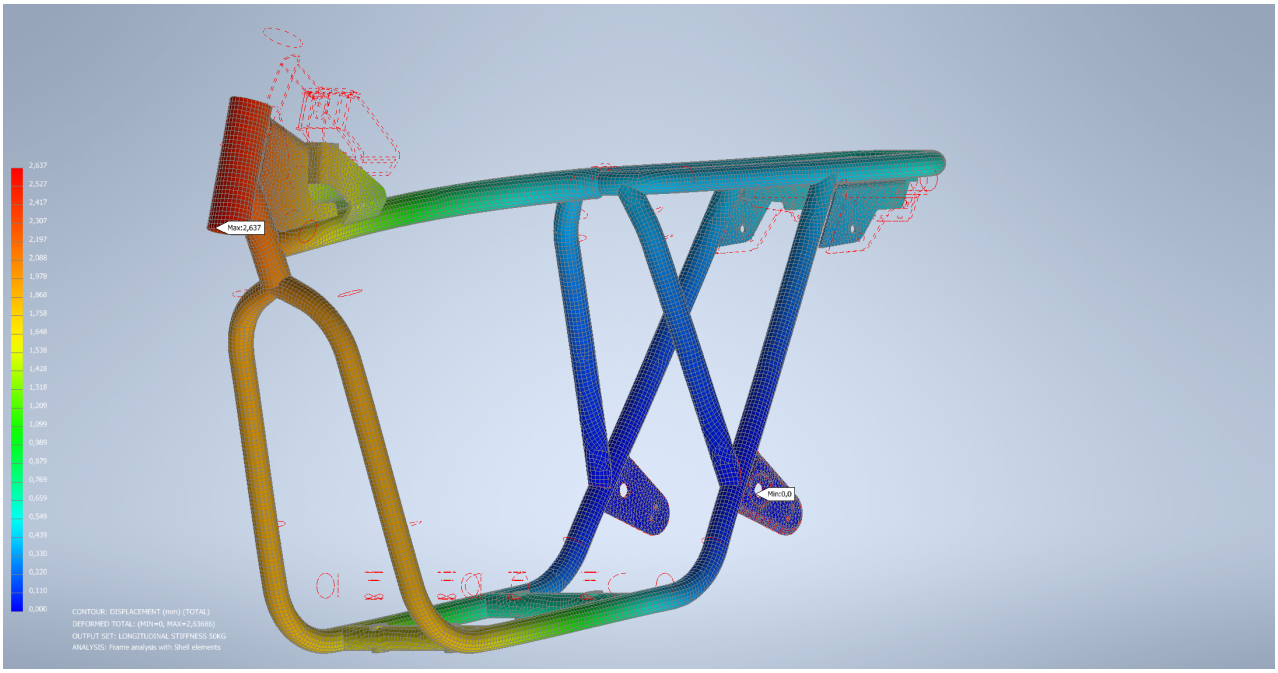

Figure A.18: *Deformation from a Longitudinal load of 491 N simulated using shell elements in Autodesk Inventor Nastran*

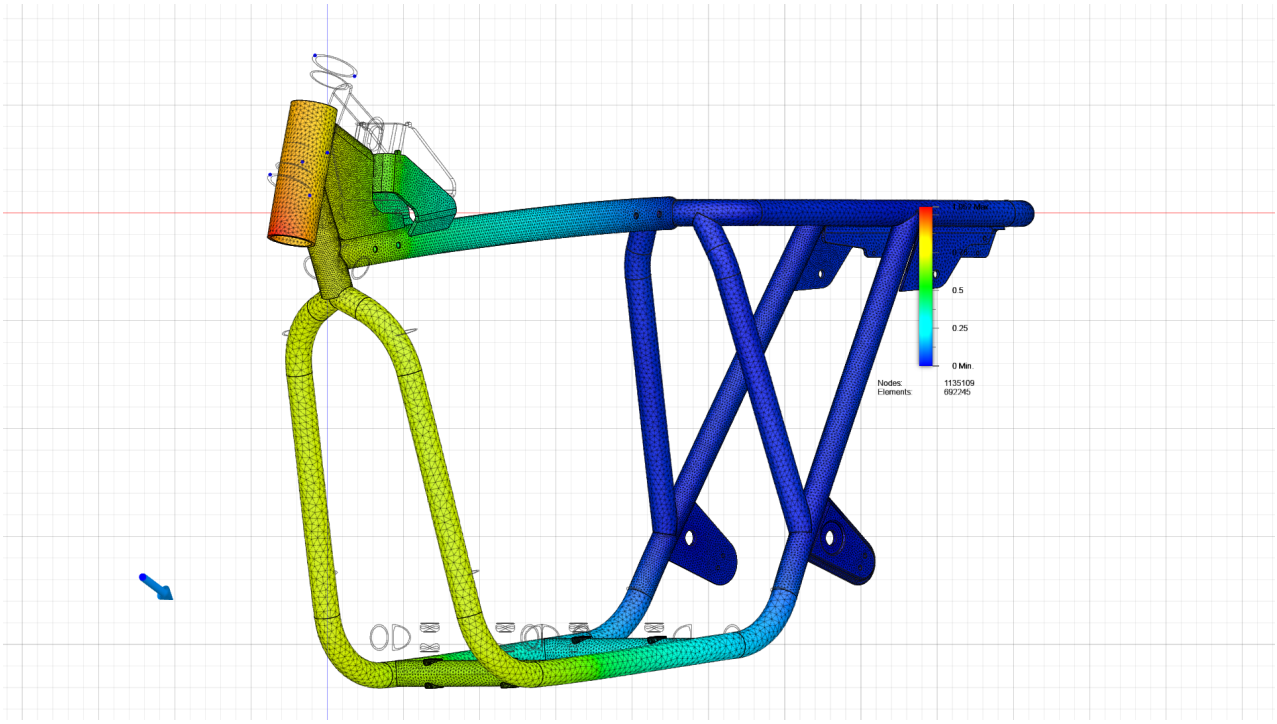

Figure A.19: *Deformation from a Longitudinal load of 491 N simulated using solid elements in Autodesk Fusion 360*

A.3.2 Stress

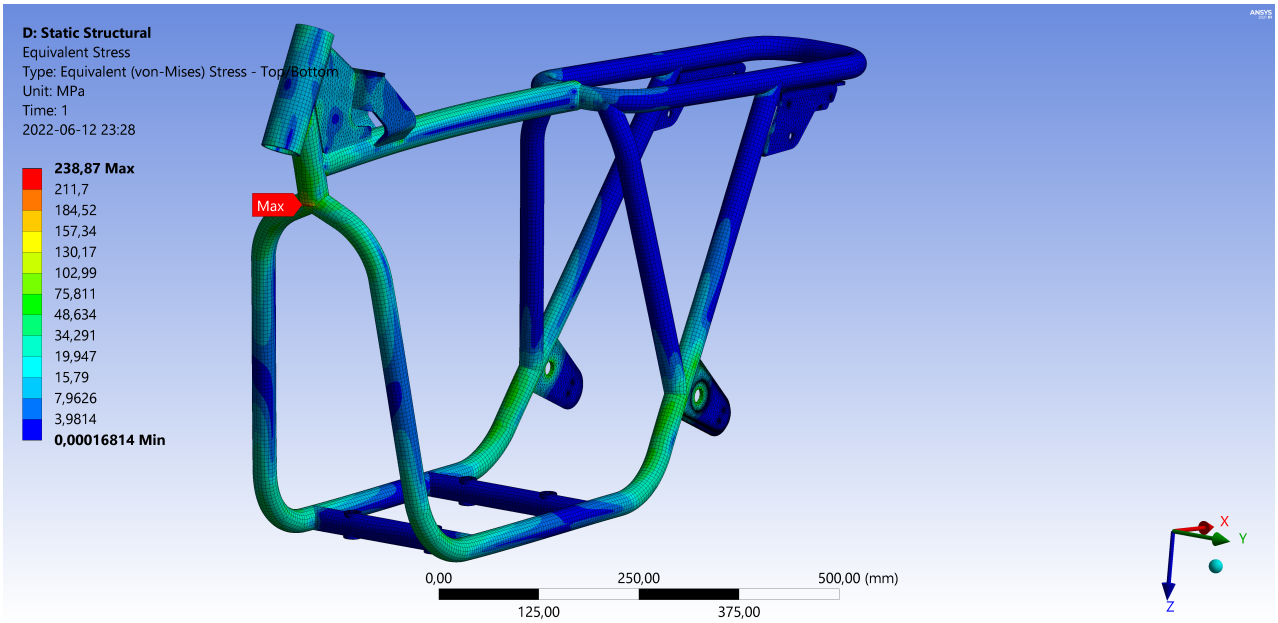

Figure A.20: *Stress plot from a Longitudinal load of 491 N using shell elements in Ansys*

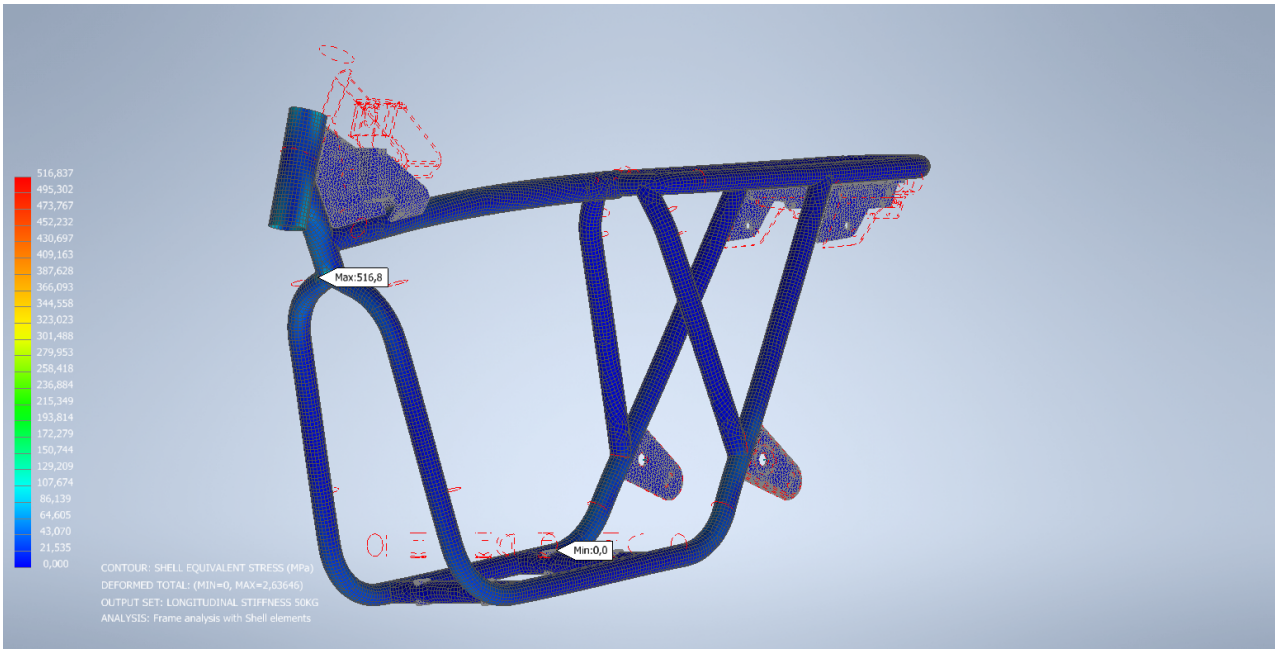

Figure A.21: *Stress plot from a Longitudinal load of 491 N simulated using shell elements in Autodesk Inventor Nastran*

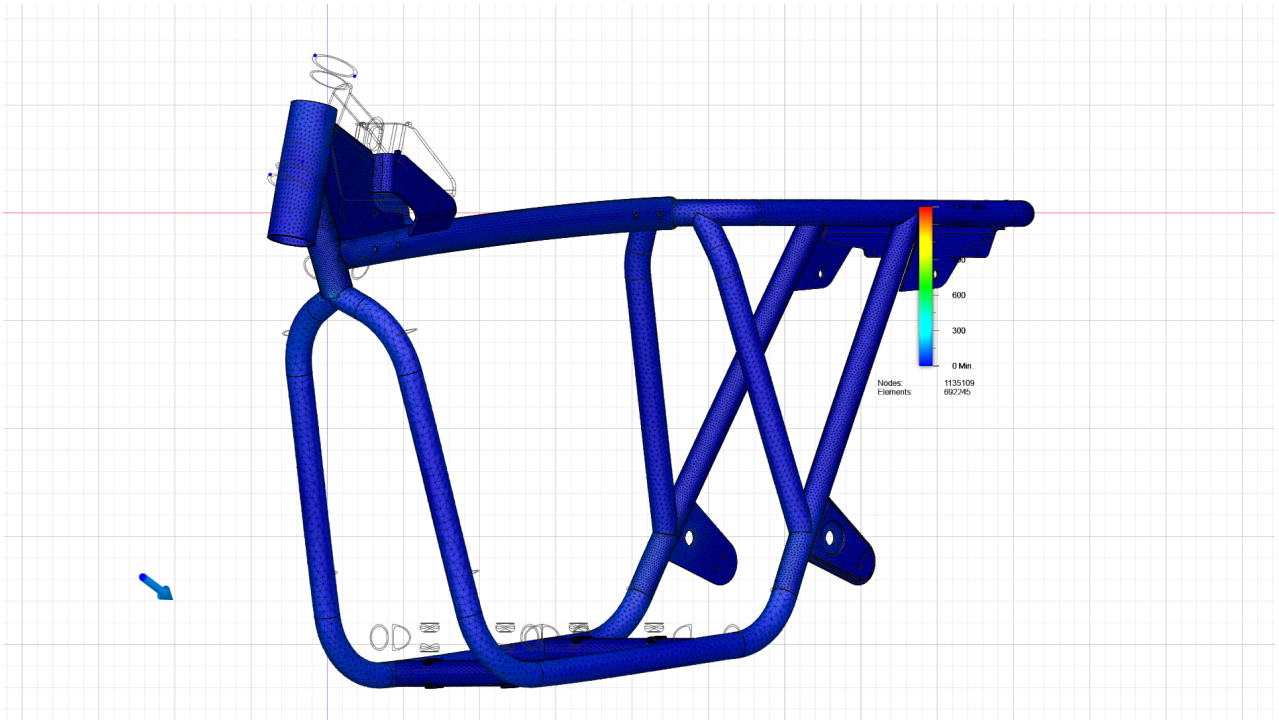

Figure A.22: *Stress plot from a Longitudinal load of 491 N simulated using Solid elements in Autodesk Fusion 360*

A.4 Stressed member

A.4.1 Battery box

Deformation

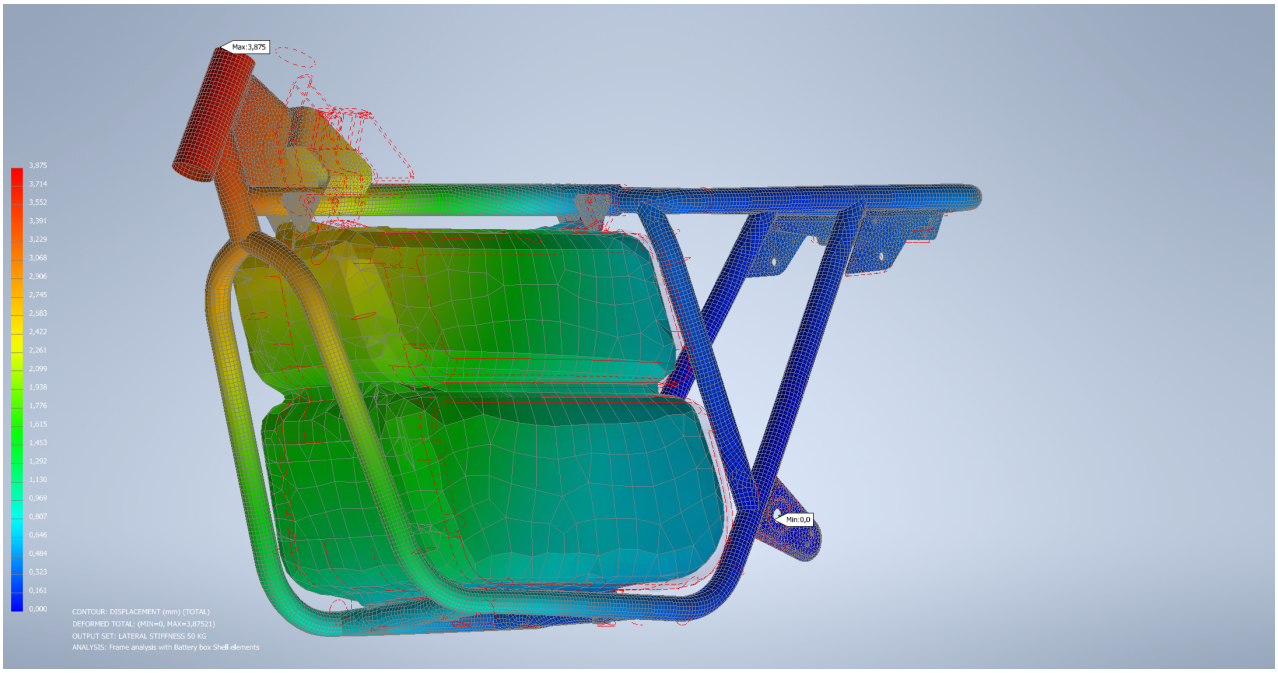

Figure A.23: *Deformation from a Lateral load of 491 N simulated using shell elements in Autodesk Inventor Nastran*

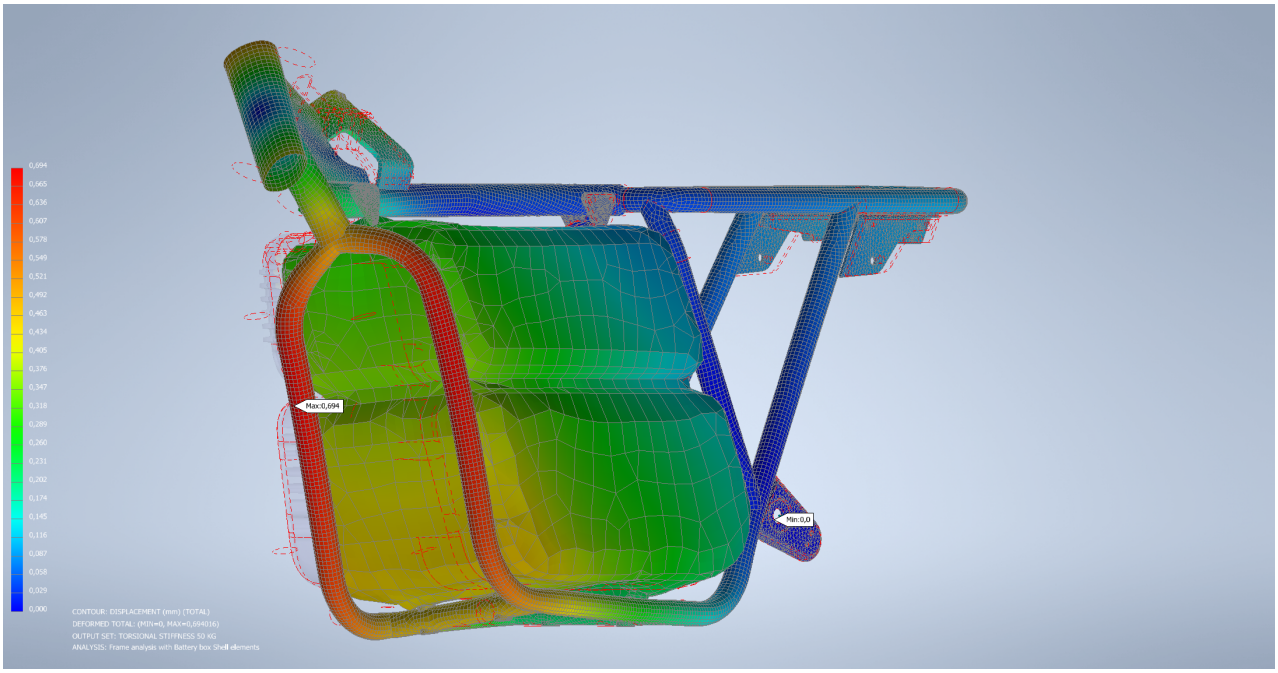

Figure A.24: *Deformation from a Torsional load of 176 Nm simulated using shell elements in Autodesk Inventor Nastran*

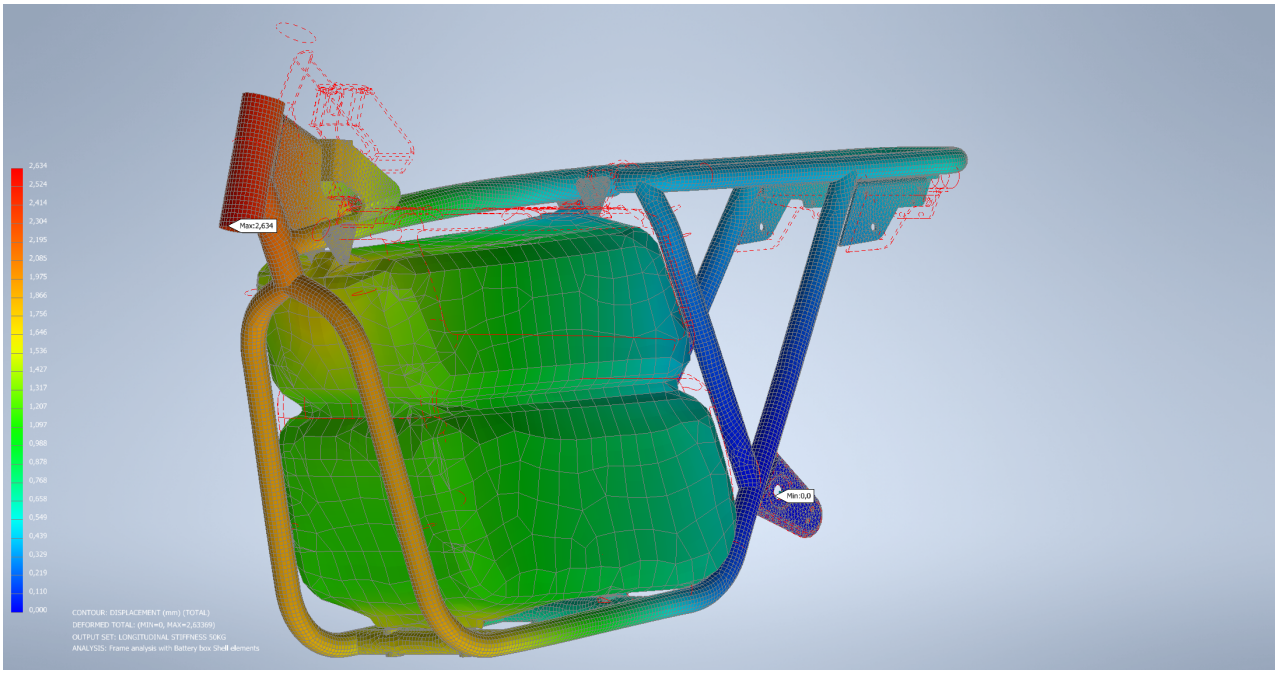

Figure A.25: *Deformation from a Longitudinal load of 1473 N simulated using shell elements in Autodesk Inventor Nastran*

Stress

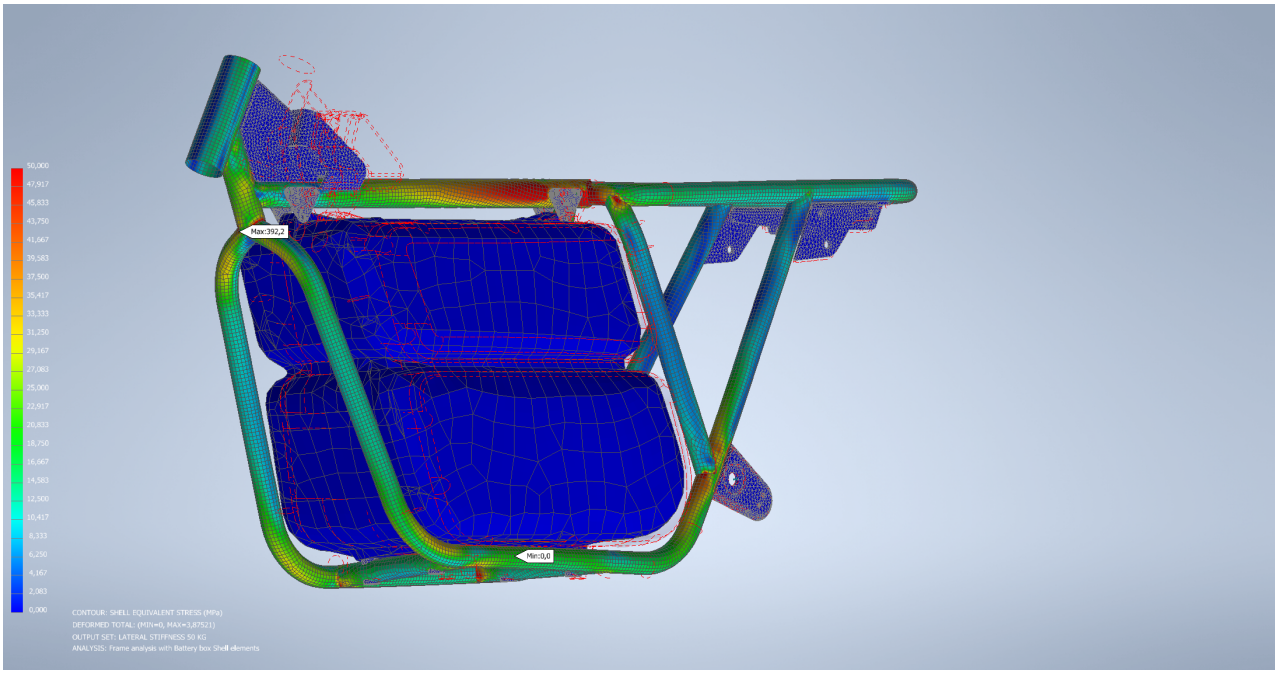

Figure A.26: *Stress plot from a Lateral load of 491 N using shell elements in Autodesk Inventor Nastran*

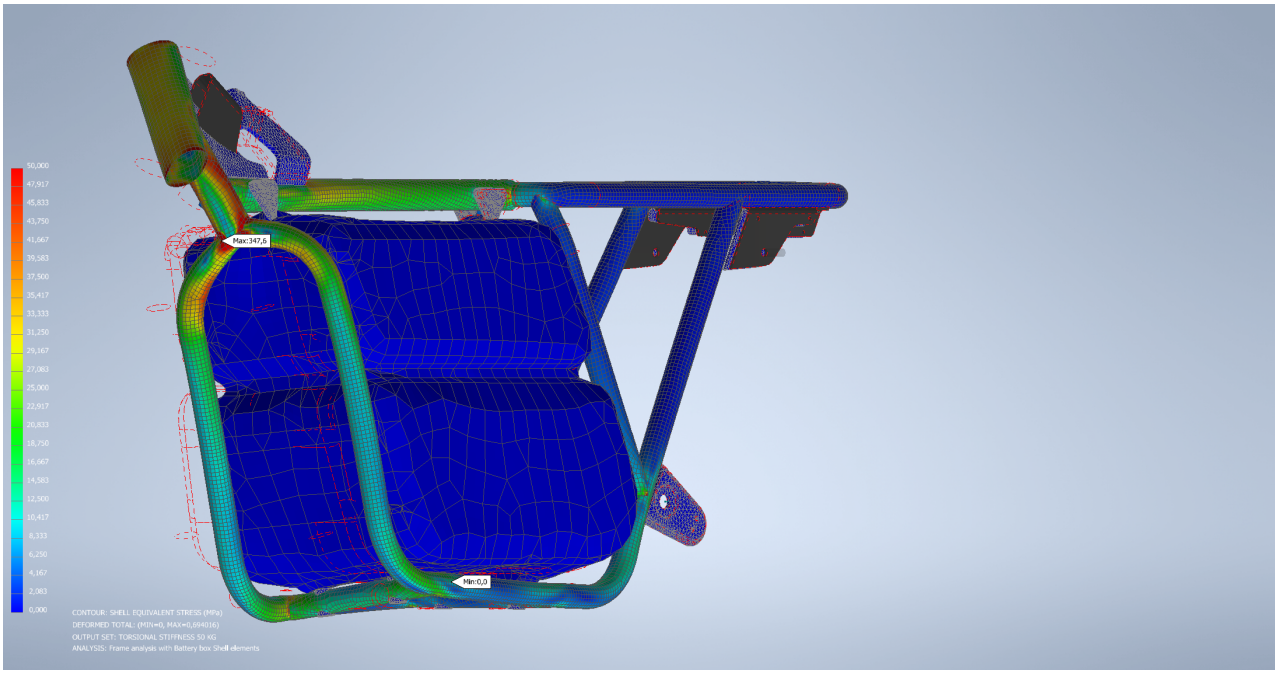

Figure A.27: *Stress plot from a Torsional load of 176 Nm simulated using shell elements in Autodesk Inventor Nastran*

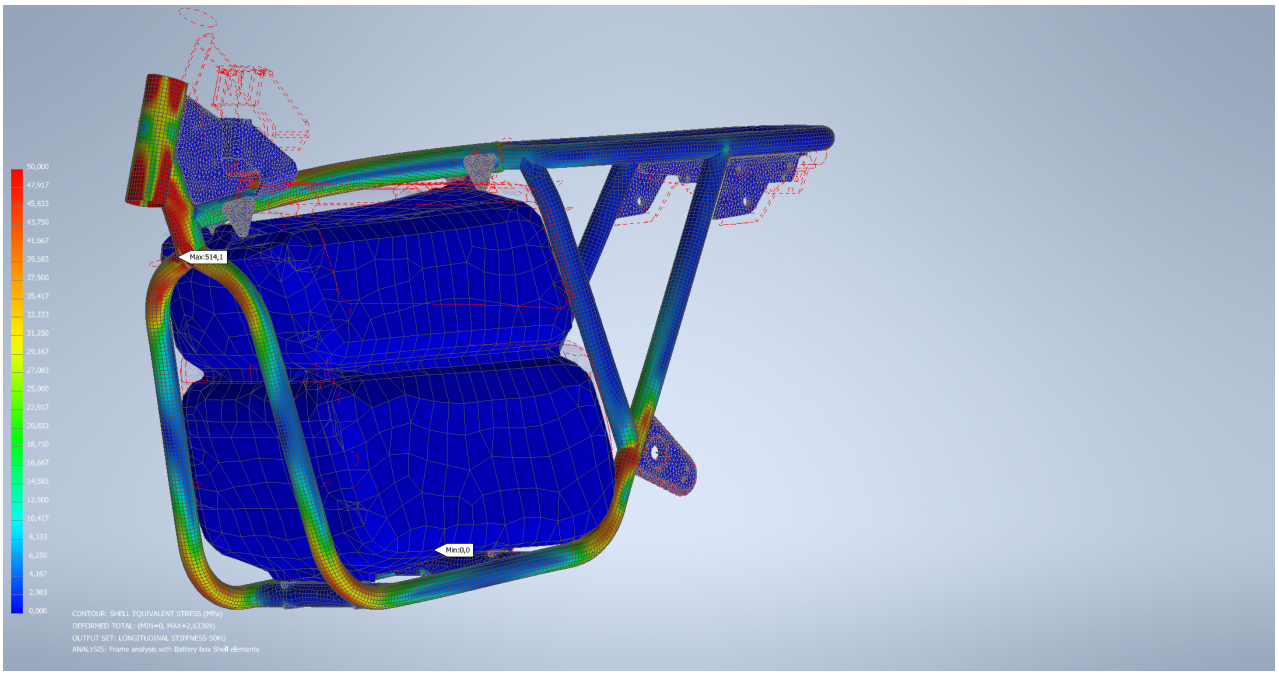

Figure A.28: *Stress plot from a Longitudinal load of 491 N simulated using shell elements in Autodesk Inventor Nastran*

A.4.2 Battery replacement

Deformation

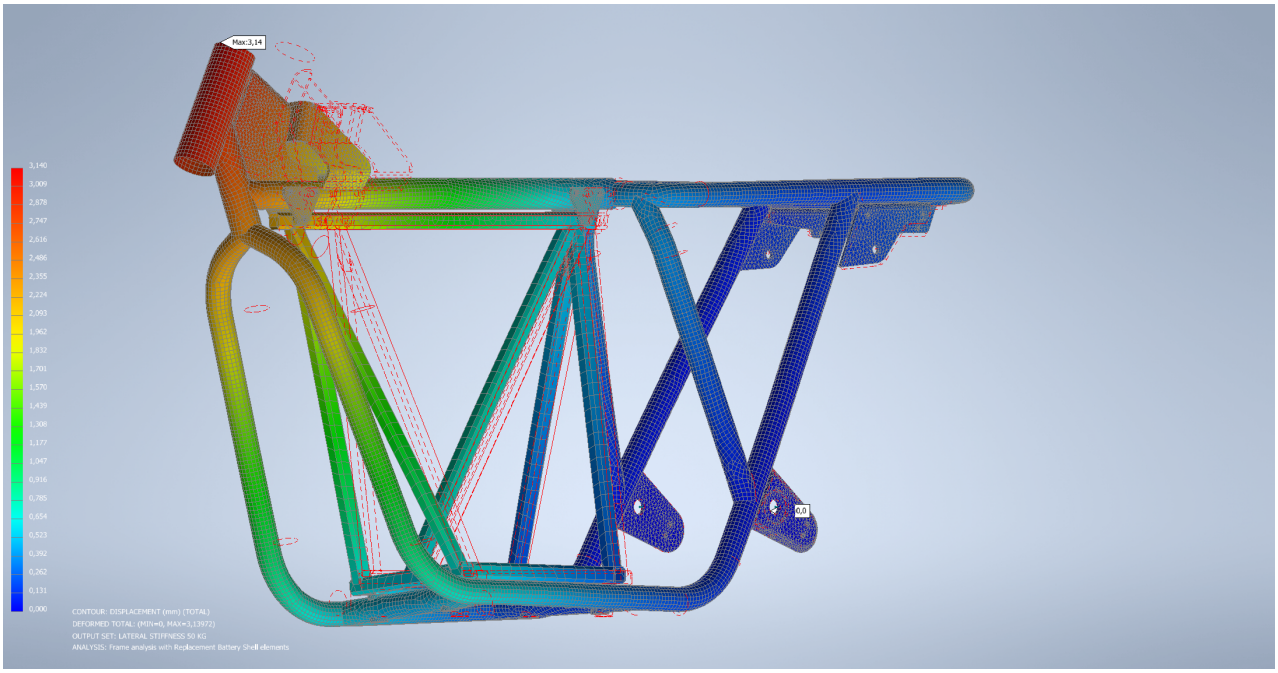

Figure A.29: *Deformation from a Lateral load of 491 N, simulated with shell elements in Autodesk Inventor Nastran*

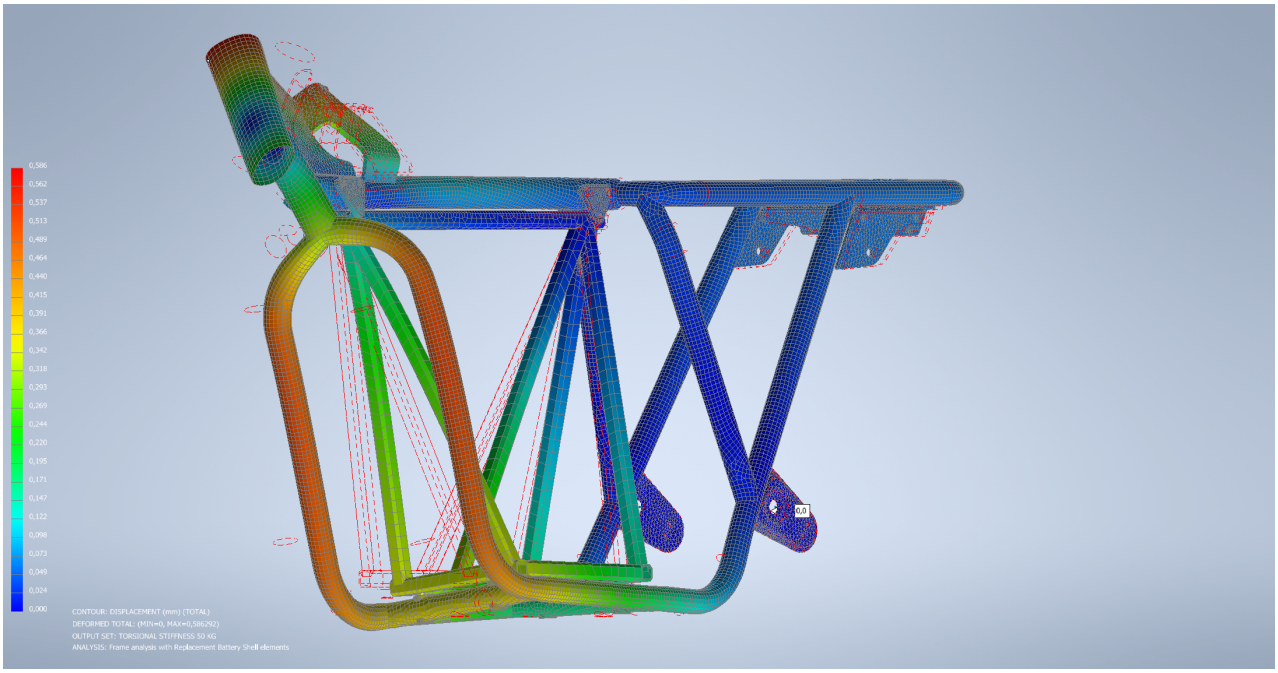

Figure A.30: *Deformation from a torsional load of 176 Nm simulated using shell elements in Autodesk inventor Nastran*

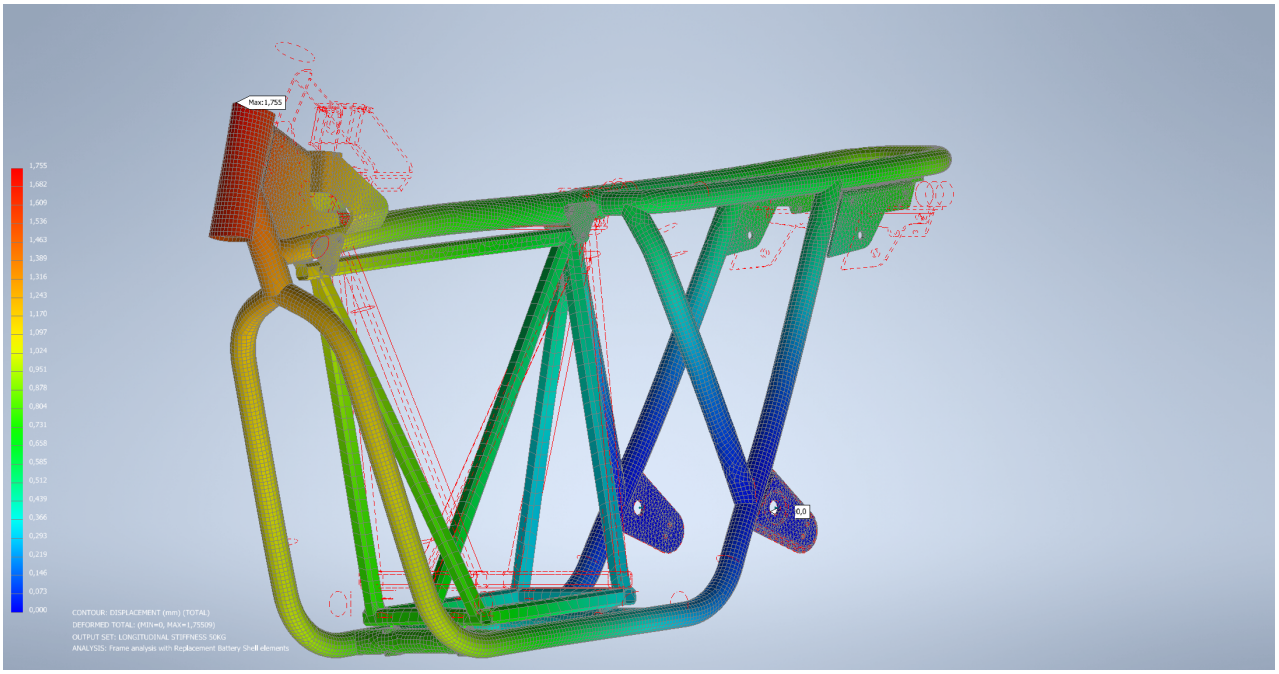

Figure A.31: *Deformation from a Longitudinal load of 491 N simulated using shell elements in Autodesk Inventor Nastran*

Stress

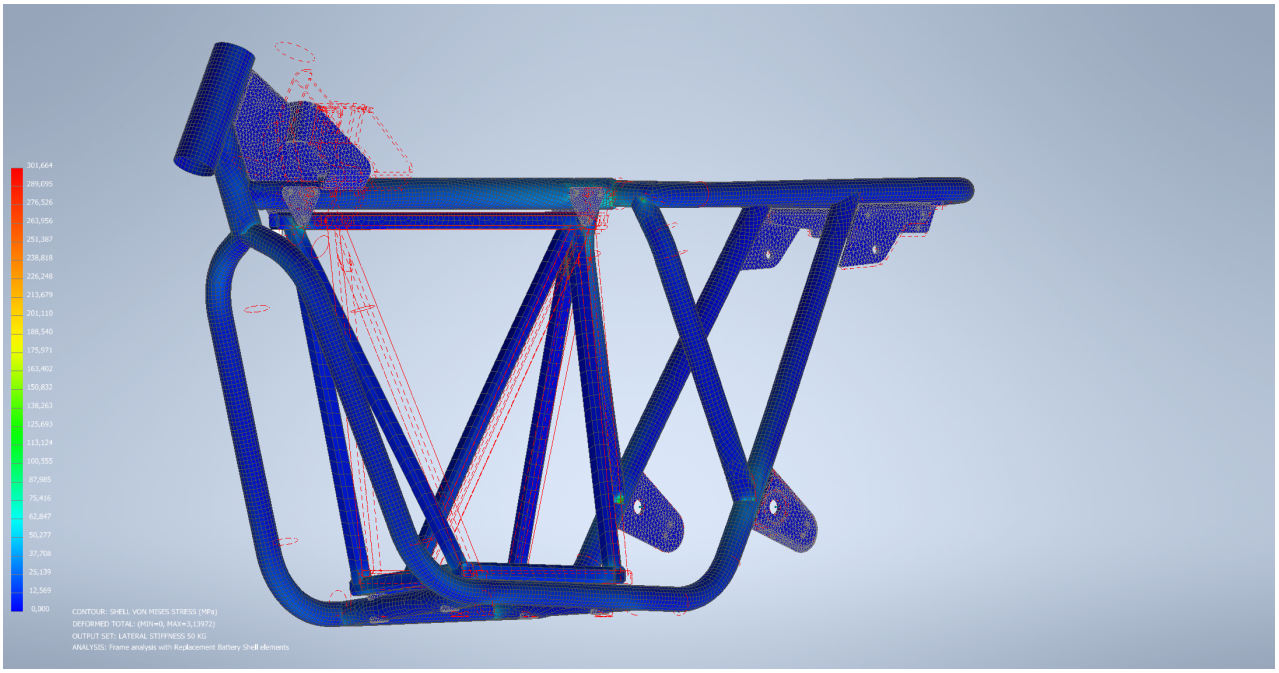

Figure A.32: *Stress plot from a Lateral load of 491 N simulated using shell elements in Autodesnk Inventor Nastran*

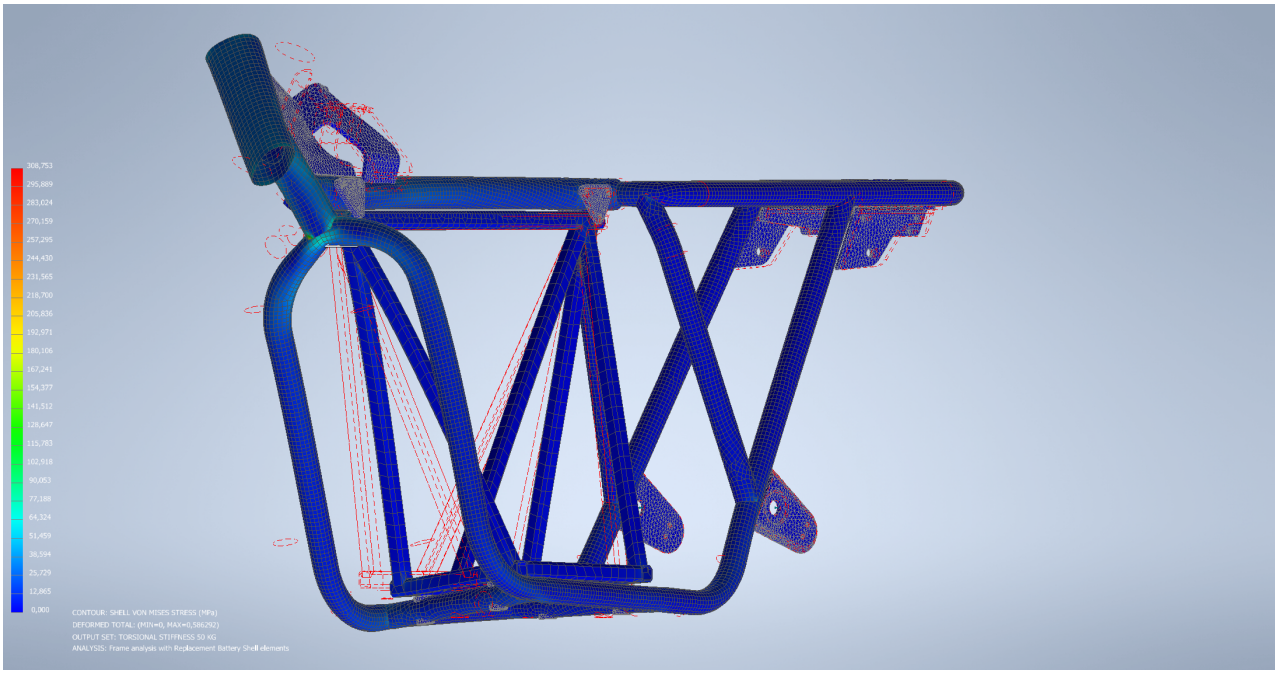

Figure A.33: *Stress plot from a Torsional load of 176 Nm simulated using shell elements in Autodesk Inventor Nastran*

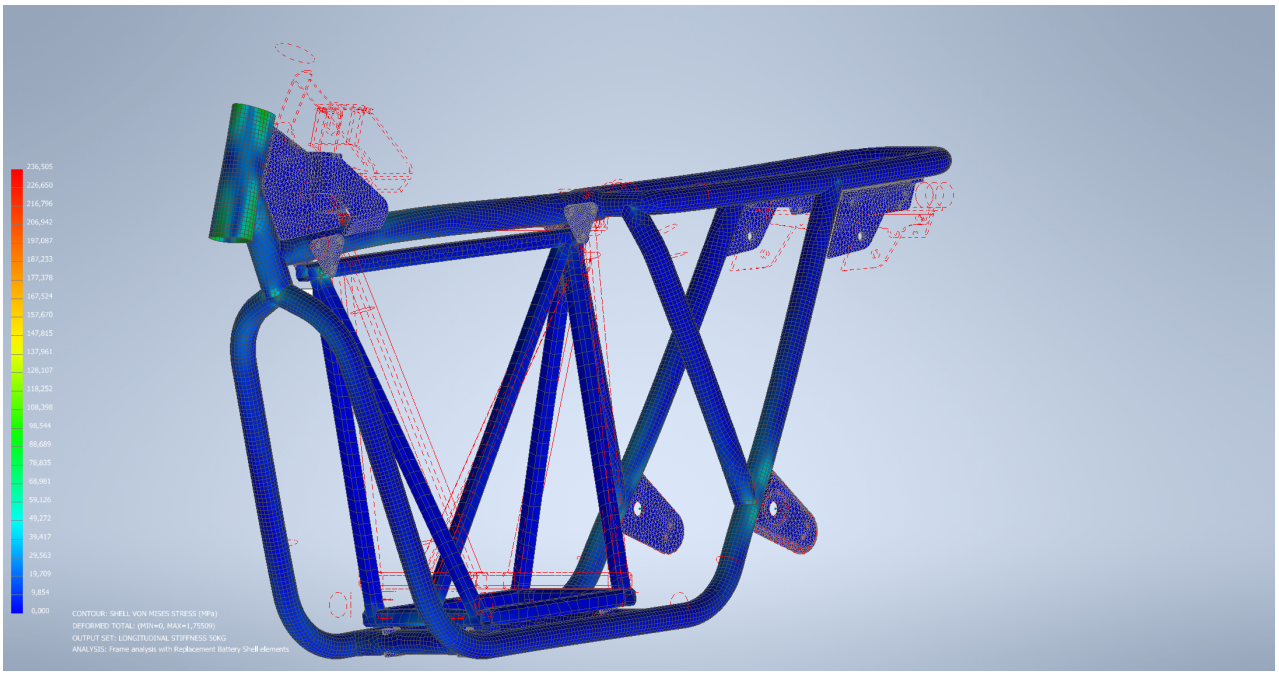

Figure A.34: *Stress plot from a Longitudinal load of 491 N simulated using shell elements in Autodesk Inventor Nastran*